Role of the human LIN complex in DNA damage induced regulation of gene expression

Dissertation zur Erlangung des

naturwissenschaftlichen Doktorgrades

der Bayerischen Julius-Maximilians-Universität Würzburg

vorgelegt von

Mirijam Mannefeld

aus

Offenburg

Würzburg, 2009

Eingereicht am:

…….

Mitglieder der Prüfungskommission:

Vorsitzender:

1. Gutachter: Prof. Dr. Stefan Gaubatz

2. Gutachter: PD Dr. Alsheimer

Tag des Promotionskolloqiums:

…….

Doktorurkunde ausgehändigt am:

…….

1 Introduction

1.1 Human cell cycle

The regulation of the human cell cycle progression is absolutely essential for proper cell proliferation. In the human body a balance between cell death and cell proliferation has to be maintained. Mammalian cells have to progress through many mitotic divisions to proliferate before they differentiate, die or enter a quiescence state. Aberrations in cell cycle progression are known to potentially lead to acceleration of cell cycle progression, aneuploidy, DNA damage and/or mutations which in turn can contribute to tumor development.

The human cell cycle can be divided into distinct phases: in the S phase (synthesis) the genetic material is duplicated once, in M phase (mitosis) the duplicated chromosomes are distributed to the two emerging daughter cells. The phases between S and M are called “G1” (first gap) and “G2” (second gap) whereas G1 takes place before the new chromosomes are synthesized in S phase and G2 before cells divide in mitosis.

The time cells need to complete one division cycle mainly depends on the cell type and the environmental circumstances but in most mammalian cell types it ranges from 10 to 30 hours. Since S and M phase only take about 1-2 h, the bigger part/bulk of important regulatory mechanisms take place during the gap phases. When a cell does not get the necessary signal for proliferation by growth factors (mitogenic signals), is terminally differentiated or does not reach the needed size, then it exits from cell cycle within the early G1 phase and enters a non-dividing, quiescent or resting phase called G0 (Molinari 2000; Malumbres and Barbacid 2001).

The transcription of genes important for G1/S as well as G2/M transition is regulated by a family of transcription factors, the E2Fs. Importantly, the function of E2Fs as transcriptional regulators is directly linked to their association with members of the pocket protein family, pRb and its relatives p130 and p107. The family of E2Fs consists of 8 E2F-proteins (E2F1-8), 6 of which (E2F1–6) need

heterodimerization with DP proteins (DP1 and DP2) for functional activity (Giacinti and Giordano 2006). The E2F transcription factor family can be divided into two functional groups. First, E2F1-3a are transcriptional activators and repressed by binding to the pocket protein pRb. E2F1-3a are generally expressed at low levels in quiescent cells but are induced to high levels during G1 phase (Dyson 1998). Second, E2F3b-8 act as transcriptional repressors with E2F4 and E2F5 mostly binding to the pocket proteins p130 and p107 to assume their repressive function/do so (Gaubatz, Lindeman et al. 2000). During G0 and G1 transcriptional repression of some E2F-responsive genes such as Plk1, Survivin (Birc5), cyclin A2, cdc2, and cyclin B1 is mediated by binding of E2F4/5 and pocket proteins to 2 specific regions which can be found within target gene promoters (Lange-zu Dohna, Brandeis et al. 2000; Zhang, Wang et al. 2007; Yang, Song et al. 2008). First, a repressive CDE (cell cycle dependent-element) and second, a CHR (cell cycle genes homology region) domain located near the CDE within the promoter region (Tommasi and Pfeifer 1995; Zhu, Giangrande et al. 2004). Together, CDE- and CHR-domains build up cis-acting elements. It is known, that transcriptional repression is mediated by binding of an E2F4- and p130-containing complex to the CDE (Tommasi and Pfeifer 1995). Although, it is known that an intact CHR element is needed for proper repression, no CHR-binding protein could be identified so far (Liu, Lucibello et al. 1998; Lange-zu Dohna, Brandeis et al. 2000). It seems that both the CDE and the CHR can bind to a set of different proteins dependent on the gene they are located in. E.g. E2F4 can bind to the CDE within the B-MYB promoter but not within the cyclin A promoter (Liu, Lucibello et al. 1998). Additionally, CDE-CHR elements are also essential for repression of G2/M gene expression after DNA damage induction (see 1.2.2). E2F4 and E2F5 are constantly expressed during the cell cycle and act only poorly as transcriptional activators probably due to their lack of a nuclear localization signal. Hence, they are dependent on their recruitment to the nucleus by p130 and p107 for fulfilling their function (Dimova and Dyson 2005).

The pocket protein family consists of 3 members, pRb, p130 and p107 which share 30 -35 % sequence homology, especially in a domain called pocket domain. All three proteins contain two conserved domains, A and B, separated

by a linker which together build the pocket domain needed for E2F binding as well as binding of other cofactors. p130 and p107 are more similar to one another than to pRb and share the ability to bind to cyclin-cdk complexes (Lipinski and Jacks 1999).

To assure, that cell cycle progression proceeds controlled and without incident, proteins are essential which drive but also monitor the march through cell division. The availability of these proteins has to be quantitatively and chronologically correct. To guarantee this, they themselves are regulated by other proteins. Additionally, to assure that errors do not remain undetected, cells detect failures in cell cycle progression at different sites within the cell cycle. Four main checkpoints are fundamental for proper ending of/accomplishing a normal division cycle: First, the “restriction point”, second, the “unreplicated DNA checkpoint”, third, the “spindle assembly checkpoint” and fourth, the “chromosome-segregation checkpoint”. Beyond the “unreplicated DNA checkpoint” the just mentioned checkpoints are constitutively active and have to be switched off in order to allow further cell cycle progression. Furthermore, separate checkpoints, which are not constitutively active, localize damage which occurred at the DNA and if possible initiate repair (Tessema, Lehmann et al. 2004).

1.2 DNA damage response

DNA damage is a common event occurring during cell cycle progression and is triggered by replication errors, endogenous factors like reactive oxygen species or by exogenous factors such as UV radiation, gamma-rays, viruses or DNA intercalating agents. Unrepaired DNA damage can amongst others lead to the loss of genomic integrity and thereby facilitating cancer development and premature ageing. Among the many different types of DNA damage, double-strand breaks (DSBs) are the most deleterious to cell survival (Shimada and Nakanishi 2006). Therefore, enabling induction of several cellular responses dealing with DNA damage compensation is the main step in avoiding severe implications for cell proliferation and living. DNA damage checkpoints are associated with chemical pathways that either end, delay or arrest cell cycle progression. In parallel to checkpoint activation, DNA repair and/or initiation of

apoptotic pathways is induced. Sensors like Rad9, Rad1, Hus1 and Rad17, Mediators (BRCA1, 53BP1 and RAD50), Transducers (ATR/ATM, CHK1 and CHK2) and effectors like p53, cdc25A,B,C and cdks, are the 4 main groups mediating a proper signal transduction from DNA damage occurrence to initiation of DNA repair, cell cycle arrest and apoptosis (Niida and Nakanishi 2006).

When DNA damage occurs, lesions within the DNA strand are recognized by multifunctional complexes such as the Mre11-Rad50-Nbs1 (MRN) complex. Their recruitment leads to the activation of DNA damage dependent signaling which in the end triggers/mediates the activation of ATM and ATR kinases. In general, ATM responds mainly to double-strand breaks (DSBs) whereas ATR mainly is activated by ssDNA and stalled DNA replication forks (Bartek and Lukas 2007).

1.2.1 G1 checkpoint

In the presence of DNA damage, the G1/S checkpoint impedes cell cycle progression and thereby prevents replication of damaged DNA. Mediator proteins such as MDC1, BRCA1 and 53BP1 collaborate with the activated ATM and ATR kinases in the phosphorylation and activation of Chk1/2. Chk1 and Chk2 themselves can now phosphorylate cdc25A leading to its re-localization into the cytoplasm via 14-3-3, thereby making it accessible for proteasomal degradation. The degradation of cdc25A results in the inactivation of cdk2 by prolonged phosphorylation events thereby preventing loading of cdc45 onto the chromatin. Since cdc45 is essential for recruitment of DNA polymerase α, cdc45 inhibition impedes new origin firing (Shimada and Nakanishi 2006).

In parallel, p53 is activated by phosphorylation via ATM/ATR and Chk1/2. Simultaneously, mdm2, an ubiquitin ligase promoting p53s nuclear export, is phosphorylated by ATM, thereby ubiquitinated and degraded and thus inhibited. As a result, p53 accumulates in the nucleus and can mediate transcriptional responses e.g. transcriptionally activate p21 (Maya, Balass et al. 2001). p21 is a common cdk inhibitor which inhibits the G1/S promoting cdk2, cdk4 and cdk6 kinases thereby leading to a G1 arrest. p21 also inhibits G1/S transition by pRb-mediated sequestration of E2F transcription factors (Bartek and Lukas 2001;

Shimada and Nakanishi 2006). In conclusion, cell cycle progression is arrested in G1 by inhibition of cdk activity thereby preventing cells to overcome the restriction point due to inhibition of pRb phosphorylation and thus E2F activation (Fig. 1.1).

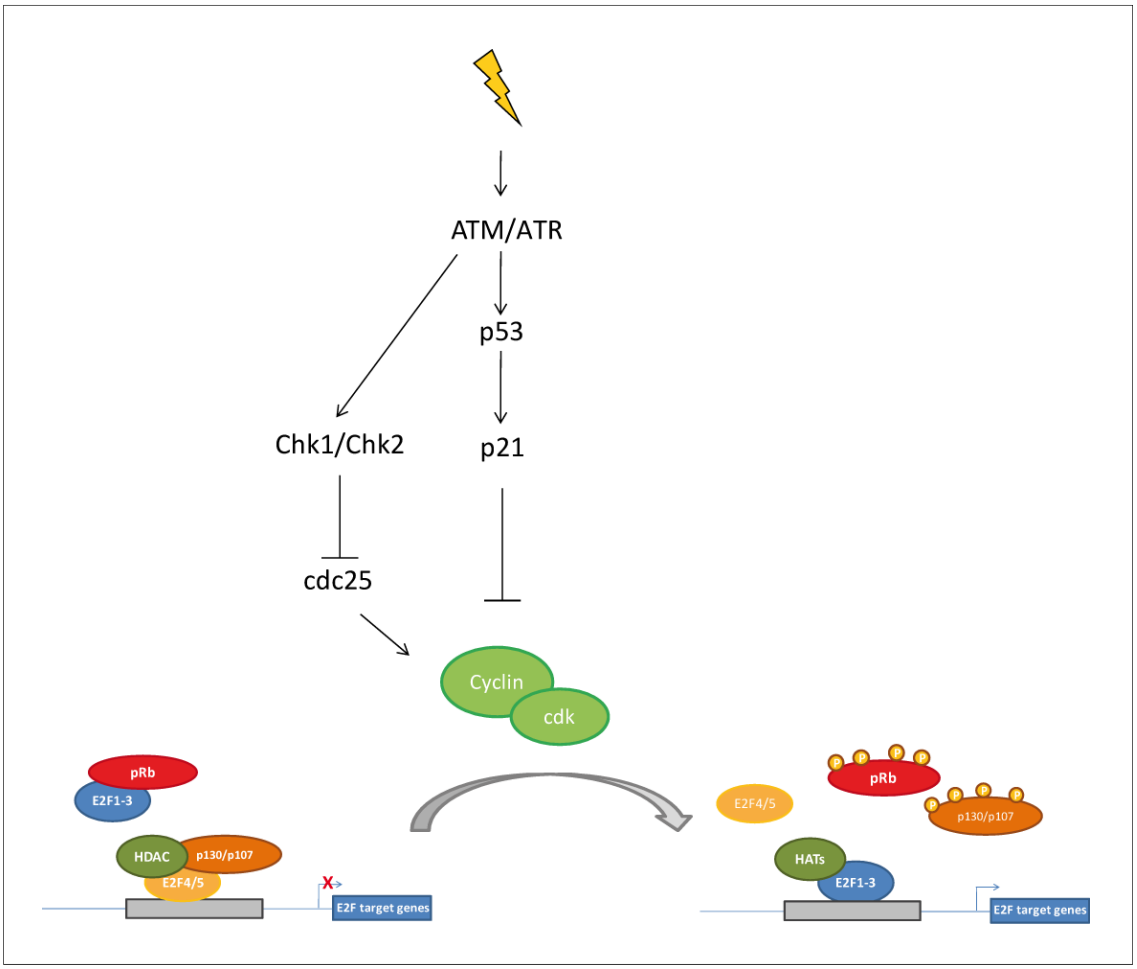

Figure 1.1: Simplified pathway leading to G1 arrest after DNA damage

Activation of Chk1/2 leads to cdc25c inhibition, thus preventing cdk activation by dephosphorylation. Additionally, p53 is activated by ATM and in turn leads to transcriptional activation of p21. As a result cdk activity is inhibited. Together, these pathways prevent cells to overcome the restriction point by inhibition of pocket protein phosphorylation.

Additionally, within the Intra S checkpoint during S phase, damaged DNA inhibits replicative DNA synthesis via two pathways: First, via the ATM/ATR-Chk1/2-cdc25A and second, via the ATM-NBS1-SMC1 pathway (Bartek and Lukas 2007).

1.2.2 G2/M checkpoint

The second main DNA damage checkpoint is the G2/M checkpoint. It prevents cells to enter mitosis with damaged DNA. Induction of G2/M arrest is independent of p53. Following DNA damage, the ATM-Chk2 and/or the ATR-Chk1 pathways are activated. Similarly to the G1/S checkpoint, this leads to the Chk1-mediated phosphorylation of cdc25C, which induces its binding to 14-3-3 proteins and thus results in its re-localization into the cytoplasm where it is degraded through the ubiquitin-proteasome pathway (Nurse 1997). Thereby, activation of cdk1 kinases by cdc25C-dependent dephosphorylation is inhibited, leading to the sequestration of cdk1 into the cytoplasm via 14-3-3σ (or 14-3-3 anchors cdk1 in the cytoplasm) and thus to the inhibition of cyclin A/B-cdk1 (Chan, Hermeking et al. 1999). Additionally, cyclin B subcellular/nuclear localization is regulated. After DNA damage the nuclear export signal within cyclin B is not inactivated by phosphorylation leading to its export into the cytoplasm (Jin, Hardy et al. 1998).

In parallel, p53 is activated after DNA damage (see 1.2.1) and thus can activate target genes important for checkpoint initiation such as 14-3-3σ, p21, GADD45 and others (Chan, Hermeking et al. 1999). p21, as a cdk inhibitor, also blocks cdk1 activity thereby enforcing the DNA damage response. Inhibitory phosphorylations of cdk1 at tyrosine 15 and threonine 14 are catalyzed by Wee1 and Myt1 additionally enforcing cdk1 inhibition (Graves, Lovly et al. 2001). Wee1, like Myt1 a protein kinase, is phosphorylated by Chk1 and thereby activated. In contrast to cdc25C, phosphorylation-induced binding of Wee1 to 14-3-3 does not lead to its degradation but rather to Wee1 stabilization and an increase in kinase activity (Wang, Jacobs et al. 2000). Additionally, binding of cdk1 and cyclin B is disrupted by GADD45. Activation of this pathway induces a fast response to DNA damage by inducing an arrest in G2/M phase mainly by inhibition of cdk1 and change in subcellular localization of cyclin B.

1.2.3 G2/M checkpoint maintenance

Besides checkpoint initiation, checkpoint maintenance is an important mechanism. Down regulation of G2/M gene expression by mostly unknown mechanisms contributes to maintenance of the G2/M checkpoint. Beyond other

factors, repression of G2/M gene expression seems to be dependent on activation of p53 as well as p21 and binding of E2F4 and p130 to CDE-CHR elements within the target gene promoters (see Fig. 1.2).

Since p53 and p21 were shown to be essential for a sustained G2 arrest after γ radiation (Bunz, Dutriaux et al. 1998) and since this pathway is activated at late times after DNA damage occurred, it was supposed, that it may play a role in sustaining or reinforcing an otherwise transient G2/M arrest established by inhibition of cdk1 (see Fig. 1.2). Otherwise it could be a fail-safe mechanism when cdk1 inhibition failed (Azzam, de Toledo et al. 1997; de Toledo, Azzam et al. 1998; Badie, Itzhaki et al. 2000; Taylor, Schonthal et al. 2001).

More precisely, p53 and p21 were shown to be essential for a sustained G2 arrest after γ radiation (Bunz, Dutriaux et al. 1998). By inactivating the p53 pathway, which occurs in most tumor cells, the G1 arrest is completely abolished while the G2 arrest is indeed initiated but in a attenuated manner/still initiated but to a lower extend (Plesca, Crosby et al. 2007). In addition, it is known that cyclin B transcriptional repression is mediated by p53 and contributes to a long-term G2 arrest. Interestingly, cyclin B overexpression alone can abrogate a p53-induced G2 arrest. Additionally, repressed level of cdc2 protein in response to p53 is also dependent on p21 and can be abrogated by the E7 protein of human papilloma virus. Since E7 itself binds and inhibits pocket proteins, this led to the assumption that pocket proteins could be involved in DNA damage-induced transcriptional repression. Finally it was shown by Taylor and colleagues, that p53 represses cdc2 transcription through a mechanism including p21 activation and binding of p130 and E2F4 to the CDE and CHR elements within the R box of the cdc2 promoter (Taylor, Schonthal et al. 2001).

E2F4 is able to form a complex with unphosphorylated p130 following radiation leading to its nuclear localization (DuPree, Mazumder et al. 2004; Crosby, Jacobberger et al. 2007). Also hypoxia induces p130 dephosphorylation and nuclear accumulation, leading to the formation of E2F4-p130 complexes which in turn occupy promoters of genes important for DNA repair (such as Rad51 and BRCA) (Plesca, Crosby et al. 2007). In addition, recent work implicated

p130 in the mechanism of G2 arrest following treatment with etoposide or adriamycin (doxorubicin) (Jackson, Agarwal et al. 2005) as well as E2F4 requirement for stable G2 arrest in response to genotoxic stress (Crosby, Jacobberger et al. 2007).

The results of these different studies support the existence of a p53- and/or p21-dependent pathway that culminates in transcriptional repression of various S/G2/M-associated genes such as cyclin A2, cyclin B1, cdk1(cdc2) and Plk1 after DNA damage (Azzam, de Toledo et al. 1997; de Toledo, Azzam et al. 1998; Badie, Itzhaki et al. 2000; Taylor, Schonthal et al. 2001). Although E2F4 and p130 as well as p53 and p21 have been implicated in DNA-damage mediated repression of genes, little is known about the exact role of this pathway in the DNA damage response and in tumor development.

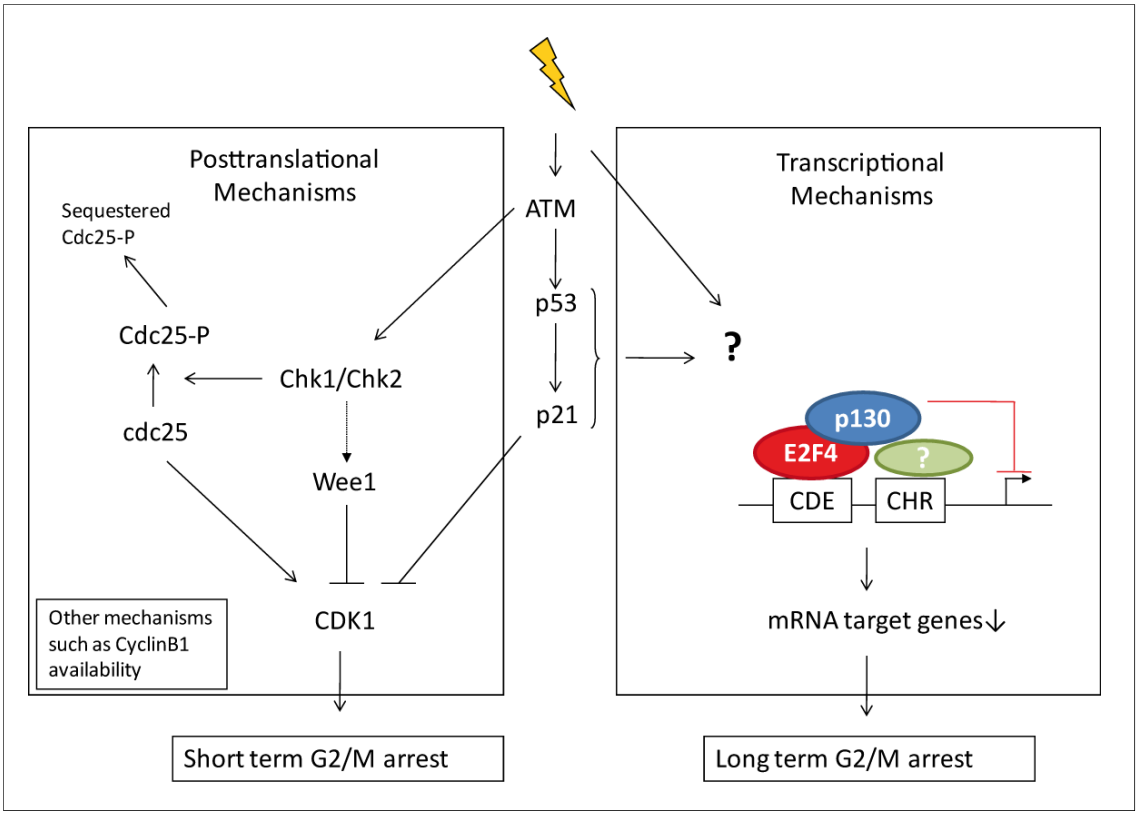

Figure 1.2: Simplified model of initiation and maintenance of G2/M arrest after DNA damage

Model showing proposed transcriptional regulation of target gene repression following genotoxic stress. It might be combined with previously proposed, largely translational DNA damage checkpoint pathways leading to initiation and maintenance of a G2/M arrest. Adapted and modified from (Badie, Itzhaki et al. 2000). See text for details.

1.2.4 Checkpoint recovery and adaptation

Checkpoint activation after DNA damage is essential to repair damaged DNA, so that cells can resume cell cycle progression and continue their physiological program. After DNA repair is completed, cells regain the ability to exit G2 arrest and reenter mitosis, referred to as checkpoint recovery. Recent work showed that checkpoint recovery is a controlled and active process which involves the ubiquitin/proteasome-dependent degradation of Claspin - needed for phosphorylation and thereby for activation of Chk1 - and Wee1 (see Fig. 1.3). During checkpoint recovery, Plk1 gene expression is reactivated leading to the phosphorylation of Claspin and Wee1 (Mamely, van Vugt et al. 2006). Thereby these two proteins are marked for degradation by $SCF^{\beta TrcP}$ (Mailand, Bekker-Jensen et al. 2006; Peschiaroli, Dorrello et al. 2006), an enzyme complex that also contributes to cdc25C degradation during initiation of G2 arrest. Since 2004 it was assumed that mostly Plk1 activity controls recovery from a DNA damage-induced G2 arrest in mammalian cells (van Vugt, Bras et al. 2004).

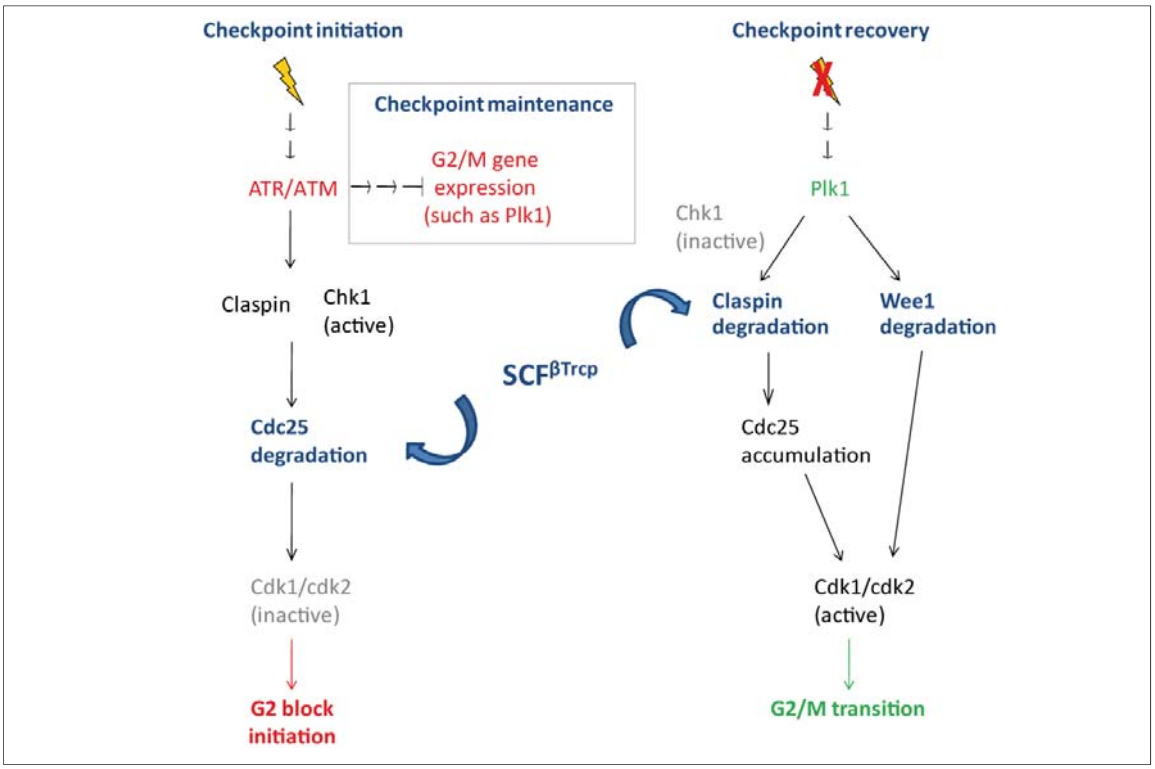

Figure 1.3: Proposed model of checkpoint initiation and recovery

During checkpoint initiation cdc25 is degraded leading to cdk1/cdk2 inactivation and a G2 arrest. When DNA damage repair is completed, Plk1 is activated by an unknown mechanism leading to Claspin and Wee1 degradation by $SCF^{\beta TrcP}$. In the end, cdk1 and cdk2 are active and cells can reenter cell cycle. Adapted and modified from (Bartek and Lukas 2007).

Related to checkpoint recovery is checkpoint adaptation, a phenomenon known from *Schizosaccharomyces cervisiae* where cells have the ability to reenter cell cycle progression after a sustained checkpoint-imposed cell cycle arrest despite the presence of DNA damage (Toczyski, Galgoczy et al. 1997). Mechanistically, checkpoint adaptation is facilitated by prematurely resumed activity of Plk1 and inhibition of Chk1/Chk2 kinases (Bartek and Lukas 2007), thus probably affecting Claspin and other factors (Fig. 1.3) (Yoo, Kumagai et al. 2004; Syljuasen, Jensen et al. 2006) before DNA damage is eliminated.

1.3 LINC – a human multiprotein complex

The human LIN complex (LINC) is an important regulator of gene expression needed for correct progression through the cell cycle. In 2007 we and others identified this stable human multiprotein complex which is composed of a core complex able to associate with different proteins in a cell cycle dependent manner. Basically, the human LIN complex (LINC or human dREAM complex) consists of 4 different LIN proteins (LIN-9, LIN-37, LIN-52 and LIN-54) and RbAp48 forming a stable core complex which can associate with either B-MYB or p130 and E2F4 (Litovchick, Sadasivam et al. 2007; Osterloh, von Eyss et al. 2007; Schmit, Korenjak et al. 2007). During G0 and G1 phase of the cell cycle LINC binds to E2F4 and p130, both proteins known to be involved in the repression of target gene expression. When cells progress through the cell cycle, the associated proteins change. In S phase, E2F4 and p130 leave the complex whereas B-MYB, an E2F target gene expressed during late G1 phase, associates to LINC (see Fig. 1.4) (Litovchick, Sadasivam et al. 2007; Schmit, Korenjak et al. 2007). Cell cycle dependent binding of p107 to LINC is controversial. Schmit and colleagues found that p107 associates to LINC together with B-MYB during S phase. A context dependent human dREAM complex was also confirmed by Pilkinton and colleagues, but in contrast, showed that p107 associates to the complex during G0 phase (Pilkinton, Sandoval et al. 2007).

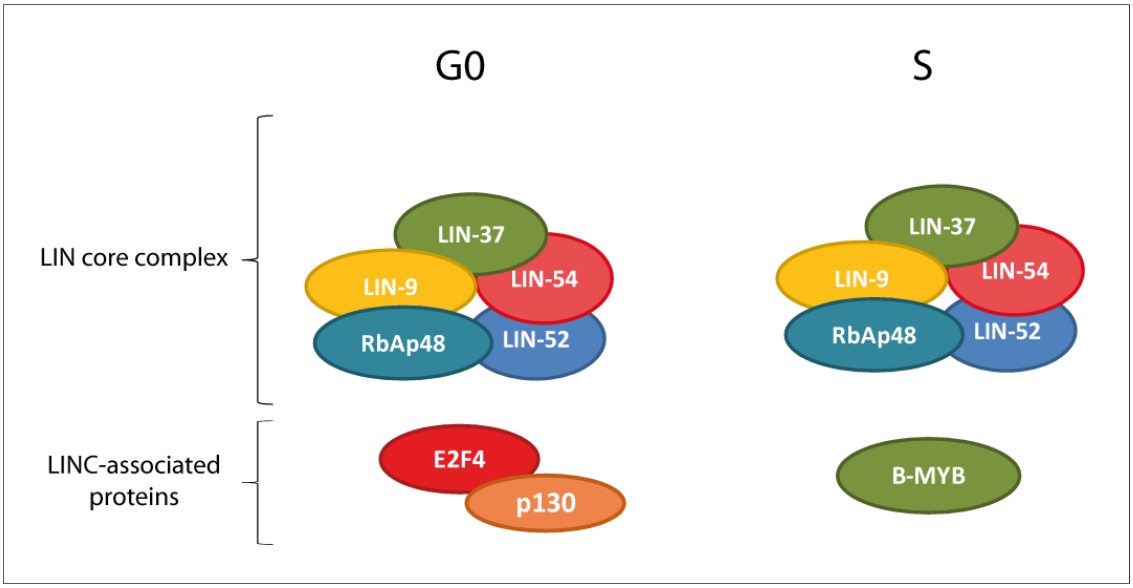

Figure 1.4: LINC composition in G0 or S phase

The LIN core complex consists of 5 different proteins, LIN-37, LIN-54, LIN-52, LIN-9 and RbAp48. Dependent on the cell cycle phase, either E2F4 and p130 (G0 phase) or B-MYB (S phase) can associate to LINC.

The human LIN complex is evolutionary conserved and homologues to dREAM/Myb-MuvB (*Drosophila melanogaster*) and DRM (*Caenorhabditis elegans*), both involved in regulation of developmental genes. In *D. melanogaster* a dREAM/Myb-MuvB complex was purified in 2004 which contains one of the two Drosophila pRb proteins (RBF1 or RBF2), the repressor E2F (dE2F2), p55CAF1, dMYB (related to B-MYB) and the 3 Myb-interacting proteins Mip40, Mip120 and Mip130 (Korenjak, Taylor-Harding et al. 2004; Lipsick 2004; Korenjak and Brehm 2005). Depletion by RNAi showed that this complex is involved in repression of developmental genes. In *C. elegans* the synMuv class B genes negatively regulate vulva development and are highly related to the subunits of a dREAM/Myb-MuvB complex in *D. melanogaster*. The different composition of dREAM-like complexes in *D. melanogaster*, *C. elegans* and *H. sapiens* are summarized in Figure 1.5.

Drosophila melanogaster			C.elegans	Homo sapiens	
(Lewis, Beall et al. 2004) 2004	(Korenjak, Taylor-Harding et al. 2004) 2004	(Beall, Manak et al. 2002) 2007	(Harrison, Ceol et al. 2006) 2006	**LINC** (Litovchick, Sadasivam et al. 2007; Schmit, Korenjak et al. 2007) **dREAM** (Litovchick, Sadasivam et al. 2007) 2007	
Myb/MuvB	**dREAM**	**tMAC**	**DRM**	**G0**	**S**
mip130	mip130	Aly	Lin-9	LIN-9	LIN-9
mip40	mip40	mip40	Lin-37	LIN-37	LIN-37
dLin-52			Lin-52	LIN-52	LIN-52
mip120	mip120	Tomb	Lin-54	LIN-54	LIN-54
p55	p55	p55	Lin-53	RbAp48	RbAp48
dDP	dDP		dpl-1	DP	DP
dE2F2	dE2F2		Efl-1	E2F4	
RBF1/2	RBF1/2		Lin-35	p130	(p107)
dMyb	dMyb				B-MYB
Rpd-3					
L(3)MBT					

Figure 1.5: Summary of pRb/E2F complexes in different species

The complexes are highly related to each other showing them to be evolutionary conserved (Korenjak, Taylor-Harding et al. 2004; Lewis, Beall et al. 2004; Harrison, Ceol et al. 2006; Beall, Lewis et al. 2007). p107 is part of LINC (Schmit, Korenjak et al. 2007) but not part of the human dREAM complex (Litovchick, Sadasivam et al. 2007) (adapted and modified from (Schmit, Korenjak et al. 2007)).

Co-immunoprecipitations from cells overexpressing different combinations of the human LINC members showed that all the tested proteins (LIN-9, LIN-52, LIN-54, LIN-37 and RbAp48) interact with each other (Schmit, Korenjak et al. 2007). Additionally, endogenous binding of all LINC components was demonstrated. Using biochemically purified nuclear cell extracts Schmit and colleagues found that LIN-9, LIN-37, LIN-54, B-MYB and RbAp48 co-fractionated over six chromatography columns. The proteins perfectly overlapped in the same fractions when checking the final eluates, strongly suggesting that they interact. In contrast, p107 only partly coeluted with components of the LIN complex. Additionally, p107 eluted in different fractions, suggesting that p107 is, beyond binding to LINC, also associated to other proteins and/or complexes.

By yeast-two-hybrid assays and GST-pulldown assays, Schmit and colleagues showed that LIN-9 directly interacts with LIN-52 and RbAP48. LIN-37 and LIN-54 did not bind directly to any other LINC component in yeast, suggesting that they have to be modified to enable binding to LINC members which probably cannot take place in yeast (Schmit, Korenjak et al. 2007).

LIN-9, a component of the LIN core complex, was first described as a DNA binding protein which interacts with pRb (Gagrica, Hauser et al. 2004). Gagrica and colleagues could show that LIN-9 acts in the pRb pathway to promote differentiation by flat cell formation in Saos-2 cells. Importantly, LIN-9 is not involved in pRb-mediated cell cycle arrest; neither in HeLa nor in Saos-2 cells. Together with pRb, LIN-9 is involved in transcriptional activation of genes important for differentiation. In contrast, pRb-mediated repression as well as E2F dependent transactivation was not significantly affected by LIN-9. Additionally, LIN-9 was shown to inhibit transformation and can substitute for the loss of pRb in oncogenic transformation (Gagrica, Hauser et al. 2004).

In zebrafish, LIN-9 is expressed throughout the embryonic development. Since LIN-9 depleted embryos have slightly smaller heads and eyes, pericardial edema and a strong trunk curvature, it seems that LIN-9 is essential for embryonic development in zebrafish. In vivo, LIN-9 depletion leads to an increase of cells with a G2/M DNA content and therefore seems to be involved in embryonic cell cycle regulation. Additionally, in LIN-9 morphant brains, apoptosis and an accumulation of mitotic cells was detectable. Via microarray experiments using LIN-9 depleted cells it was shown, that LIN-9 regulates a cohort of genes required for mitosis in zebrafish, e.g. cdc2, plk1 and cdc20 (Kleinschmidt, Wagner et al. 2009).

1.3.1 LINC in target gene activation

Transcriptional activation of many E2F-target genes is delayed during cell cycle progression (G2/M genes such as Aurora A, Plk1 and cyclin B) compared to the early E2F-responsive genes (G1/S genes such as PCNA, cdc6 and RR1). Recently, we showed that in human cells the delayed expression of a set of E2F target genes responsible for G2/M transition (G2/M genes) is dependent on the

function of LINC together with the associated protein B-MYB (Fig. 1.6) (Schmit, Korenjak et al. 2007).

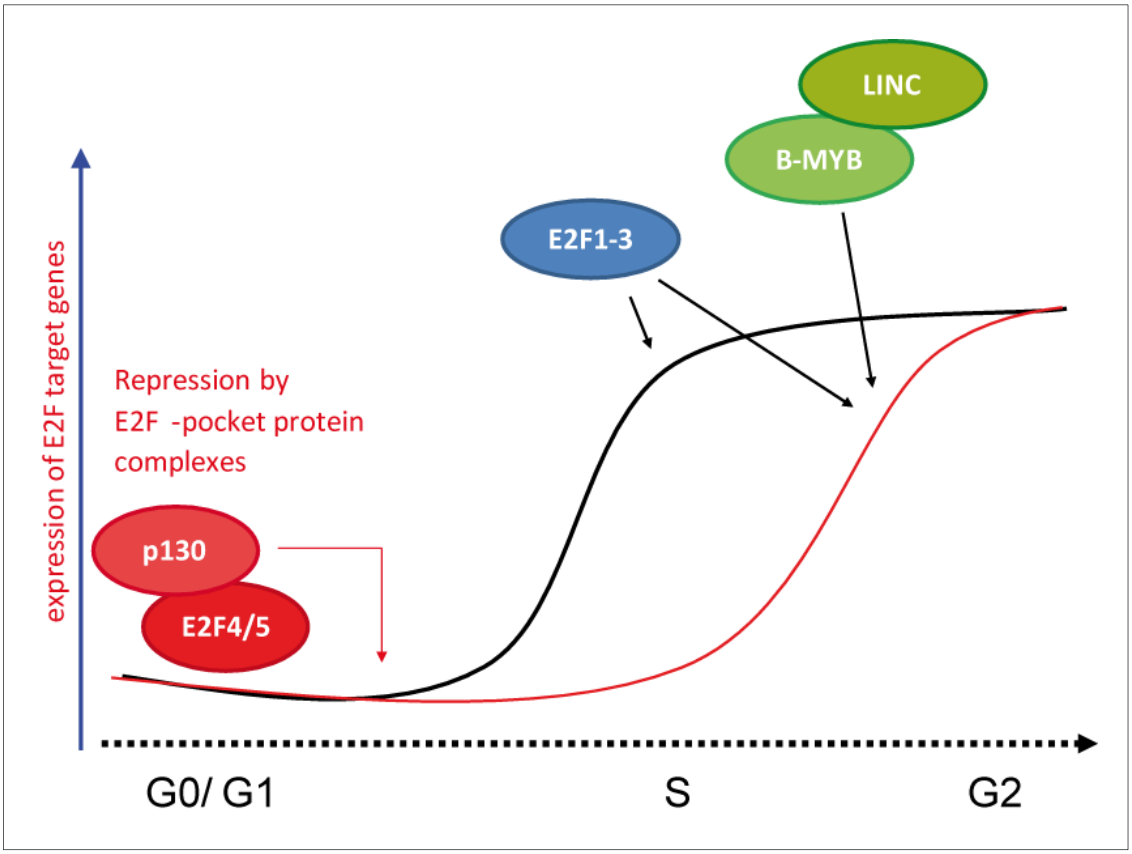

Figure 1.6: Illustration of E2F target gene expression during cell cycle

E2F target genes are expressed in two "waves" during cell cycle progression. First, gene expression is repressed in G0/G1 phase by repressive E2F-pocket protein complexes (E2F4/5-p130). During G1/S transition E2F1-3 activate target gene expression (black curve) and thereby enable the cells to enter S phase. Genes essential for further cell cycle progression, entry into mitosis and chromosome segregation are expressed delayed and additionally need association of LINC and B-MYB for transcriptional activation.

The important role of LINC in activating G2/M gene expression was shown by depletion of different LINC components, e.g. LIN-9. Microarray analyses after depletion of LIN-9 showed that G2/M gene expression, normally activated during S phase, is decreased leading to an arrest in the G2/M phase of the cell cycle (Osterloh, von Eyss et al. 2007; Schmit, Korenjak et al. 2007). Similarly to depletion of LIN-9, depletion of LIN-54 and LIN-52 leads to a decrease in G2/M gene expression (Schmit, Korenjak et al. 2007). Therefore, regulation of G2/M gene expression is not an isolated function of LIN-9 but is mediated by its cooperation with the other components of the LIN complex. Solely depletion of LIN-37 showed no change in G2/M gene expression, suggesting that LIN-37 is

not required for G2/M gene activation. Target genes of LINC are summarized in Figure 1.7.

Unigene ID	symbol	name	function
Hs. 93002	UBCH10	Ubiquitin-conjugating enzyme E2C	exit of mitosis
Hs. 514527	BIRC5	Baculoviral IAP repeat-containing 5 (Survivin)	mitotic checkpoint
Hs. 334562	CDC2	Cell division cycle 2	entry into mitosis
Hs. 14559	Cep55	Centrosomal protein, 55 kDa	cytokinesis
Hs. 58974	CCNA2	Cyclin A2	entry into S- and M-phase
Hs.23960	CCNB1	Cyclin B1	entry into mitosis
Hs. 75573	CENPE	Centromere protein E	mitotic spindle checkpoint
Hs. 469649	BUB1	Budding uninhibited by benzimidazoles 1	spindle checkpoint
Hs. 250822	AURKA	Serine/threonine kinase 6; Aurora A	mitotic spindle
Hs. 592049	PLK1	Polo-like kinase 1	entry into mitosis

Figure 1.7: List of important LINC target genes

Summary of downregulated G2/M genes in LIN-9 depleted BJ cells (adapted from (Osterloh, von Eyss et al. 2007)). In the text cdc2 is also referred to as cdk1.

By Chromatin-immunoprecipitations (ChIP) Schmit and colleagues showed that the ability of LINC to regulate gene expression seems to be dependent on its binding to target gene promoters. Proteins of the LIN core complex bind constantly to the promoters of target genes during G0 and S phase. In contrast, promoter binding of LINC-associated proteins like E2F4 and B-MYB differs during cell cycle progression.

The activating properties of LINC during S phase are probably at least partially due to its binding partner B-MYB, which is a known transcription factor involved in transcriptional activation of G2/M genes. Until now, it is unknown if LINC function involves the co-activation of gene expression by recruitment of chromatin modifying proteins or solely by recruitment of B-MYB to target gene promoters.

1.3.1.1 B-MYB

B-MYB is a ubiquitously expressed transcription factor known to induce genes necessary for cell cycle progression, e.g. cyclin A. B-MYB, like its family members A-MYB and C-MYB, is able to bind to the consensus DNA sequence C/TAACNG. In the absence of co-factors, B-MYB is a poor transcriptional activator probably due to the binding of co-repressors like N-COR or SMRT, which maintain B-MYB in a repressed state (Li and McDonnell 2002). During S phase, B-MYB is phosphorylated by cyclinA-cdk2 complexes, leading to its full activation but also to the induction of accelerated protein turnover by ubiquitination and subsequent proteasome-induced degradation (Ziebold, Bartsch et al. 1997; Johnson, Schweppe et al. 1999; Charrasse, Carena et al. 2000; Sala 2005). Additionally, other transcriptional co-factors bind to B-MYB to either enhance or repress its transcriptional activity, e.g. cyclinD1, PAPR1 or CBP/p300. PARP1 for example, binds to B-MYB as a co-activator dependent on the integrity of cdk2 phosphorylation sites on B-MYB (Santilli, Cervellera et al. 2001). In contrast, cyclin D interacts with the B-MYB transcriptional domain thereby suppressing B-MYB transactivation by interfering with CBP/p300 (Horstmann, Ferrari et al. 2000). A hypothesis is that cyclin D holds B-MYB inactive during G1 until cyclin D itself is destroyed in late G1, thereby coordinating B-MYB with the cell cycle. Activation of B-MYB then induces transcription of its target genes in S or later cell cycle phases. Before, it was already assumed that pocket proteins like p107 or p130 maintain a repressed state of the “B-MYB complex” until further cell cycle progression induced detachment of pocket protein family members, enabling the transcriptional activation of target genes (Sala 2005). Depletion of B-MYB in human fibroblasts by RNAi leads to a partial arrest in the G2/M phase and apoptosis showing the importance of B-MYB for G2/M gene expression (Santilli, Cervellera et al. 2001). Our recent data showed that B-MYB together with LINC regulates transcriptional activation of genes essential for G2/M transition, such as cdk1 and cyclin B1, during the S phase (Schmit, Korenjak et al. 2007).

1.3.2 LINC in target gene repression

Furthermore, LINC target genes are known to be down regulated during G0/G1 phase of the cell cycle and additionally after activation of the DNA damage-induced G2/M checkpoint (cyclinA2, cyclinB1, cdk1 (cdc2) and Plk1). Since LINC also binds to G2/M gene promoters during G0, a function for LINC in repressing G2/M gene expression was assumed. But so far, the involvement of LINC in the repression of gene expression is controversial. Litovchick and colleagues showed that depletion of LINC components led to the de-repression of G2/M gene expression in G0 (Litovchick, Sadasivam et al. 2007). In contrast, Schmit and colleagues showed that depletion of LINC components only lead to a decreased G2/M gene expression in S phase but has no impact on the repression of target gene expression in G0 (Schmit, Korenjak et al. 2007). Probably this difference is due to the different setup of the experiments. Both groups used the same cell line but in contrast to Schmit and colleagues, Litovchick and colleagues first depleted components of the LIN complex and then starved the cells by serum-starvation. Therefore, LINC may play a role in establishing the repressive state but is not essential for its maintenance (Litovchick, Sadasivam et al. 2007; Schmit, Korenjak et al. 2007).

Still, the mechanisms leading to LINC-dependent activation or repression of gene expression as well as the mechanisms leading to the change in LINC composition during cell cycle progression are unknown.

1.4 Aim of this project

From previous studies we know that LINC plays an important role in transcriptional activation of genes essential for G2/M transition (Osterloh, von Eyss et al. 2007; Schmit, Korenjak et al. 2007). Since it is known that down regulation of a similar set of genes is essential for sustained G2 arrest after DNA damage (see 1.2.2), the goal was to analyze whether LINC plays a role in regulating the DNA damage response.

Because it is known that LINC composition changes when cells progress through the cell cycle, the aim of this project was to test whether LINC composition differs when comparing normal growing and DNA damaged cells.

The second important goal was to analyze the impact of LINC on G2/M gene expression after DNA damage induction. Additionally, the pathway leading to a decrease in G2/M gene expression after DNA damage was analyzed in more detail.

Third, because p53 deficient cells prematurely exit the DNA-damage mediated G2 arrest, it was analyzed whether LINC together with B-MYB also function in this process.

The final question was whether B-MYB expression levels correlate with the p53 status in human tumors.

2 Materials and methods

2.1 Materials

2.1.1 Chemical stocks

Unless indicated otherwise, commonly used chemicals were purchased from Applichem, Invitrogen, Roth and Sigma with analysis quality.

	Stock concentration
Ammonium Persulfate (APS)	10 % in H_2O
Ampicillin	100 mg/ml in H_2O
Bovine serum albumin (BSA)	20 mg/ml in H_2O
dNTP Promega or Invitrogen	2 mM dATP, dCTP, dGTP dTTP each
Doxorubicin	1.7 mM
Ethidium bromide	10 mg/ml in H_2O
Luminol	250 nM in DMSO
Nocodazole	3.31 mM
ONPG	6 mg/ml in H_2O
p-Coumaric acid	90 nM in DMSO
Phenylmethylsulphonyl fluoride (PMSF)	10 mg/ml in isopropanol
Ponceau S solution	0.1 % Ponceau S in 5% acetic acid
Propidium Iodide (PI)	1 mg/ml in H_2O
Proteinase K	10 mg/ml in 50 mM Tris pH 8.0 / 1 mM $CaCl_2$
Random Primer	500 µg/ml in H2O
RNaseA	10 mg/ml in 10 mM Tris pH 7.4 / 150 mM NaCl
Salmon sperm ssDNA	10 mg/ml in H_2O
Sodium dodecyl sulfate (SDS)	10 % (w/v) in H_2O
Thymidine	200 mM in H_2O

2.1.2 Buffers

2.1.2.1 General buffers

5 x DNA loading buffer	15 % Ficoll 0.05 % Bromphenol blue 0.05 % Xylene Cyanol 0.05 M EDTA in 1 x TAE
2 x HBS	280 mM NaCl 1.5 mM Na_2HPO_4 50 mM HEPES-KOH, pH 7.05
Luria Bertani (LB) Agar	40 g powder in 1 l H_20, autoclave
Luria Bertani (LB) Medium	25 g powder in 1 l H_20, autoclave
Phosphate buffered saline (PBS)	13.7 mM NaCl 0.3 mM KCl 0.64 mM Na_2HPO_4 0.15 mM KH_2PO_4 adjust pH to 7.4 with HCl
Protease inhibitors (PI) Stock concentrations	0.1 mg/ml Aprotinin 10 mg/ml AEBSF 0.5 mg/ml Bestatin 0.5 mg/ml E64 1 mg/ml Leupeptin 0.1 mg/ml Pepstatin
RNA Isolation reagent	Thermo Fisher Scientific

TAE (1 x)	40 mM Tris base 5 mM glacial acetic acid 10 mM EDTA, pH 8.0
TBS (1 x)	50 mM Tris-HCl, pH 7.4 150 mM NaCl
TE	10 mM Tris, pH 7.5 1 mM EDTA, pH 8.0 in H_2O

2.1.2.2 Buffers for whole-cell lysates

TNN buffer	50 mM Tris, pH 7.5 120 mM NaCl 5 mM EDTA, pH 8.0 0.5 % NP-40 10 mM $Na_4P_2O_7$ 2 mM Na_3VO_4 100 mM NaF Protease inhibitors (PI) 1:100 (add freshly) PMSF 1:200 (add freshly)
Bradford solution	50 mg Coomassie Brillant Blue G250 23.75 ml ethanol 50 ml 85 % (v/v) o-Phosphoric acid ad 500 ml ddH_2O filter twice

2.1.2.3 Buffers for immunoprecipitation and immunoblotting

Coomassie staining solution	250 ml methanol 35 ml acetic acid 1 g Coomassie Blue R-250 ad 500 ml H_2O

Destain	250 ml methanol 35 ml acetic acid ad 500 ml H_2O
Acrylamide solution for SDS gels	30 % (w/v) Acrylamide 0.8 % (w/v) N,N´-Methylenbisacrylamide
SDS running buffer	576 g Glycine 120 g Tris 40 g SDS ad 4 l H_2O
Blotting buffer (1 x)	0.6 g Tris base 2.258 g Glycine 150 ml methanol ad 1 l H_2O
Blocking solution	3 % (w/v) milk powder in TBST
3 x Electrophoresis sample buffer (3 x ESB)	300 mM Tris-HCl pH 6.8 15 mM EDTA 150 mM DTT 12 % (w/v) SDS 15 % (w/v) glycerol 0.03 % (w/v) bromphenol blue
TBS (1x)	50 mM Tris, pH 7.5 150 mM NaCl Adjust to pH 7.4
TBST	0.05 % Tween in 1x TBS

Substrate solution	10 ml 100 mM Tris-HCl pH 8.5
	50 µl 250 mM Luminol
	22 µl 90 mM p-coumaric acid
	3 µl 30 % H_2O_2

2.1.2.4 Buffers for chromatin immunoprecipitation

Cell lysis buffer	5 mM PIPES, pH 8.8
	85 mM KCl
	0.5 % NP-40
Nuclei lysis buffer	50 mM Tris, pH 8.1
	10 mM EDTA
	1 % SDS
IP dilution buffer	0.01 % SDS
	1.1 % Triton
	1.2 mM EDTA
	16.7 mM Tris, pH 8.2
	167 mM NaCl
Elution buffer	50 mM Tris, pH 8.0
	1 % SDS
	10 mM EDTA
LiCl wash buffer	0.25 M LiCl
	0.5 % NP-40
	0.5 % Sodium deoxycholate (DOC)
	1 mM EDTA
	10 mM Tris, pH 8.0
Blocking buffer	3 ml IP-dilution buffer
	150 µl BSA (20 mg/ml)
	30 µl ssDNA (10 mg/ml)

2.1.2.5 Buffers for flow cytometry (FACS) analysis

Sodium citrate	38 mM in H_2O
1 x binding buffer	10 mM HEPES, pH 7.4 0.14 M NaCl 2.5 mM $CaCl_2$
Incubation buffer	0.5 g BSA ad 100 ml 1 x PBS

2.1.3 Antibodies

2.1.3.1 Primary antibodies

Antibody against	Company	Origin	Application	Dilution	Internal number
LIN-9	Not commercially available	Rabbit polyclonal serum (Osterloh, von Eyss et al. 2007)	IP	1:50	# 136
			WB	1:500	# 137
			ChIP	40 µg	# 136 affinity purified
LIN-37	Not commercially available	Rabbit polyclonal serum (Schmit, Korenjak et al. 2007)	IP	1:50	# 131
			WB	1:500	
LIN-54	Not commercially available	Rabbit polyclonal serum (Schmit, Korenjak et al. 2007)	IP	1:50	# 129
			WB	1:500	

p130 (C-20)	Santa Cruz Sc-317	Rabbit polyclonal (100 µg/ml)	WB	1:1000	# 33
			ChIP	4 µg	
E2F4 (C-20)	Santa Cruz Sc-866	Rabbit polyclonal (200 µg/ml)	WB	1:1000	# 6
			ChIP	4 µg	
B-MYB (N-19) (N-19-X)	Santa Cruz Sc-724 Sc-724	Rabbit polyclonal	IP	1:100	# 79
			WB	1:1000	# 79
			ChIP	10 µg each	# 159 # 79
β-Tubulin (D-10)	Santa Cruz Sc-5274	Mouse monoclonal	WB	1:2500	# 161
p107 (C-18)	Sc-318	Rabbit polyclonal (100 µg/ml)	WB	1:1000	# 32
p21 (OP64)	Calbiochem	Mouse monoclonal	WB	1:1000	# 146
IgG (I5006)	Sigma	Rabbit polyclonal (1 mg/ml)	ChIP	4 µg	# 104
Phospho-H3-Alexa Fluor 488 (AB # 9708)	Cell signalling	Mouse monoclonal	FACS	1:10 in 100 µl for 1 x 10^5 cells	
Annexin-V-FITC #556419	BD Bioscience	Protein linked to FITC	FACS	1:20 in 100 µl for 1 x 10^5 cells	

2.1.3.2 Secondary antibodies

Antibody against	Company	Application	Dilution
Anti-mouse IgG HRP linked	GE Healthcare NXA931	WB	1:5000
Protein A HRP linked	GE Healthcare NA9120	WB	1:5000

2.1.4 Primers

Unless otherwise indicated primers were intended for human sequences and purchased from Metabion or Roth.

2.1.4.1 Primers for quantitative real time PCR

Primer number	Sequence	Application	
SG 645	GCCCAATACGACCAAATCC	GAPDH	sense
SG 646	AGCCACATCGCTCAGACAC		antisense
SG 620	GGCAGACCGAGATGAATCCTCA	S14	sense
SG 621	CAGGTCCAGGGGTCTTGGTCC		antisense
SG 956	TGGAGAACTTGGAAATGGAAA	PCNA	sense
SG 957	GAACTGGTTCATTCATCTCTATGG		antisense
SG 628	TCACTGTCTTGTACCCTTGTGC	p21	sense
SG 629	GGCGTTTGGAGTGGTAGAAA		antisense
SG 570	GGAGAACGCTCTGTCAGCA	BUB-1	sense
SG 571	TCCAAAAACTCTTCAGCATGAG		antisense
SG 680	AAGATCTGGAGGTGAAAATAGGG	Plk1	sense
SG 681	AGGAGTCCCACACAGGGTCT		antisense
SG 574	CGCCTGAGCCTATTTTGGT	cyclin B1	sense
SG 575	GCACATCCAGATGTTTCCATT		antisense
SG 572	GGTACTGAAGTCCGGGAACC	cyclin A2	sense
SG 573	GAAGATCCTTAAGGGGTGCAA		antisense
SG 576	TGGATCTGAAGAAATACTTGGATTCTA	cdc2 (cdk1)	sense
SG 577	CAATCCCCTGTAGGATTTGG		antisense

SG 568	GCCCAGTGTTTCTTCTGCTT	Birc5	sense
SG 569	CCGGACGAATGCTTTTTATG		antisense
SG 590	TGCCGAGCTCTGGAAAAA	Ubch10	sense
SG 591	AAAAGACGACACAAGGACAGG		antisense
SG 630	TCCACACTGCCCAAGTCTCT	B-MYB	sense
SG 631	AGCAAGCTGTTGTCTTCTTTGA		antisense
SG 580	CCCCACCACGGTTACATTAT	LIN-9	sense
SG 581	CGGCGACTGTCCTAATAAAGG		antisense

2.1.4.2 Primers for chromatin immunoprecipitation

Primer number	Sequence	Application	
SG 540	GGCAGCAAGAGTCACTCCA	GAPDH2	sense
SG 541	TGTCTCTTGAAGCACACAGGTT		antisense
SG 781	CTGGCTGCTGCGCGA	PCNA	sense
SG 782	CACCACCCGCTTTGTGACT		antisense
SG 548	AGTGAGTGCCACGAACAGG	cyclin B1	sense
SG 549	GCCAGCCTAGCCTCAGATTT		antisense
SG 924	GGAATCTCGATGTAAACACAATATCA	Cdc2	sense
SG 925	TGTTCGCTCCGTTCTTCTTT	(cdk1)	antisense
SG 612	CCATTAACCGCCAGATTTGA	Birc5	sense
SG 613	GCGGTGGTCCTTGAGAAAG		antisense
SG 552	GCCCTTTAATGGTTAGCGTTT	Ubch10	sense
SG 553	GCTGCCATTAACTAACGAATCC		antisense

2.1.5 siRNA sequences

Unless otherwise indicated siRNA Oligos were purchased from MWG or Dharmacon.

siRNA against	Sequence	Target	Internal number
LIN-9	GGAAGAGAGATCAGCATTA	(Schmit, Korenjak et al. 2007)	Lin-9.4

B-MYB	GCAGAGGACAGTATCAACA	{1165-1183}	B-MYB.5
Ctrl	TAGCGACTAAACACATCAA	non targeting	Ctrl.1

2.1.6 Cell lines, cell culture media and treatment

DMEM (4.5 g Glucose/L-Glutamine)	Cambrex
Penicillin/Streptomycin (10 U/µl each)	Cambrex
Trypsin (EDTA) (200 mg/l)	Cambrex
Foetal Bovine Serum (FCS)	Invitrogen

HCT-116 wt, HCT-116 p53 negative, HCT-116 p21 negative, MCF-7, T98G and U2OS cells were cultured in DMEM with 10 % FCS and 1 % PenStrep.

2.1.7 Markers

1 Kb DNA Ladder	Fermentas
SDS Page Ruler Mix	Fermentas

2.1.8 Kits

Jetstar Plasmid Purification Midi/Maxi Kit	Genomed
Plasmid Mini/Midi/Maxi Kit	Promega
Plasmid Midi/Maxi Kit	Invitrogen
QIAquick PCR Purification Kit	Qiagen
Absolute QPCR SYBR Green Mix	Thermo Fisher Scientific

2.1.9 Beads

Protein A Sepharose	Pierce
Protein G Sepharose	Pierce

2.2 Methods

2.2.1 Cell culture

2.2.1.1 Passageing of cells

Eukaryotic cells were cultivated in tissue culture incubator at 37 °C and 5 % CO_2. For passageing, the cells were washed once with 1 x PBS and briefly incubated with trypsin/EDTA at 37 °C. The detached cells were then plated on new cell culture dishes.

2.2.1.2 Transient transfection

U2OS, 293T and HeLa cells were transfected using calcium phosphate. To do so, 20 – 40 µg plasmid DNA was mixed with 50 µl of 2.5 M $CaCl_2$ and ddH_2O to a final volume of 500 µl. 500 µl 2 x HBS was bubbled while the DNA/$CaCl_2$ mixture was added drop wise. This solution was slowly added to the plated cells. After 12 – 18 h the cells were washed with 1 x PBS and left growing another 24 – 36 h in normal medium.

HCT-116 (wt, p21-/-, p53-/-) cells were transfected using Oligofectamine (Invitrogen) or Metafecten (Biontex) according to the manufacturer's protocol.

2.2.1.3 Synchronization of U2OS cells by thymidine

For synchronization, 5 x 10^5 U2OS were plated on a 10 cm plate. 24 h later cells were treated with 2.5 mM thymidine for 6 h. The cells were then arrested at the G1/S border of the cell cycle and could be released into the cell cycle by washing twice with 1 x PBS and adding 10 % FCS medium.

2.2.1.4 Treatment

For treatment, either 1 x 10^5 cells were plated in a 6-well-dish or 5 x 10^5 cells on a 10 cm plate. After 24 h, cells were treated with 1 µM doxorubicin for 2 h, afterwards washed twice with 1 x PBS and left growing in normal medium. When cells were additionally treated with 1 µM nocodazole, it was added to the medium after the doxorubicin removal and PBS washing step.

2.2.1.5 Cell cycle phases: flow cytometry (FACS)

For FACS measurement, the cells were harvested by trypsinization and centrifuged for 10 – 20 min at 1200 rpm and 4 °C. After washing the pellet with 1 x PBS, the cells were fixed with 80 % ethanol. Fixation was performed at -20 °C over night. The next day, cells were again washed with 1 x PBS and incubated with 100 µg/ml RNAse A in 38 mM sodium citrate for 30 min at 37 °C. The cells were stained by addition of 30 - 50 µl propidium-iodide [1 mg/ml] for 10 -15 min at room temperature (RT) and measured by FACS.

In order to determine the fraction of cells in M phase, cells were stained with propidium-iodide and an antibody specific for phospho-histone H3 (Ser10). Cells were harvested by trypsinization, washed in 1 x PBS and fixed in 2 % paraformaldehyde in 1 x PBS for 10 min at 37 °C. After 1 min on ice the cells were permeabilized for 30 min at 4 °C by adding 90 % ice cold methanol and stored at -20 °C over night. 5 x 10^5 cells were washed with 3 ml incubation buffer, resuspended in 90 µl incubation buffer and blocked for 10 min at room temperature (RT). By addition of 10 µl phospho-histone H3 (Ser10) antibody the cells were stained for 1.5 – 2 h at room temperature (RT) in the dark. After a second washing step with incubation buffer, cells were incubated with 50 µg/ml PI and 0.7 mg/ml RNaseA for 30 min at 37°C and analyzed by FACS to determine the fraction of phospho-histone H3 positive cells.

Apoptotic cells were stained with propidium-iodide and FITC-coupled Annexin-V. Therefore, cells were harvested by trypsinization, washed twice with 1 x PBS and resuspended in 1 x binding buffer resulting in a concentration of 1 x 10^6 cells/ml. 100 µl cell solution were stained by addition of 5 µl Annexin-V-FITC and 10 µl PI [50 µg/ml] for 30 min at RT in the dark. After addition of 400 µl 1 x binding buffer, the fraction of apoptotic cells was determined by FACS analysis.

2.2.2 Expression analysis

2.2.2.1 RNA Isolation

RNA was isolated from cells using a RNA isolation reagent from Thermo Fisher Scientific. After removing the medium from the cell culture plate, 0.5 – 1 ml reagent was added onto the plate and cells were scraped into reaction tubes.

100 – 200 µl chloroform was added and vortexed for 15 s. The samples were centrifuged at 12000 rcf for 30 min at 4 °C and the upper aqueous phase was transferred to a new reaction tube. RNA was precipitated with 500 µl isopropanol at 12000 rcf for 30 min at 4 °C. The pellet was washed with 70 – 80 % ethanol and resuspended in 20 – 25 µl RNaseA-free water.

2.2.2.2 Reverse transcription

1 – 2 µg RNA were mixed with 0.5 µl random primer [0.5 µg/µl] and brought to 9.5 µl with water. After incubation at 70 °C for 5 min, the samples were left for 1 min at 4 °C and then mixed with 5 µl M-MLV 5 x reaction buffer, 6.25 µl dNTPs [2mM], 0.5 µl Ribolock RNase inhibitor [40 U/µl], 0.5 µl M-MLV-RT [200U] and 2.75 µl H_2O. For cDNA synthesis, the samples were incubated at 37 °C for 60 min and then inactivated for 15 min at 70 °C.

2.2.2.3 qRT-PCR

To determine the amount of a specific mRNA compared to a housekeeping gene, the following reaction was prepared:

12.5 µl Absolute Q-PCR Sybr Green Mix

10.5 µl H2O

1 µl fw / rev primer mix (10 pmol/µl each)

1 µl cDNA or precipitated Chromatin

PCR program (40 cycles):

95 °C 15 min

95 °C 15 s

60 °C 1 min

The relative expression of a gene compared to a housekeeping gene was calculated with this formula: $2^{-\Delta\Delta Ct}$

with $\Delta\Delta Ct = \Delta Ct$ (sample) – ΔCt (reference)

and ΔCt = Ct(gene of interest) – Ct (housekeeping gene)

The standard deviation of ΔΔCt was calculated with $s=\sqrt{(s_1^2+s_2^2)}$

with s_1 = standard deviation (gene of interest)

and s_2 = standard deviation (housekeeping gene)

The margin of error for $2^{-\Delta\Delta Ct}$ was determined by this formula:

$$2^{-\Delta\Delta Ct +/-s}$$

and the error used for the error bars was calculated with:

$$error = 2^{-\Delta\Delta Ct +s} - 2^{-\Delta\Delta Ct}$$

Values in chromatin immunoprecipitations are shown as % of input:

$$\% \text{ input} = 2^{\text{Ct (1\% Input)} - \text{Ct (IP)}}$$

Standard deviation, error margins and error were calculated as shown above.

2.2.3 Biochemical methods

2.2.3.1 Whole cell lysates

MCF-7, HCT-116 and U2OS were scraped with PBS and centrifuged for 5 min at 3000 rpm and 4 °C. The pellet was lysed for 20 min on ice using 10 times its amount of TNN buffer (with freshly added PI [1:100] and PMSF [1:200]). The lysates were spinned at 14000 rpm for 10 min at 4 °C. The supernatant was transferred in a new reaction tube and kept on ice until subsequent processing.

2.2.3.2 Protein concentration

Protein concentration was measured with Bradford solution on the basis of a known BSA straight calibration line as described by Bradford (Bradford 1976). 5 µl of the whole lysate were mixed with 1 ml Bradford solution and extinction was measured at 595 nm and compared to a standard BSA dilution series.

2.2.3.3 Immunoprecipitation

For immunoprecipitation 1 – 2 mg of the whole cell lysate was used and incubated with the desired antibody over night on a rotating wheel at 4 °C. After

addition of 40 µl beads (protein-A-sepharose for polyclonal and protein-G-sepharose for monoclonal antibodies), the mixture was left on a rotating wheel for another 1 h at 4 °C. The beads were washed 5 times with TNN buffer and drained with a Hamilton syringe. 30 µl 3 x ESB buffer was added and boiled at 95 °C for 5 min. Optional the samples were stored at – 20 °C.

In parallel, 10 - 20 % of the protein amount used for immunoprecipitation was boiled with 3 x ESB at 95 °C for 5 min and optional stored at -20 °C.

2.2.3.4 SDS-polyacrylamide gel electrophoresis

SDS-PAGE analysis was performed using the discontinous method (Laemmli, 1970). For electrophoretic separation, an 8 – 14 % SDS-acrylamide gel was prepared and after polymerization, a stacking gel was poured on the top. The gels were prepared as follows:

Separating gel (10 %):	Stacking gel (5 %)
5 ml Acrylamid/Bisacrylamid	1.6 ml Acrylamid/Bisacrylamid
3.7 ml 1.5 M Tris/HCl pH 8.8	1.4 ml 0.5 M Tris/HCl pH 6.8
75 µl 20 % SDS	50 µl 20 % SDS
10 µl TEMED	10 µl TEMED
100 µl 10 % APS	50 µl 10 % APS
6.1 ml H_2O	6.9 ml H_2O

Electrophoresis was carried out for 1 h at 35 mA/gel. The gels were then used for immunoblotting.

2.2.3.5 Immunoblotting

The transfer of proteins from the gel to a PVDF membrane was done via electroblotting using a BioRad Wet Blot gadget. The PVDF membrane was incubated in methanol for 1min and then rinsed in blotting buffer. The membrane was placed onto a layer of blotting buffer soaked Whatman filter papers. The gel was applied onto the membrane and another soaked Whatman filter paper was placed on the top. This “sandwich” was enclosed by two sponges and put into a BioRad Wet Blot gadget filled with 1 x blotting buffer. Blotting was carried out for 2 h at 300 mA. The equal and complete transfer was

checked by staining the membrane with Ponceau S staining solution and subsequent rinsing with H_2O.

For blocking, the membrane was transferred in blocking solution and incubated at RT for 30 min to 2 h. The desired antibodies were added to fresh blocking solution in the required dilution and incubated with the membrane over night at 4 °C. After washing the membrane 3 times with TBST for 5 – 10 min, it was incubated with the appropriate secondary HRP-conjugated antibodies for 2 h at RT. The membrane was washed 3 times for 5 - 10 min with TBST and specific bands were then detected using a Luminol-substrate-solution. Finally, the membrane was wrapped in plastic foil and exposed to an ECL- or X-Ray-film.

2.2.3.6 Affinity purification of polyclonal antisera

For chromatin immunoprecipitation self-made polyclonal antibodies had to be affinity purified. To do so, 1 ml protein-A-sephrose beads were packed into a column and washed with 20 ml 10 mM Tris/HCl pH 7.5. 1ml antibody serum was diluted in 10 ml 20 mM Tris/HCl pH 7.5, added onto the beads and incubated on a rotating wheel for 30 min to 1 h at RT. After discarding the flow-through, the beads were first washed with 20 ml 10 mM Tris/HCl pH 7.5, second with 20 ml 10 mM Tris/HCl pH 7.5 / 500 mM NaCl and third with 20 ml 10 mM Tris/HCl pH 7.5. For elution, 50 µl Tris/HCl pH 8.0 were provided into multiple reaction tubes in which the different antibody fractions were eluted using 500 µl of 100 mM glycin pH 2.5 for each fraction. 20 µl of each fraction was mixed with Bradford solution and peak fractions were pooled. For more precise usage in ChIP assays, the antibody concentration was measured with Bradford solution (see 2.2.3.2).

2.2.3.7 Chromatin immunoprecipitation

The protocol used is based on the protocol described in (Wells, Boyd et al. 2000).

Proteins were crosslinked to the DNA by adding 270 µl formaldehyde to 10 ml medium. After 10 min, the reaction was stopped by addition of 1250 µl 1M Glycine and incubation for 5 min. The cells were then washed 2 times with 1 x PBS and scraped into 15-ml falcons. The cell number per plate was analyzed

by trypsinizing and counting a separate dish. According to the cell number, pellets of 8 x 10^6 cells were separated and centrifuged at 1200 rpm for 10 min at 4 °C. The pellets were shock-frozen in liquid nitrogen and either stored at – 80 °C or immediately lysed for 10 min using 10 times its amount of cell lysis buffer (containing freshly added PI 1:100 and PMSF 1:200). After centrifugation at 2800 rpm for 5 min at 4 °C, nuclei were lysed in 800 µl nuclei lysis buffer (containing freshly added PI 1:100 and PMSF 1:200). Lysed nuclei were sonified to fracture the chromatin in 500 – 2000 bp fragments. The optimal conditions for the different cell types used were as follows:

For all cell types:	10 s pulse
	45 s pause
MCF-7	20 % amplitude
	8 repeats
HCT-116 wt	10 % amplitude
	6 repeats
HCT-116 p53 -/-	20 % amplitude
	6 repeats
HCT-116 p21 -/-	20 % amplitude
	8 repeats

To remove cell debris, the chromatin was centrifuged at 14000 rpm for 15 min at 4 °C. 50 µl chromatin was used to control the chromatin size.

To do so, 50 µl of the chromatin were mixed with 2 µl 5 M NaCl, 1 µl RNaseA [10 mg/ml], covered with mineral oil and incubated over night at 65 °C to reverse the crosslink. The following day, after 3 h incubation with 2 µl Proteinase K, the chromatin size was analyzed on a 1.2 % agarose gel.

The remaining supernatant was transferred to a new 15-ml falcon, diluted 1:10 with dilution buffer (containing PI and PMSF) and precleared with 240 µl

blocked protein-A-sepharose beads on a rotating wheel for 0.5 – 1 h at 4 °C. 4 immunoprecipitations were set up from the initial 8 x 10^6 cells. 1 % of the chromatin was taken as input and kept at 4°C over night. After addition of the antibodies, the samples were incubated at 4 °C over night on a rotating wheel. After addition of 40 – 80 µl blocked protein-A-sepharose beads, the mixture was incubated on a rotating wheel for 1 – 3 h at 4 °C. The beads were washed 7 times, each with 1 ml LiCl-washing buffer and eluted at 28 °C with 120 µl elution buffer shaking at 1400 rpm for 15 min. A second elution step was performed at 28 °C for 15 min using 150 µl elution buffer and both supernatants were brought together in a new reaction tube. For reverse crosslink 10 µl 5 M NaCl was added to the eluted mixture and covered with mineral oil. The inputs were brought to 250 µl with elution buffer, mixed with 10 µl 5 M NaCl and 1 µl RNaseA [10 mg/ml] and also covered with mineral oil. Reverse crosslink was performed over night at 65 °C. Proteins were degraded by incubation with 2 µl proteinase K [10 mg/ml] for 3 h at 55 °C.

Phenol/chloroform extraction was performed. 250 µl sample were mixed with 230 µl phenol/chloroform (1:1) for 15 s and after centrifugation at 14000 rpm for 5 min at RT, the aqueous phase was transferred into a new reaction tube. The DNA was purified using the Qiagen DNA Purification Kit according to the manufacturer's manual.

1 µl of purified chromatin was used for quantitative PCR analysis and precipitated samples were compared to input chromatin. The values were calculated as described in 2.2.2.3

2.2.4 Molecular biology

2.2.4.1 Isolation of plasmid DNA from bacteria

For plasmid isolation, a single colony was picked from a LB agar plate after transformation and cultured in 5 ml LB-medium at 37 °C for 4 - 8 h. This culture was transferred into either 50 – 100 ml (Midi preparation) or 200 – 400 ml (Maxi preparation) LB medium containing ampicillin and left growing over night in a shaker at 37 °C. Plasmids were purified with Midi- or Maxi-Kits from Genomed, Qiagen, Promega or Invitrogen according to the manufacturer's instructions.

3 Results

3.1 LINC composition after DNA damage induction

The LIN core complex is known to be associated to p130 and E2F4 during G0 phase of the cell cycle. As cells progress through the cell cycle LINC associates to B-MYB and p107 leading to the activation of G2/M target gene expression (Schmit, Korenjak et al. 2007). From published studies it is well known, that G2/M gene expression is decreased after DNA damage. However, the mechanism and the pathways that mediate this down regulation are largely unknown. Interestingly, many G2/M gene promoters contain CDE-CHR elements which are reported to be bound by p130 and E2F4 after DNA damage induction (Taylor, Schonthal et al. 2001). To analyze whether LINC plays a role in the DNA damage response, I compared its composition before and after doxorubicin treatment (Cummings and Smyth 1993; Fornari, Randolph et al. 1994; Nitiss 2002).

3.1.1 Binding studies in p53 wt cells

First, I determined the composition of LINC after doxorubicin treatment using immunoprecipitation studies in MCF-7 cells (Fig. 3.1 A). B-MYB binding to LIN-9 decreased 18 h to 24 h after DNA damage induction via doxorubicin whereas p130 binding to LIN-9 increased 6 h after treatment (Fig. 3.1 A). Interestingly, p130 seems to be able to bind to LIN-9 for the first time 6 h after doxorubicin was added to the medium, at the same time when also p21 protein levels are elevated. Additionally, at the same time a faster migrating form of p130 appeared on the SDS gel. Such changes in the running properties are often due to posttranslational modifications and in the case of p130 probably due to phosphorylation events (Cobrinik 2005). In parallel, I assayed for the cell cycle distribution using flow cytometry analysis (FACS) (Fig. 3.1 B). The first difference in cell cycle distribution occurred 18 h after DNA damage was induced. At that time the cells showed an arrest in G1 as well as in G2 phase of the cell cycle with only a few cells left in S phase. Notably, the change in LINC composition after DNA damage induction occurred before an effect on cell cycle

distribution could be detected. Therefore, I suggest that the switch in LINC composition is no indirect effect triggered by cell cycle inhibition.

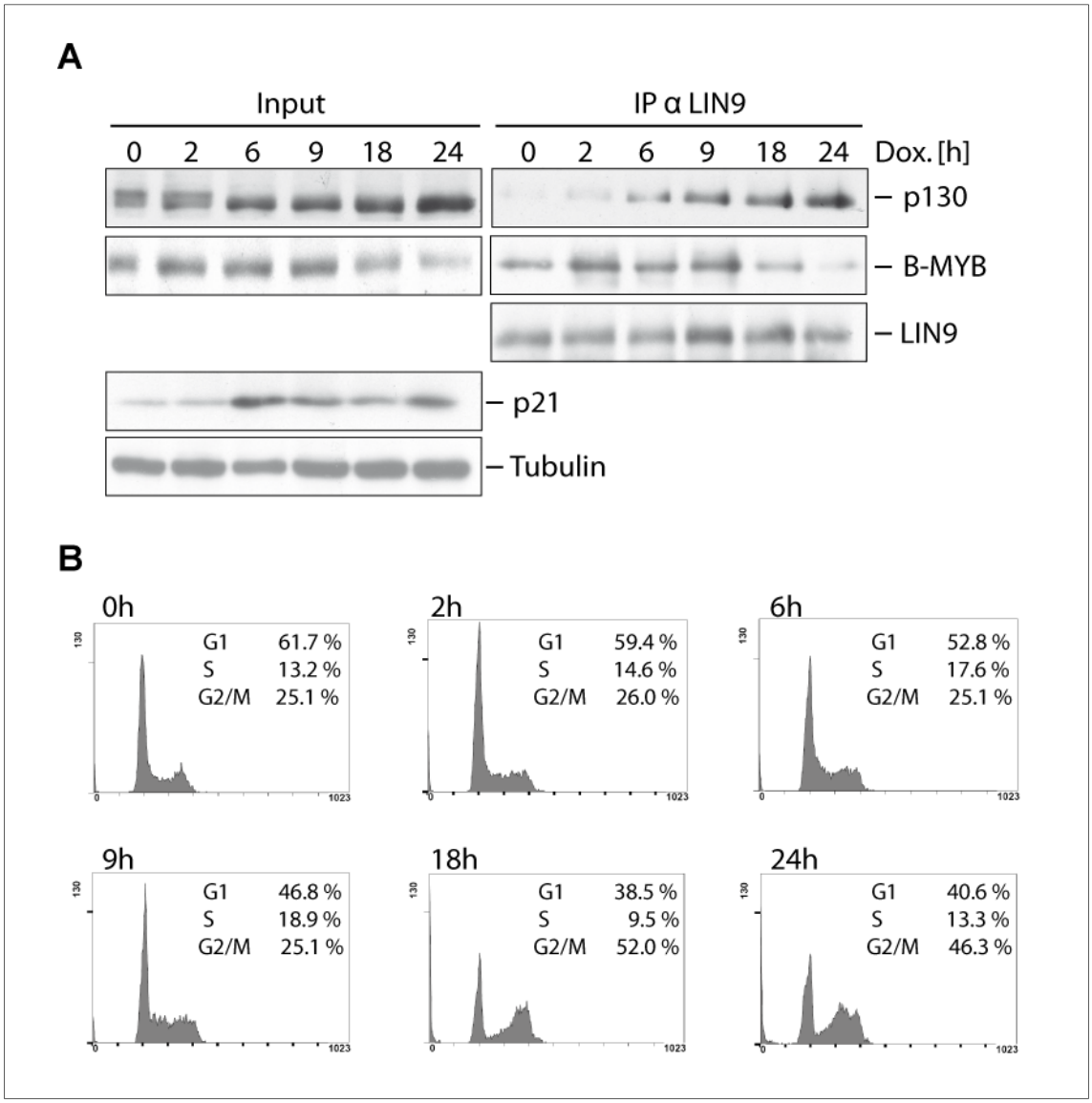

Figure 3.1: LINC composition after doxorubicin treatment

MCF-7 cells were treated with 1 µM doxorubicin for 2h, washed twice and left growing in normal media for the indicated times. (A) Lysates were precipitated with LIN-9 antibody and bound proteins were detected via immunoblotting with the indicated antibodies. (B) MCF-7 cells were stained with propidium iodide (PI) and analyzed in a flow cytometer (FACS machine) to determine cell cycle distribution.

To test whether the LIN core complex maintains its structure after doxorubicin treatment I checked for the binding of the different LINC core proteins (Schmit, Korenjak et al. 2007) in immunoprecipitation and immunoblot experiments (Fig. 3.2). After DNA damage induction p130 again showed a change in its migration pattern accompanied by an increased binding to LIN-9. In contrast, the other

core proteins LIN-54 and LIN-37 were constantly bound to LIN-9, independently of DNA damage (Fig. 3.2).

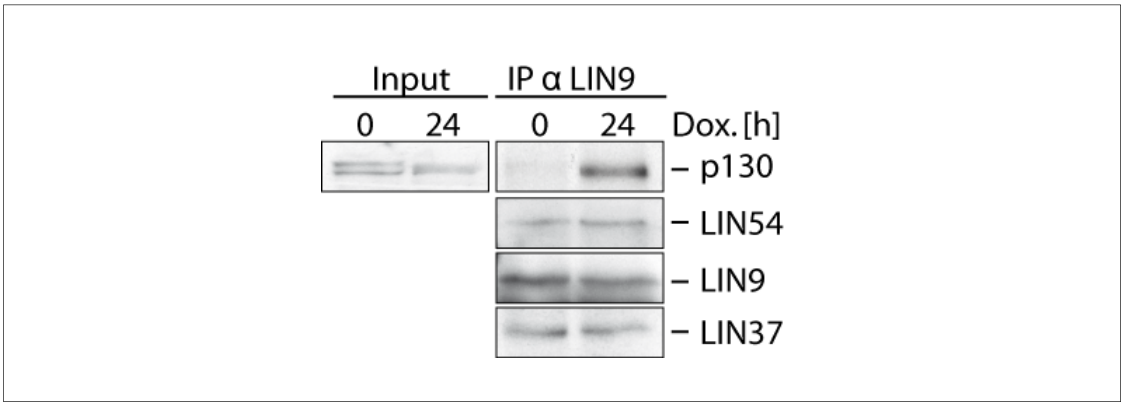

Figure 3.2: Composition of the LIN core complex after DNA damage

MCF-7 cells were treated with 1 µM doxorubicin for 2h, washed twice with1 x PBS and left growing in normal media for the indicated times. Lysates were precipitated with LIN-9 antibody and bound core proteins were detected via immunoblotting.

To analyze whether LINC rearrangement after doxorubicin treatment is independent from the used DNA damage-inducing agents, immunoprecipitations were performed after treating MCF-7 cells with either etoposide or cisplatin (Fig. 3.3) (Leng and Brabec 1994; Hande 1998; Barabas, Milner et al. 2008). In both cases, p130 binding to LIN-9 increased, after 24h in the case of etoposide and after 48h in the case of cisplatin. B-MYB binding to LIN-9 decreased as expected (Fig. 3.3 A and B). In parallel, FACS analyses were performed to determine cell cycle distribution (Fig. 3.3 C and D). After etoposide treatment most of the cells accumulated in G1 and G2 phase of the cell cycle, while cisplatin treated cells showed a moderate G2 block but high levels of cells in sub-G1 (Fig. 3.3 C and D). Therefore, I suggest that LINC rearrangement is not dependent on the used DNA damage-inducing agent, but instead occurs after DNA damage induction in general.

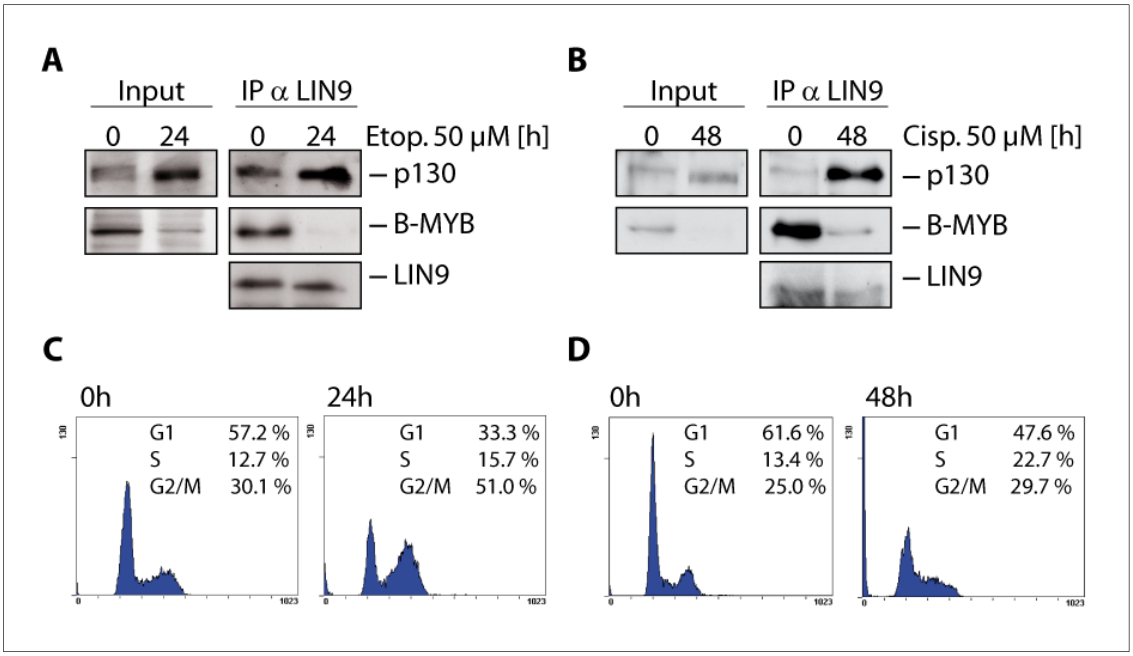

Figure 3.3: LINC composition after treatment with etoposide or cisplatin

(A, B) MCF-7 cells were treated with 50 µM etoposide (A) or 50 µM cisplatin (B) for the indicated times. Lysates were incubated with LIN-9 antibody over night. Bound B-MYB and p130 proteins were detected using immunoblotting. (C, D) MCF-7 cells were treated with 50 µM etoposide (C) or 50 µM cisplatin (D) for he indicated times. To determine the cell cycle distribution the cells were stained with PI and measured by FACS.

3.1.2 p130 and B-MYB do not bind to LINC simultaneously

After I demonstrated that both B-MYB and p130 bind to LIN-9 between 6 and 18 h after DNA damage induction (Fig. 3.1) immunoprecipitations were performed to determine if B-MYB and p130 bind simultaneously to LIN-9. Immunoprecipitations against B-MYB following p130 detection via immunoblotting showed that endogenous B-MYB does not bind to p130 at any time point I tested after doxorubicin treatment (Fig. 3.4). Thus, I conclude that B-MYB and p130 cannot be found in the same complex after DNA damage induction.

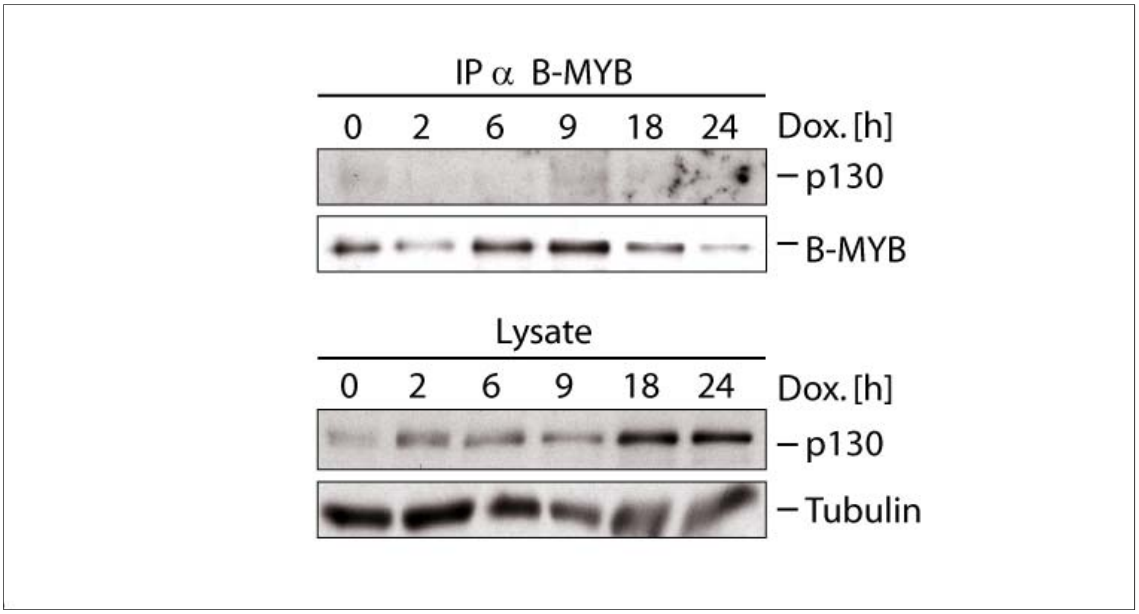

Figure 3.4: B-MYB and p130 do not bind to LIN-9 simultaneously

MCF-7 cells were treated as described in the legend of Figure 3.1 for the indicated times. Lysates were harvested and incubated with B-MYB antibody over night. Bound p130 was detected using immunoblotting.

3.1.3 Change in LINC composition is a direct effect of DNA damage induction

To address the question, if changes in LINC composition after DNA damage are caused indirectly by the incidental G1 block, I took advantage of the U2OS cell line which can be easily synchronized by addition of thymidine (van Vugt, Bras et al. 2004). After synchronization, U2OS cells were released into S phase and treated with 1 µM doxorubicin. To compare LINC composition in DNA damaged U2OS cells and undamaged cells enriched in G2/M, U2OS cells were additionally treated with 1 µM nocodazole (Fig. 3.5 A) (Jordan, Thrower et al. 1992). Figure 3.5 C shows the cell cycle distribution after treatment with different agents. Both, doxorubicin (C) and nocodazole (D) treated cells arrested in the G2/M phase of the cell cycle. In addition, FACS analyses were performed before the cells were released into the cell cycle (A) and at the time they were treated with doxorubicin and/or nocodazole (B) to confirm synchronization with thymidine was successful (Fig. 3.5 C). LIN-9 was immunoprecipitated by addition of LIN-9 antibody and bound p130 or B-MYB protein was detected by immunoblot analysis (Fig. 3.5 B). As shown before (compare Fig. 3.1 and 3.3), after DNA damage induction p130-binding to LIN-9

was induced whereas binding of B-MYB to LIN-9 decreased (Fig. 3.5 B). Interestingly, in U2OS cells treated with nocodazole (D) alone, no binding of p130 to LIN-9 could be detected although B-MYB binding to LIN-9 was strongly reduced and p130 showed an even bigger change in its running properties compared to doxorubicin treated cells (C). Thus it appears that the switch in LINC composition is as direct effect triggered by DNA damage induction and not a secondary effect triggered by the G1 arrest seen in asynchronously growing cells (Fig. 3.1).

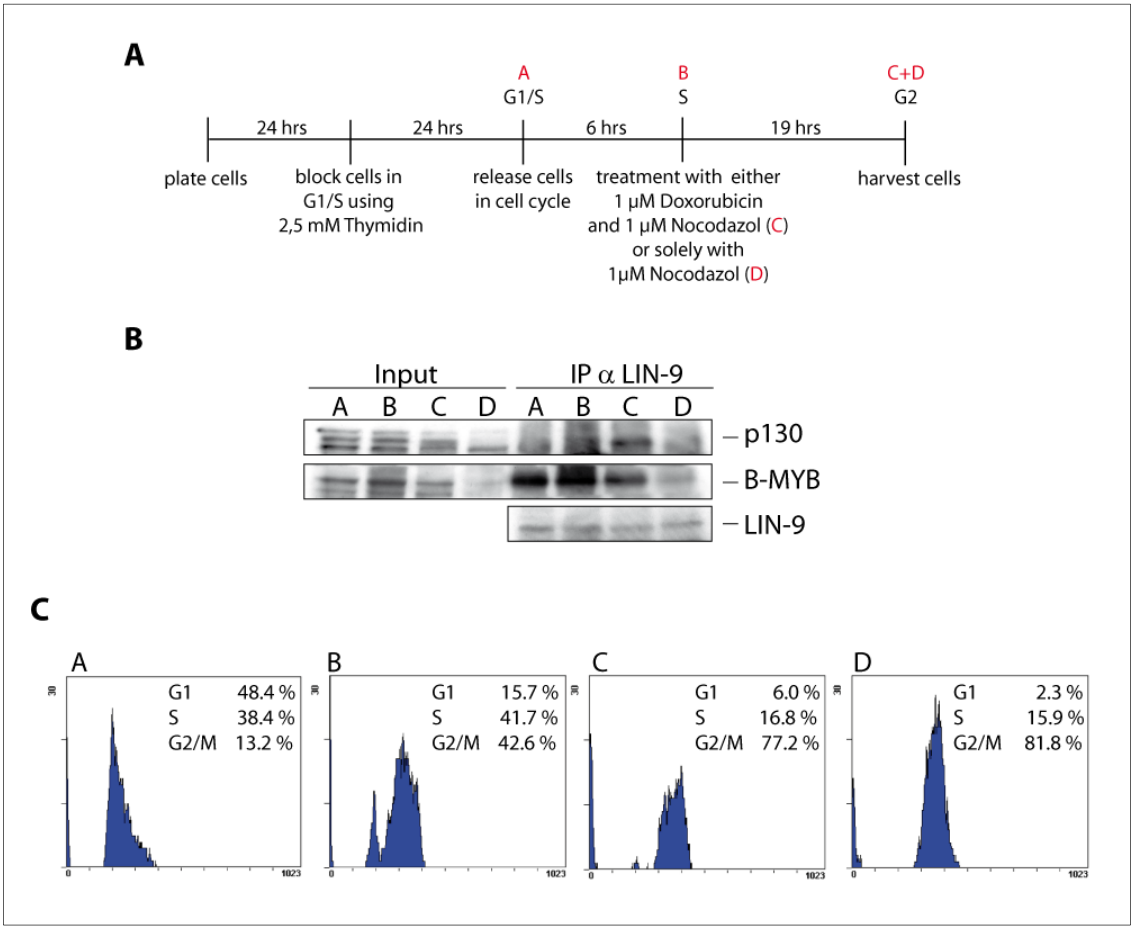

Figure 3.5: Change in LINC composition is a direct effect of DNA damage induction

(A) Experimental setup is shown in the scheme. After blocking the cells in G1/S phase by treatment with 2.5 mM thymidine, cells were released into the cell cycle by washing twice with 1 x PBS. 6 h later cells were treated with 1 µM doxorubicin and/or 1 µM nocodazole for another 19 h. (B) For immunoprecipitation experiments the lysates were incubated with LIN-9 antibody over night. The bound proteins were detected via immunoblotting using the indicated antibodies. (C) To determine the distribution within the cell cycle, U2OS cells were stained with PI and measured by FACS.

3.1.4 p130 phosphorylation status is crucial for binding to LINC

It is known that p130 (as well as the other pocket proteins) is highly regulated by its phosphorylation status (Cobrinik 2005). In addition, I observed a change in the running properties of p130 after DNA damage induction at the same time when it binds to LIN-9 (Fig. 3.1 A, 3.2 A, 3.3 A and 3.5 B). Therefore, I next wanted to know if the rearrangement of LINC after DNA damage is induced by the dephosphorylation of p130.

Thus, MCF-7 cells were treated with 1 µM doxorubicin and binding of LIN-9 to p130 was analyzed by immunoprecipitation. These experiments showed that only the faster migrating form of p130 is able to bind to LIN-9 (Fig. 3.6). In contrast, the slower migrating hyperphosphorylated form of p130 present in untreated cells exhibited no binding to LIN-9 at all.

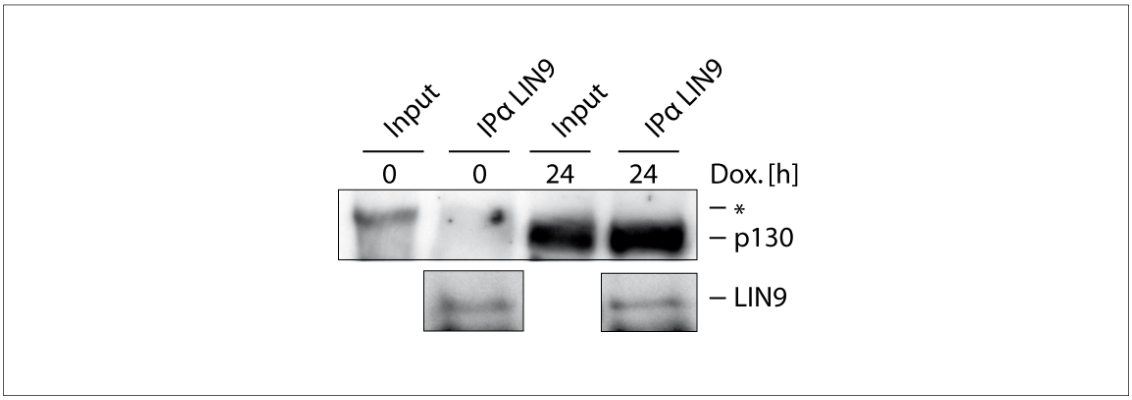

Figure 3.6: p130 phosphorylation status is crucial for binding to LIN-9

MCF-7 cells were treated with 1 µM doxorubicin for 2 h, washed twice with 1 x PBS and left growing for 24 h in normal media. Lysates were incubated with an antibody directed against LIN-9. Bound p130 was detected via immunoblotting.

3.2 Pathways leading to LINC switch

In Figure 3.5 and 3.6 I showed that LIN-9 only bound to the partially dephosphorylated form of p130 after DNA damage. Additionally, in Figure 3.1 A I could show that the induction of p21 correlated with the appearance of hypophosphorylated p130 and with binding of p130 to LIN-9. These findings suggest that the phosphorylation status of p130 determines LINC composition. Importantly, p21 induction, as a consequence of DNA damage-dependent p53 activation, does lead to the dephosphorylation of pocket proteins by inhibiting cyclin-cdk complexes. Thus, it is possible that p21 mediates the rearrangement

of LINC in response to DNA damage. To test this hypothesis I performed more binding studies. First, I used cell lines deficient for p21 or p53. Secondly, Nutlin-3 was used to activate p53 DNA damage independent in wildtype cells (Vassilev 2005; Wang, Jonca et al. 2007; Shangary and Wang 2009).

3.2.1 Binding studies in p21 negative cells after DNA damage induction

To get more information about the pathway leading to the change in LINC composition, I took advantage of HCT-116 cells and isogenic p21 -/- cells in which p21 was deleted by homologues recombination (Bunz, Dutriaux et al. 1998).

I analyzed LINC composition via immunoprecipitations and immunoblot analyses in both the HCT-116 wt (p21 +/+) and p21 deficient (p21 -/-) cells. Consistent with our results before (Fig. 3.1 A), LIN-9 bound to p130 after DNA damage induction in HCT-116 p21 +/+ cells (Figure 3.7 A). In contrast, in p21 -/- HCT-116 cells, doxorubicin treatment did not induce binding of p130 to LIN-9. Furthermore, after treatment p130 only showed a change in its migration pattern in p21 +/+ and not in p21 -/- cells. As a control in both cell lines p21 protein levels were analyzed by immunoblotting and were upregulated in HCT-116 p21 +/+ cells 8 h after doxorubicin addition. In contrast, as anticipated, no p21 was detected in p21 -/- HCT-116 cells. In parallel, the cell cycle distribution of these cells was analyzed using FACS analysis (Figure 3.7 B). 24 h after doxorubicin treatment, both p21 +/+ and p21 -/- cells accumulated mainly in G2/M. This experiment confirmed that p21 indeed is essential for binding of p130 to LIN-9 and therefore is part of the pathway leading to the switch in LINC composition.

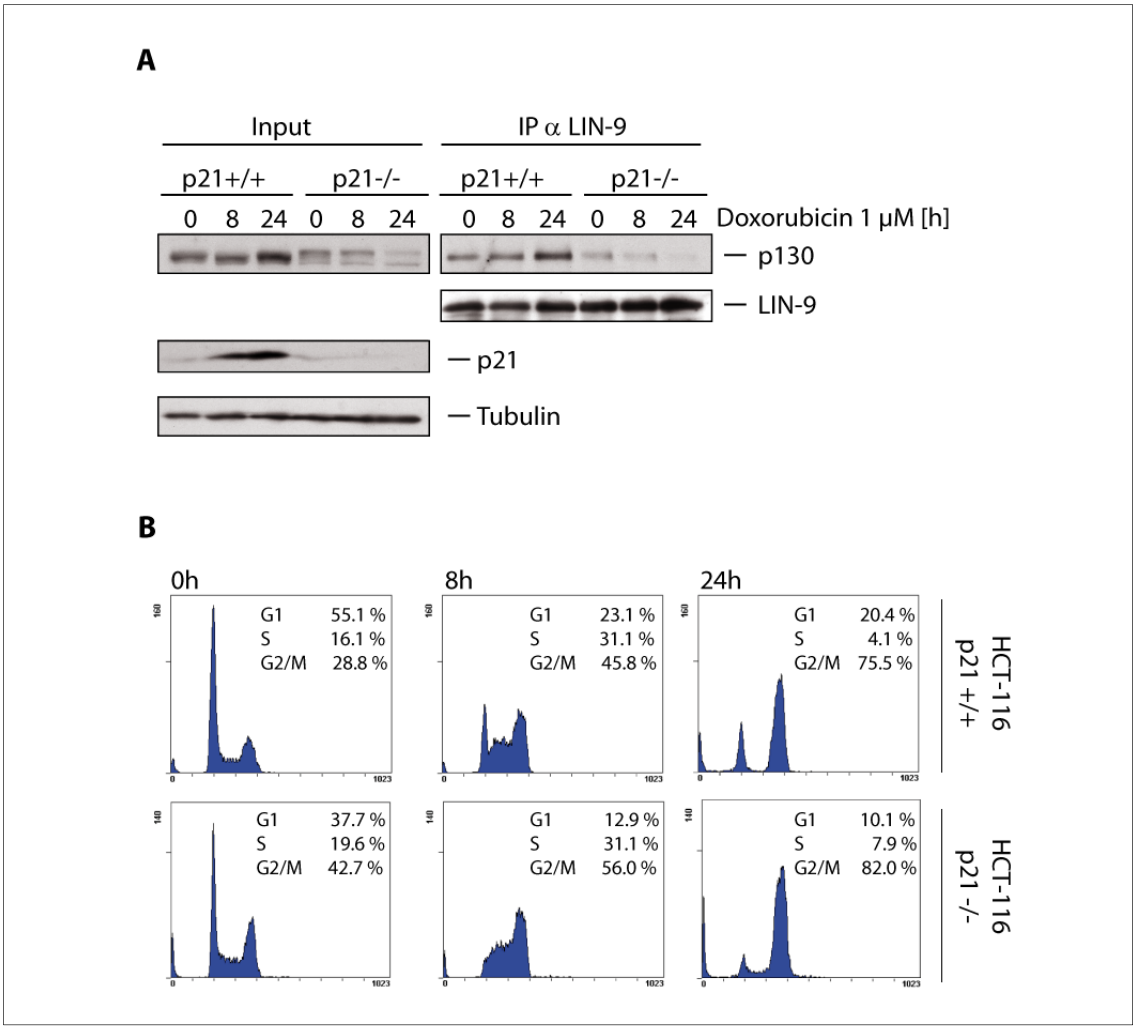

Figure 3.7: p21 is required for LINC rearrangement after DNA damage induction

HCT-116 p21 +/+ and p21 -/- cells were treated with 1 µM doxorubicin for 2 h, washed with 1 x PBS and left growing in normal media for the indicated times. (A) Lysates were incubated with antibody against LIN9 and bound proteins were detected using immunoblotting. (B) Cells were stained with PI and DNA content was measured by FACS.

3.2.2 Binding studies in p53 negative cells after DNA damage induction

Because induction of p21 is mostly dependent on p53 activation (Niida and Nakanishi 2006), I next asked if p53 is also a part of the pathway leading to LINC rearrangement. Therefore, I used HCT-116 wildtype (p53 +/+) cells and HCT-116 cells deficient for p53 (p53 -/-) and treated them with doxorubicin. After performing immunoprecipitations and immunoblot analyses I found that LINC switches in composition in HCT-116 p53 +/+ cells but not in p53 -/- cells (Fig. 3.8 A). In contrast to the situation in p53 +/+ cells, no binding of p130 to LIN-9 and no decreased binding of B-MYB to LIN-9 was observed in p53 -/-

cells. Instead, binding of B-MYB to LIN-9 even increased in these cells after DNA damage induction (Fig. 3.8 A). Additionally, I analyzed cell cycle distribution of p53 +/+ and p53 -/- cells after DNA damage induction and could show that both cell lines mainly block in the G2/M phase of the cell cycle with only a small amount of cells arresting in G1 phase (Fig. 3.8 B). Altogether, this result showed that p53 is essential to switch composition of LINC after DNA damage.

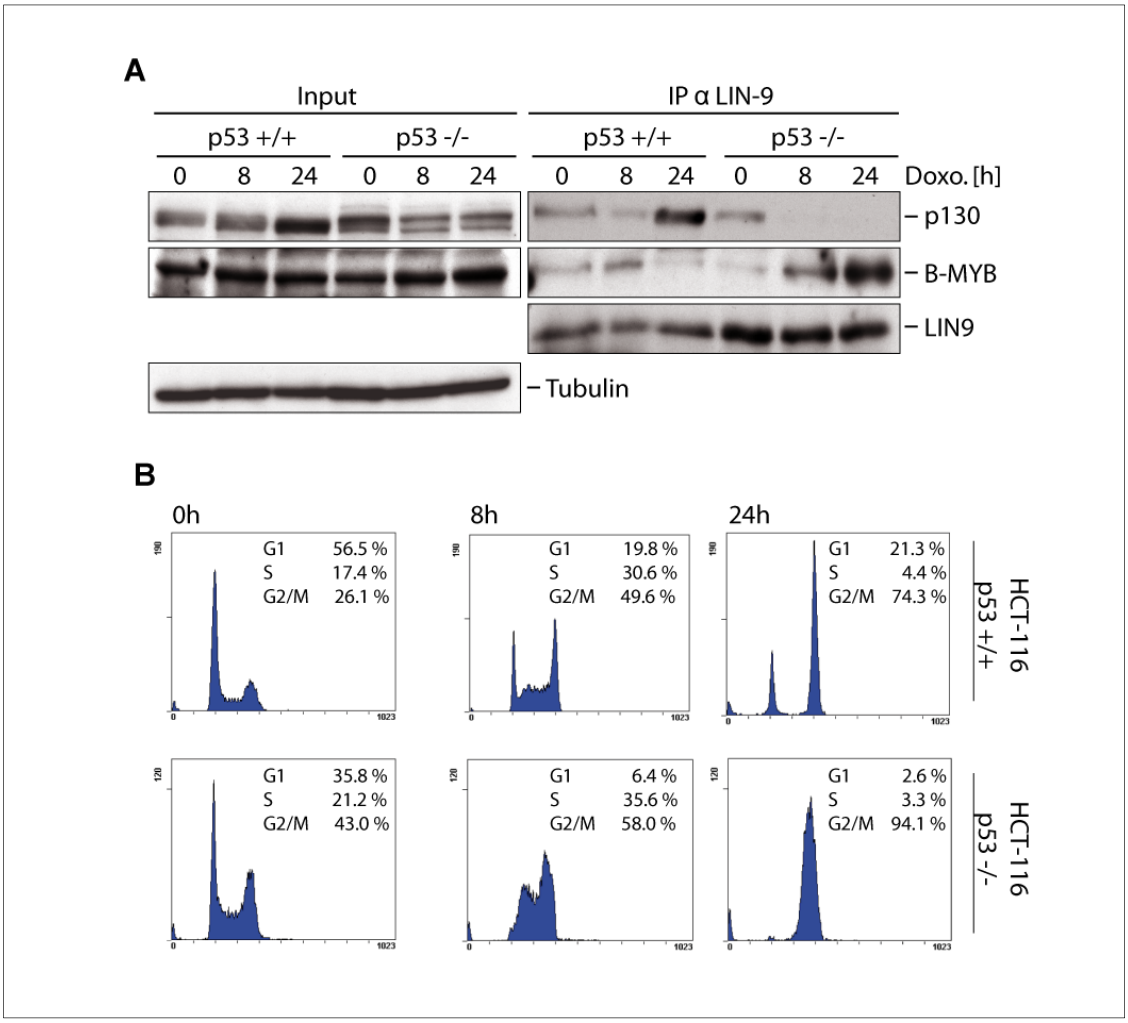

Figure 3.8: p53 is required for LINC rearrangement after DNA damage induction

HCT-116 wildtype and p53 -/- cells were treated with 1 µM doxorubicin for 2 h, washed twice with 1 x PBS and left growing for the indicated times. (A) LIN-9 was immunoprecipitated over night. Bound proteins were detected via immunoblotting. (B) To determine the distribution within the cell cycle, HCT-116 p53 +/+ and -/- cells were stained with PI and measured by FACS.

3.2.3 Binding studies in p53 wt cells after Nutlin-3 treatment

To test whether p53 activation is not only necessary (see 3.2.2) but also sufficient to switch LINC from a B-MYB-associated to a p130-associated complex, I performed immunoprecipitation assays in MCF-7 cells treated with Nutlin-3 (Vassilev 2005; Wang, Jonca et al. 2007). As an inhibitor of mdm-2, addition of Nutlin-3 leads to the stabilization and therefore also the activation of p53. After performing immunoprecipitations against LIN-9, I analyzed the bound proteins via immunoblot analysis. As depicted in Figure 3.9 A and B, binding of p130 and E2F4 to LIN-9 increased after 8 h of Nutlin-3 treatment whereas binding of B-MYB and p107 decreased around 14h after treatment. In parallel, FACS analyses were performed (Fig. 3.9 C), showing that MCF-7 cells mainly arrest in the G1 phase of the cell cycle (66.5%) when treated with Nutlin-3. These results led to the conclusion, that p53 activation after DNA damage is not only necessary but also sufficient to switch the LIN complex.

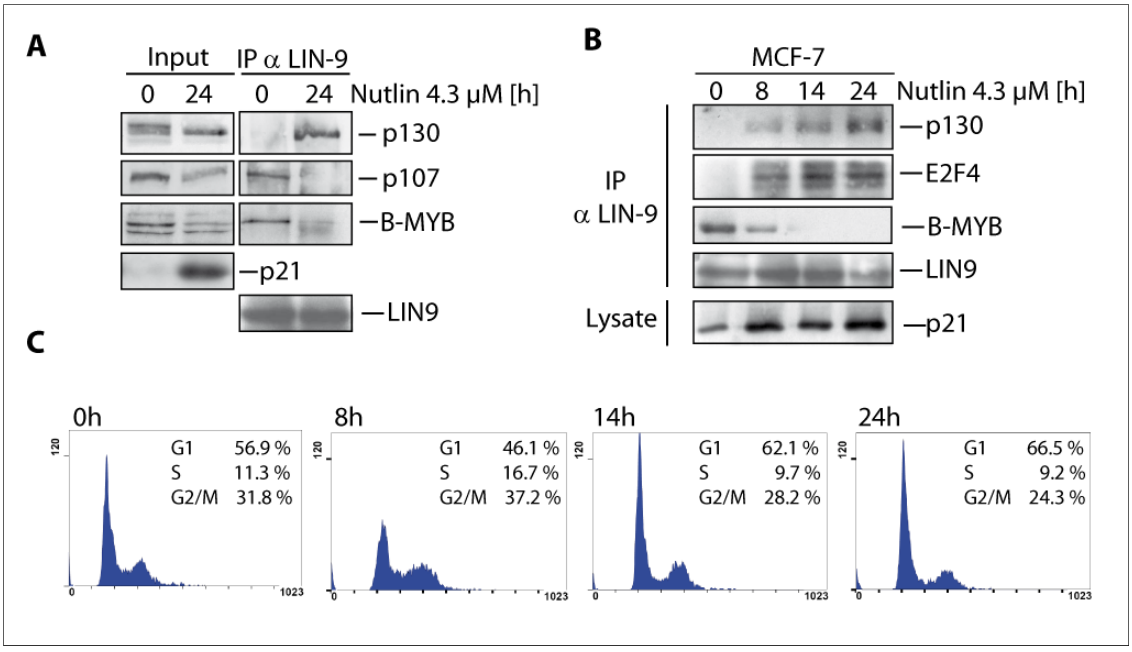

Figure 3.9: p53 activation is sufficient to induce LINC rearrangement

MCF-7 cells were treated with 4.3 µM Nutlin-3 for the indicated times. (A,B) Lysates were incubated with LIN-9 antibody over night. The next day bound proteins were detected in immunoblot analysis. (C) Nutlin-3 treated cells were harvested with trypsin and stained with PI. Distribution within the cell cycle was quantified using FACS analysis.

3.3 Regulation of G2/M gene expression

It is known, that LINC associates dynamically with p130, E2Fs and B-MYB in a cell cycle dependent manner. In the G0 phase of the cell cycle p130 and E2F4 are bound to the LIN complex. During S phase, p130 and E2F4 are replaced by B-MYB and p107 which leads to an activation of mitotic gene expression. Given that the activating LIN complex is disrupted after DNA damage induction, I studied the gene expression profiles of mitotic genes after DNA damage induction.

3.3.1 G2/M gene expression in p53 wt and p53 negative cells

First, I wanted to find out if the rearrangement of LINC after DNA damage induction has an impact on G2/M gene expression and thereby perhaps influences the maintenance of the G2 arrest. Therefore, I used MCF-7 cells, treated them with doxorubicin and analyzed target gene expression using quantitative Real Time PCR analysis (qPCR) 48 h later (Fig. 3.10). As a result of p53 activation, p21 gene expression was increased whereas the gene expression of Ubch10, Birc5 and cyclin B1, known mitotic genes, was strongly decreased. Proliferating cell nuclear antigen (PCNA) is an E2F-responisve gene activated during G1/S transition and served as a control because it is regulated neither by LINC nor by B-MYB. In spite of that, PCNA showed a slight decrease in gene expression. Finally, the alteration in LINC composition after DNA damage induction is accompanied by a downregluation of G2/M target gene expression.

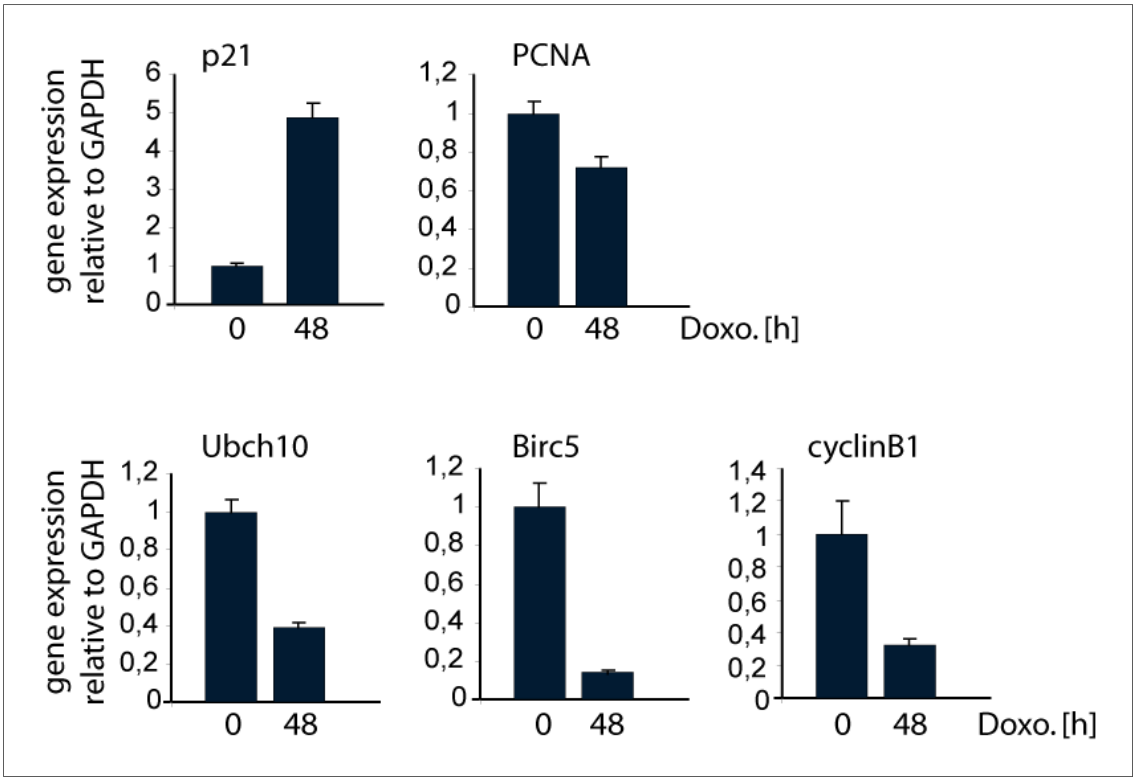

Figure 3.10: LINC target gene expression decreases in MCF-7 cells after doxorubicin treatment

MCF-7 cells were treated with 1 µM doxorubicin for 2 h, washed twice with 1 x PBS and left growing for 48 h. After RNA purification, cDNA was synthesized and gene expression quantified using qPCR analysis. Primers were used, which are specific for regions of G2/M genes (Ubch10, Birc5 and cyclin B1), G1/S genes (PCNA), DNA damage induced genes (p21) and unregulated control genes (GAPDH). Target gene expression is shown compared to GAPDH expression.

To assure that this effect is not restricted to the MCF-7 cell line but occurs in other cell lines as well, I performed qPCR analysis in HCT-116 cells. As shown in Figure 3.11, in HCT-116 p53 +/+ cells, all analyzed G2/M genes showed a decreased expression after DNA damage induction. In contrast, HCT-116 p53 -/- cells showed no decrease but even an increase in basal G2/M gene expression levels (2-fold) as well as in expression levels (4- to 8-fold) after doxorubicin treatment. This is probably due to the increased binding of B-MYB to LIN-9 shown before in Figure 3. 8 A. Repeatedly, PCNA served as a control and showed a slight increase in gene expression after treatment. This experiment confirmed that the down regulation of G2/M gene expression after doxorubicin treatment is dependent on p53, like the switch in LINC composition shown before in Figure 3.8 A.

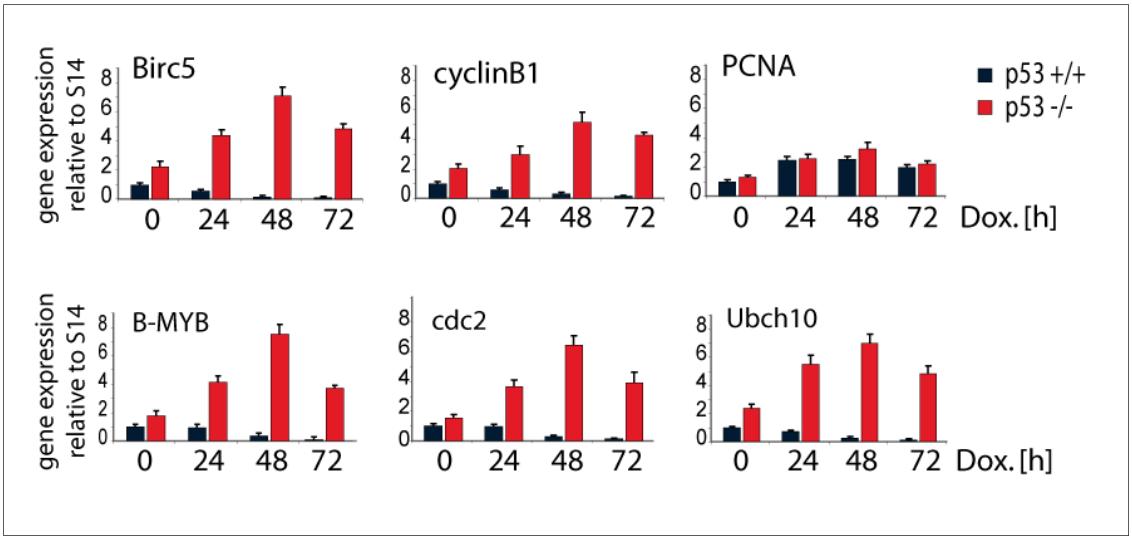

Figure 3.11: G2/M gene expression in HCT-116 p53 +/+ and –/- cells after doxorubicin treatment

HCT-116 cells p53 +/+ (blue bars) and p53 -/- (red bars) cells were treated with 1 µM doxorubicin for 2 h, washed twice with 1 x PBS and left growing for the indicated times. RNA was purified and cDNA synthesized. qPCR analysis was performed with primers annealing in the regions of G2/M genes (Birc5, cyclin B1, cdc2 (cdk1) and Ubch10), G1/S genes (B-MYB and PCNA) or unregulated control genes (S14). Target gene expression is shown compared to S14.

Next, I asked if p53 activation by addition of Nutlin-3 is sufficient to trigger a decrease in G2/M gene expression since I showed that treatment with Nutlin-3 results in a switch in LINC composition (Fig. 3.9). Therefore, I treated MCF-7 cells with Nutlin-3 and analyzed gene expression profiles via qPCR. Gene expression of mitotic genes (cdc2 (cdk1) and cyclin B1) was decreased after treatment with Nutlin-3 as expected (Fig. 3.12 A). As a result of p53 activation, p21 gene expression increased. RR1 and cdc6 are G1/S genes and also displayed a decrease in gene expression after Nutlin-3 treatment. The distribution of MCF-7 cells within the cell cycle after Nutlin-3 treatment is depicted in Figure 3.12 B showing that most of the cells arrested in the G1 phase of the cell cycle. Finally, this shows that p53 activation independently of DNA damage induction is sufficient to induce down regulation of G1 and G2/M gene expression.

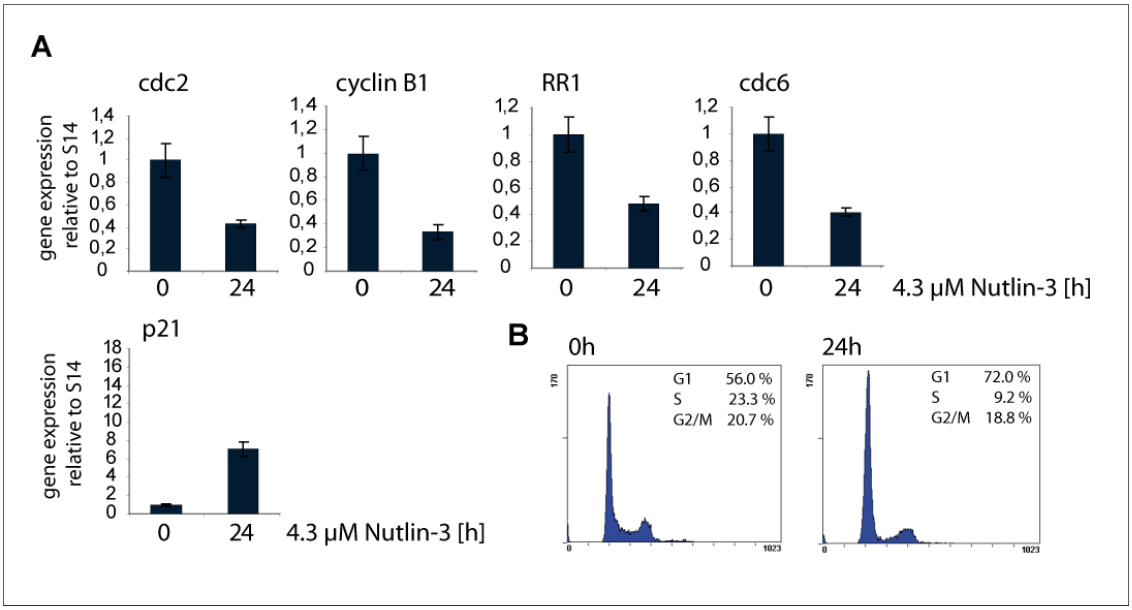

Figure 3.12: G2/M gene expression of MCF-7 cells after Nutlin-3 treatment

MCF-7 cells were treated with 4.3 µM Nutlin-3 for the indicated times. (A) After the cells were harvested, RNA was purified and cDNA synthesized. qPCR was performed using primers annealing in the regions of G2/M genes (cdc2 (cdk1), cyclin B1), G1/S genes (RR1, cdc6), DNA damage induced genes (p21) or unregulated control genes (S14). Target gene expression is shown compared to S14. (B) To determine the distribution within the cell cycle MCF-7 cells were stained with PI and measured by FACS.

3.3.2 Regulation of G2/M gene expression is a direct effect

To get more insight into the regulation of mitotic gene expression after DNA damage induction I performed chromatin immunoprecipitation analyses. MCF-7 cells were treated with doxorubicin, chromatin was prepared and immunoprecipitated with antibodies directed at E2F4 and B-MYB (Fig. 3.13 A). As a control, an unspecific IgG antibody was used. After doxorubicin treatment a difference in the protein accumulation at the tested promoters could be observed. Specifically, E2F4 was enriched at the promoters of G2/M target genes (cyclin B1, Ubch10 and Birc5) whereas B-MYB binding to these promoters slightly decreased after doxorubicin treatment. Analysis of the PCNA promoter served as a control and showed an increased accumulation of E2F4 after DNA damage but no binding of B-MYB before or after DNA damage. In parallel, FACS analyses were performed and showed the cells arresting mainly in the G1 phase of the cell cycle (Fig. 3.13 B). In conclusion, the rearrangement of LINC after DNA damage induction could also be seen on promoter level.

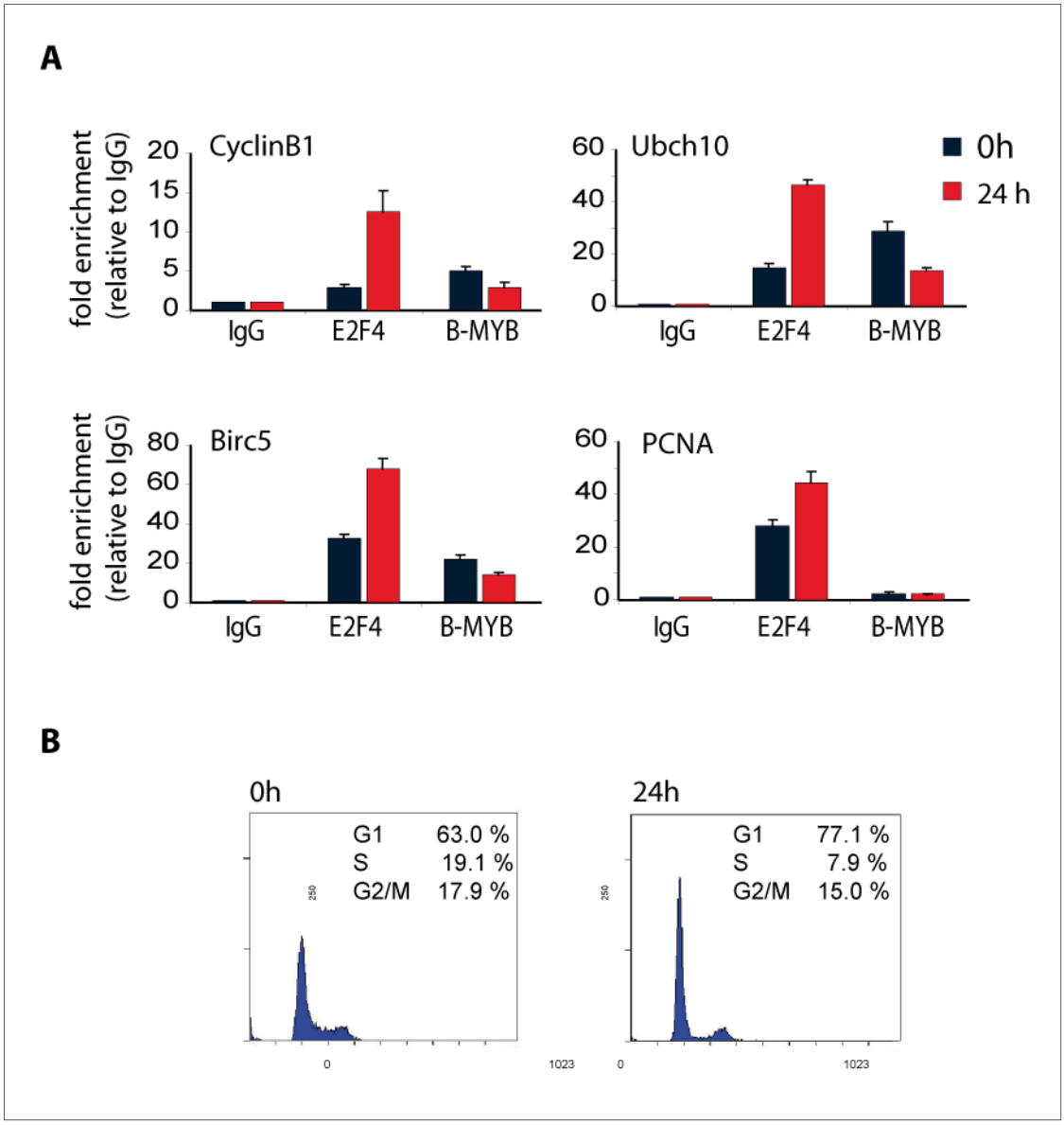

Figure 3.13: Chromatin immunoprecipitation (ChIP) analysis in MCF-7 cells after doxorubicin treatment

MCF7- cells were either left untreated (blue bars) or treated with doxorubicin for 2 h (red bars), washed twice with 1 x PBS and left growing in normal medium for the indicated times. (A) Cell lysates were incubated with the antibodies indicated below the graphs. The bound chromatin was quantified via qPCR analyses using primers annealing to the promoters of G2/M genes (cyclin B1, Ubch10 and Birc5) and G1/S genes (PCNA). (B) To determine the distribution within the cell cycle, treated and untreated MCF-7 cells were stained with PI and measured by FACS.

To determine if the differences between p53 +/+ and p53 -/- cells seen on gene expression level (Fig. 3.8) after DNA damage are due to differences in LINC accumulation at these promoters, I performed ChIP analyses with HCT-116 p53 +/+ and p53 -/- cells. As displayed in Figure 3.14, in p53 +/+ cells E2F4 as well as p130 showed an increased enrichment at the G2/M target gene promoters (Ubch10, cyclin B1 and Birc5) after DNA damage. In contrast, B-MYB

decreased after DNA damage. LIN-9 as a component of both the “activating” as well as the “repressing” complex was detected at all analyzed promoters at all analyzed time points. Only for the Birc5 promoter a slight increase in LIN-9 enrichment was detectable. Before and after DNA damage induction E2F4 and p130 accumulated at the PCNA promoter. In contrast, neither LIN-9 nor B-MYB bound to its promoter. Unlike the situation in p53 +/+ cells, p53 -/- cells showed a decreased binding of p130 and E2F4 to G2/M gene promoters after doxorubicin treatment. LIN-9 enrichment at the promoters did not change. Surprisingly, B-MYB binding to some G2/M gene promoters (such as cyclin B1 and Birc5) increased after DNA damage induction in p53 -/- cells. E2F4 and p130 accumulation at the PCNA promoter decreased in p53 -/- cells, especially when cells were treated with doxorubicin. As expected, neither LIN-9 nor B-MYB bound to its promoter. GAPDH is a housekeeping gene and therefore no binding of any tested protein to its promoter could be detected.

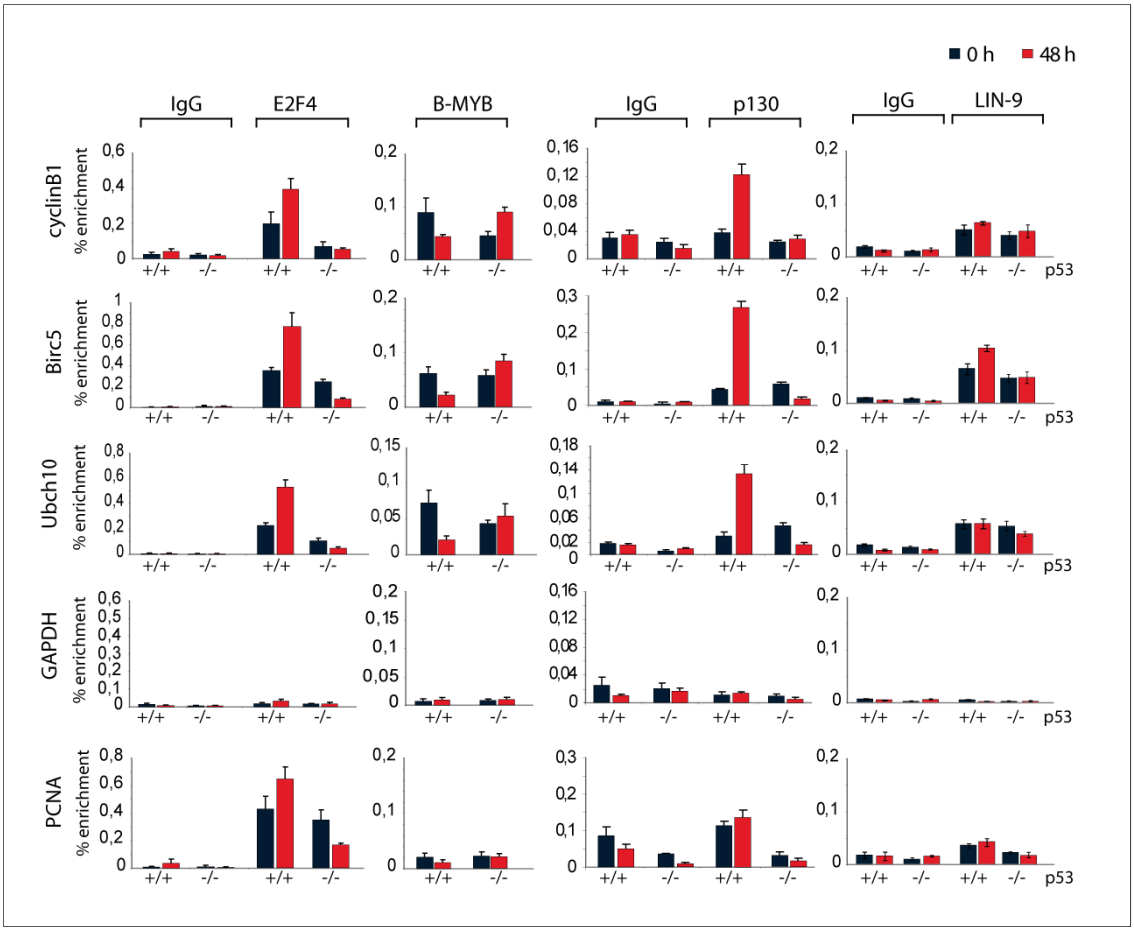

Figure 3.14: ChIP analysis in HCT-116 p53 +/+ and p53 -/- cells after 48 h of doxorubicin treatment

HCT-116 p53 +/+ and -/- cells were left either untreated (blue bars) or treated with 1 µM doxorubicin (red bars), washed twice with 1 x PBS and left growing in normal medium for another 48 h. Pellets were harvested and lysates were incubated with antibodies indicated at the top of the graph. The bound chromatin was quantified via qPCR analyses using primers annealing to the promoters of G2/M genes (cyclin B1, Ubch10,cdc2 (cdk1) and Birc5), G1/S genes (PCNA) and unregulated control genes (GAPDH).

To get more information about the situation at the promoters at earlier time points I decided to perform ChIP assays 24 h after doxorubicin treatment (Fig. 3.15). Again, for the G2/M promoters Birc5, Ubch10 and cyclin B1 a strong increase of E2F4 and p130 binding was detected after 24h of treatment in HCT-116 p53 +/+ cells. In contrast, in HCT-116 p53 -/- cells neither E2F4 nor p130 were recruited to the promoters after DNA damage but rather showed a decreased attachment to the tested gene promoters compared to untreated p53 -/- cells.

In contrast to the situation 48 h after doxorubicin treatment, 24 h after doxorubicin treatment B-MYB showed a constant binding to the tested G2/M

gene promoters in HCT-116 p53 +/+ cells. Nevertheless, in p53 -/- cells 24 h after DNA damage induction a clear increase in bound B-MYB could be shown. In p53 +/+ and p53 -/- cells as well as in untreated or treated cells, LIN-9 constantly bound to the different promoters. GAPDH as a housekeeping gene was used as a negative control since none of the tested proteins is known to bind to its promoter.

Additionally, for both ChIP assays (Fig. 3.14 and 3.15) FACS analysis were performed (Figure 3.16). The cell cycle distribution of both cell lines was nearly identical showing mainly a G2/M block from about 76 % to 91 % after doxorubicin treatment.

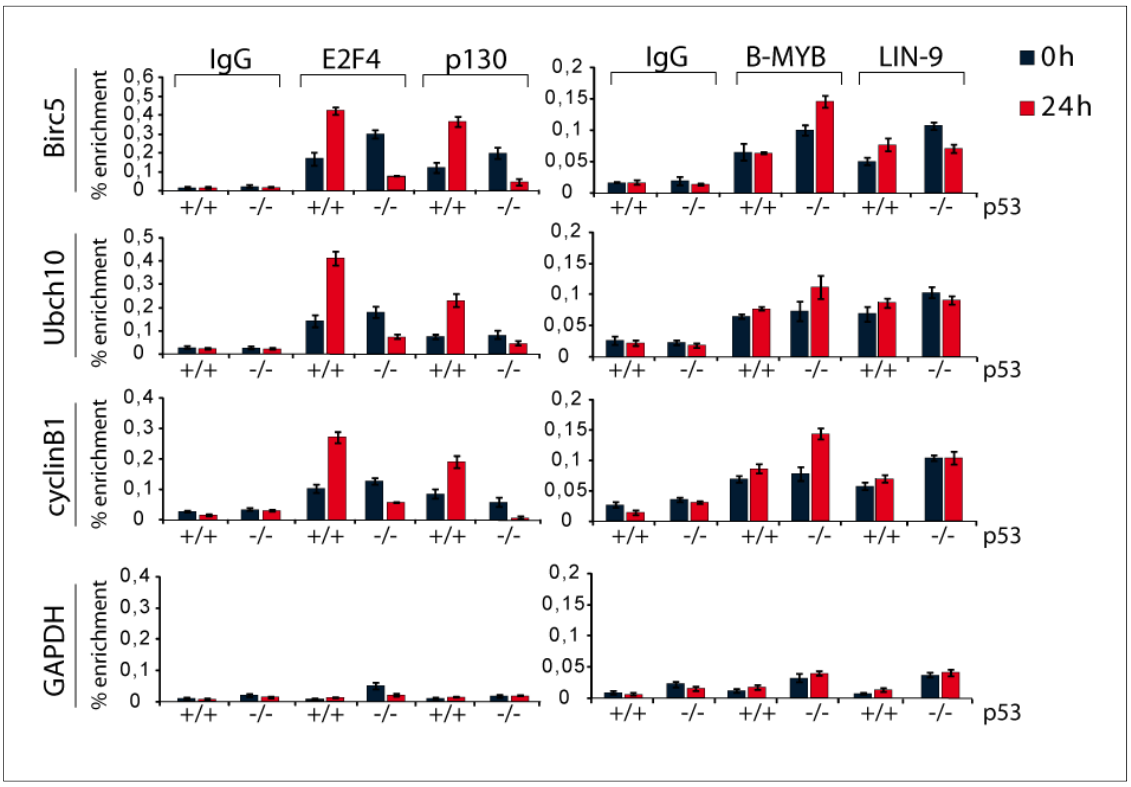

Figure 3.15: ChIP analysis in HCT-116 p53 +/+ and p53 -/- cells after 24 h of doxorubicin treatment

HCT-116 p53 +/+ and -/- cells were left either untreated (blue bars) or treated with 1 µM doxorubicin (red bars), washed twice with 1 x PBS and left growing in normal medium for another 24 h. Pellets were harvested and lysates were incubated with antibodies indicated at the top of the graph. The bound chromatin was quantified via qPCR analyses using primers annealing to the promoters of G2/M genes (cyclin B1, Ubch10 and Birc5) and unregulated control genes (GAPDH).

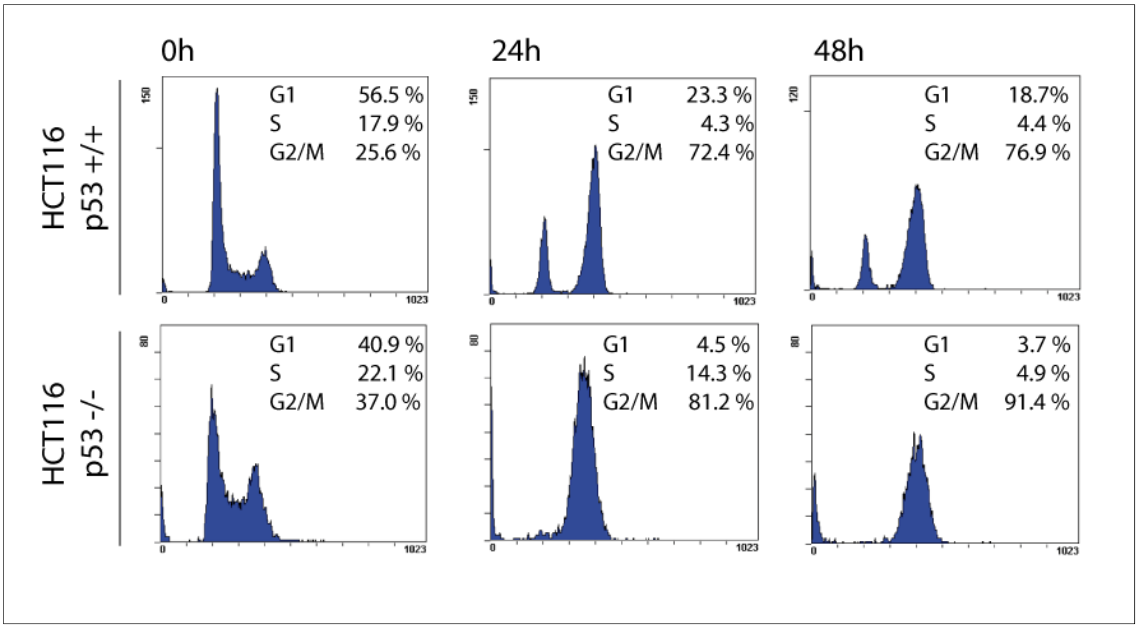

Figure 3.16: FACS analysis of HCT-116 p53 +/+ and -/- cells after doxorubicin treatment

HCT-116 p53 +/+ and -/- cells were treated with 1 µM doxorubicin for 2 h, washed twice with 1 x PBS and left growing in normal medium for 24 h or 48 h. To determine the distribution within the cell cycle, HCT-116 p53 +/+ and -/- cells were stained with PI and measured by FACS.

As we know, not only the induction of DNA damage but also the p53 activation using Nutlin-3 led to a decrease in G2/M gene expression in MCF-7 cells (Fig. 3.12). Therefore, I performed chromatin immunoprecipitations with Nutlin-3-treated MCF-7 cells. As before, I analyzed the binding of known LINC components as well as the binding of LINC-associated proteins to promoters of responsive G2/M genes (Fig. 3.17 A). The experiment showed an enrichment of E2F4 and p130 at the tested G2/M gene promoters (Ubch10 and Birc5) after treatment with Nutlin-3. B-MYB, as a part of the activating LIN complex, showed a decreased binding to the same G2/M gene promoters. LIN-9, as a member of the core module, bound constant to the tested G2/M promoters. In this experimental setup, the addition of LIN-9 preimmuneserum served as a direct control for accumulation of LIN-9 at the promoters. As mentioned before, GAPDH again served as a control showing that none of the tested proteins bound at its promoter. In Figure 3.17 B, the corresponding FACS profile depicts that Nutlin-3-treated MCF-7 cells arrested mainly in the G1 phase of the cell cycle.

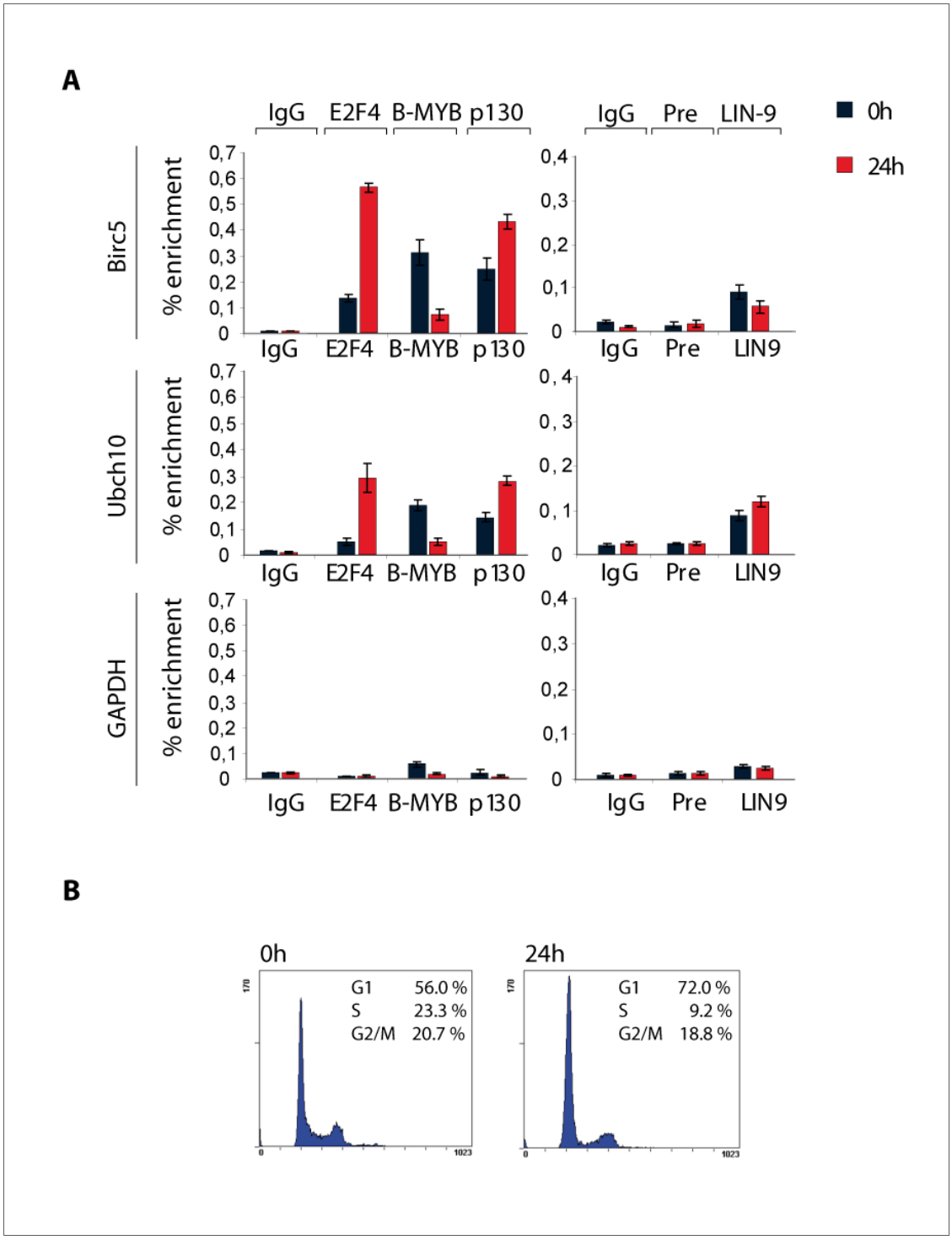

Figure 3.17: ChIP analysis in MCF-7 cells after 24 h of Nutlin-3 treatment

MCF-7 cells were either left untreated (blue bars) or incubated with 4.3 µM Nutlin-3 for 24 h (red bars). (A) Pellets were harvested and lysates were incubated with antibodies indicated below the graphs. Pre: LIN-9 preimmuneserum. The bound chromatin was quantified via qPCR analyses using primers annealing to the promoters of G2/M genes (Ubch10 and Birc5), G1/S genes (PCNA) and unregulated control genes (GAPDH). (B) To determine the distribution within the cell cycle, treated and untreated MCF-7 cells were stained with PI and measured by FACS.

3.3.3 Deregulated G2/M gene expression in p53 negative cells after DNA damage induction is partially rescued by depletion of LIN-9 and/or B-MYB

So far I could show that p53 -/- cells exhibit an increased G2/M gene expression when treated with DNA damaging agents like doxorubicin. It is possible that this is at least partially due to an enrichment of B-MYB at their promoters. But to what extent does B-MYB contribute to the increased G2/M gene expression? To address this question, I depleted B-MYB from p53 +/+ and p53 -/- cells, treated them with doxorubicin and performed qPCR analysis (Fig. 3.18 A). On RNA level, depletion of B-MYB resulted in a knock down from about 50 - 80 %. Cellular B-MYB expression levels decreased in p53 +/+ cells after treatment with doxorubicin and are further decreased by depletion of B-MYB. In untreated p53 -/- cells B-MYB expression levels were already increased compared to p53 +/+ cells but were even higher after doxorubicin treatment. Depletion of B-MYB in p53 -/- cells did not completely inhibit upregulation of B-MYB expression after DNA damage induction but reduced it significantly. In both tested cell lines, no effect on gene expression due to B-MYB depletion could be detected for PCNA, a G1/S gene known to be not responsive to B-MYB.

G2/M gene expression of p53 +/+ cells decreased after DNA damage induction when a ctrl siRNA was used and further decreased after depletion of B-MYB. In p53 -/- however, G2/M gene expression as well as B-MYB expression increased after doxorubicin treatment showing the same effect as in Figure 3.11. Strikingly in 53 -/- cells, depletion of B-MYB partially inhibited the DNA damage-induced increase in G2/M gene expression, e.g. Birc5, cdc2 (cdk1) and Ubch10. More precisely, by depletion of B-MYB I diminished target gene expression about 40 – 60 %. As depicted in Figure 3.18 B, also on protein level the effect of B-MYB depletion was clearly detectable. In p53 +/+ cells, B-MYB depletion led to a stronger decrease in protein levels of cdc2 (cdk1) and cyclin B1. Similarly, in p53 -/- cells depletion of B-MYB resulted in a decrease of cdc2 (cdk1) and cyclin B1 protein levels when compared to p53 -/- cells treated with a control siRNA.

This indicates that B-MYB plays at least a partial role in the upregulation of G2/M gene expression in p53 -/- cells after DNA damage induction.

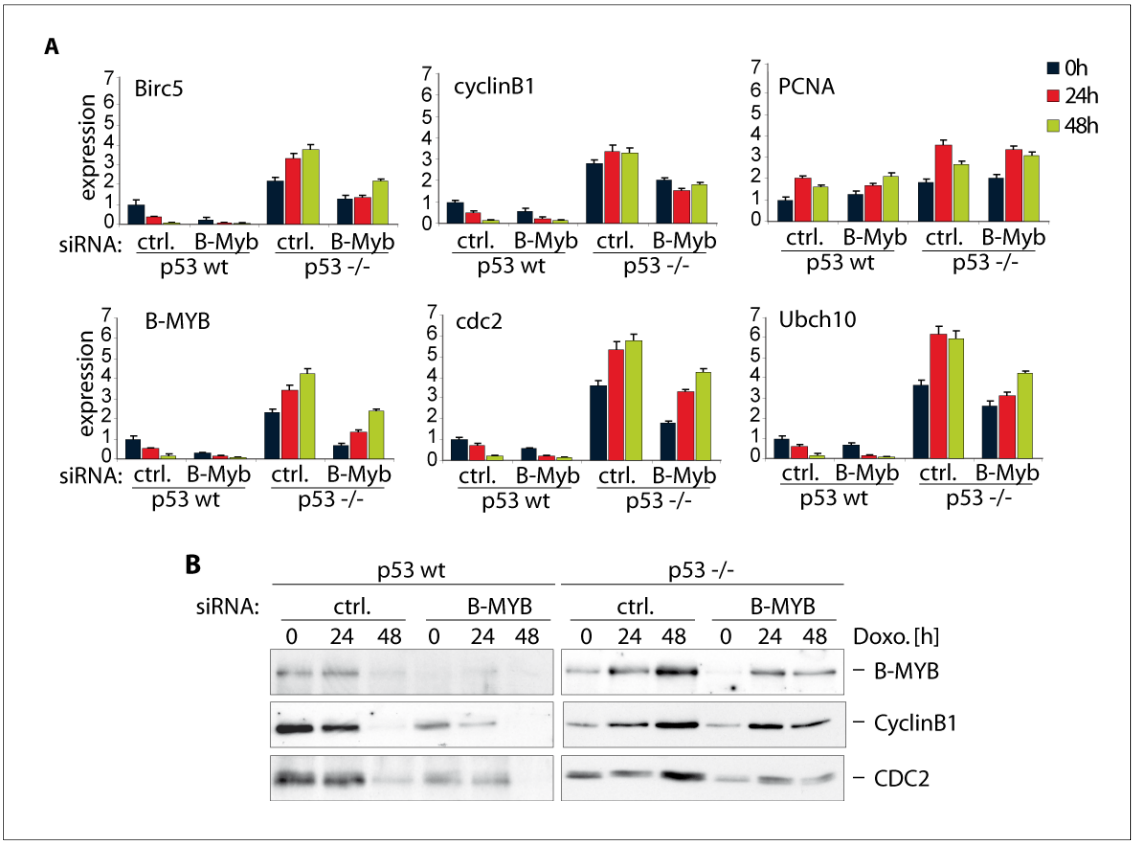

Figure 3.18: B-MYB is involved in upregulation of G2/M gene expression in HCT-116 p53 -/- cells after doxorubicin treatment

HCT-116 p53 +/+ and -/- cells were treated either with a control siRNA (ctrl) or a siRNA directed against B-MYB (B-MYB). After depletion, both cell lines were left untreated (blue bars) or treated with doxorubicin for 2 h, washed twice with 1 x PBS and left growing for 24 h (red bars) or 48 h (green bars). (A) RNA was purified and cDNA synthesized. Gene expression was quantified via qPCR analysis using primers annealing in regions of G2/M genes (Birc5, cyclin B1, Ubch10, cdc2 (cdk1)), G1/S genes (B-MYB, PCNA) or unregulated control genes (S14). Target gene expression is shown compared to S14 expression. (B) Amounts of protein were detected via immunoblotting using the antibodies indicated on the right.

It is known that B-MYB associates with LINC in the S phase of the cell cycle. In this period, B-MYB and LINC bind to G2/M gene promoters leading to the activation of G2/M gene expression (Schmit, Korenjak et al. 2007). To examine if the activation of G2/M gene expression after doxorubicin treatment in p53 -/- cells is an isolated function of B-MYB (Fig. 3.18) or mediated by the LIN complex, I depleted LIN-9 by siRNA. Additionally, to analyze if LIN-9 and B-MYB have additive functions in increasing the G2/M gene expression in p53 –/- cells after DNA damage induction, a double knock down of these two proteins

was established. Therefore, I again used HCT-116 p53 -/- cells, depleted either one of the two proteins or both proteins simultaneously and checked gene expression profiles via qPCR (Fig. 3.19 A). To verify the knock down, LIN-9 and B-MYB expression levels were also tested, showing that LIN-9 expression was decreased about 80 % and B-MYB expression about 60 - 80% in both the single and the double knock down experiment.

After doxorubicin treatment, B-MYB depletion – as shown before in Figure 3.18 – led again to a decrease in gene expression of Birc5, cyclin B1 and Ubch10 when compared to ctrl siRNA treated p53 -/- cells. Strikingly, gene expression of the tested G2/M genes was also significantly reduced in LIN-9 depleted cells. Depletion of both proteins simultaneously did not show an additional decrease in G2/M gene expression when compared to the levels of gene expression after LIN-9 or B-MYB depletion alone. Gene expression of PCNA did not change significantly independently of which siRNA was used. Importantly, the described effects were also apparent on protein level (Fig. 3.19 B). Altogether this strongly suggests that increased G2/M gene expression in p53 -/- cells after DNA damage induction is not only dependent on B-MYB function but is in fact due to the activating LIN complex.

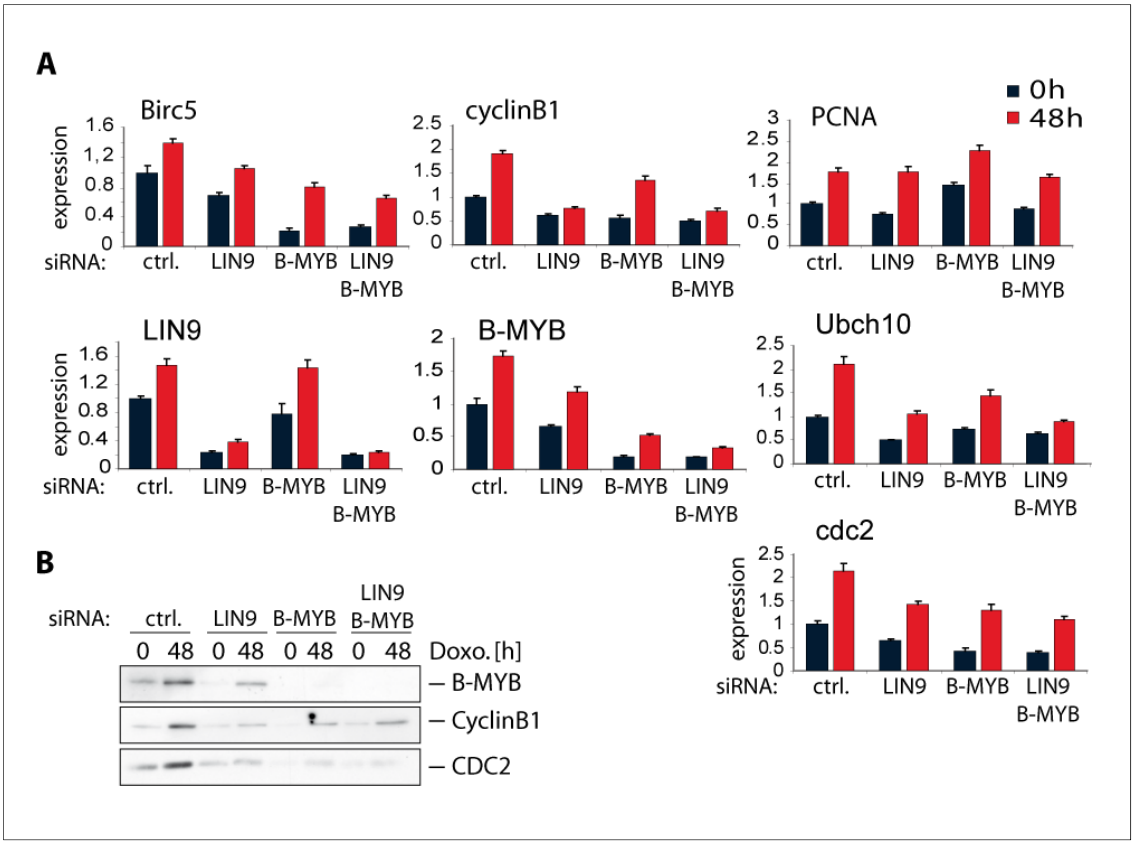

Figure 3.19: G2/M target gene levels after depletion of B-MYB and/or LIN-9 and doxorubicin treatment in HCT-116 p53 -/- cells

HCT-116 p53 -/- cells were treated with siRNAs either directed against a control gene (ctrl), LIN-9 (LIN-9), B-MYB (B-MYB) or both genes (LIN-9 + B-MYB). After treatment with doxorubicin for 2 h, the cells were washed twice with 1 x PBS and left growing in normal medium for 48 h (red bars). Gene expression of cells not treated with doxorubicin is shown by the blue bars. (A) RNA was purified and cDNA synthesized. Gene expression was quantified via qPCR analysis using primers annealing in regions of G2/M genes (Birc5, cyclin B1, Ubch10, cdc2 (cdk1)), G1/S genes (B-MYB, PCNA), the LIN-9 gene (LIN-9) or unregulated control genes (S14). Target gene expression is shown compared to S14 expression. (B) Amounts of protein were detected via immunoblotting using the antibodies indicated on the right.

3.4 Premature mitotic entry of p53 negative cells after DNA damage partially depends on B-MYB and LIN-9

Considering that B-MYB and LIN-9 are responsible for the increased expression of G2/M genes in p53 -/- cells after DNA damage induction, I finally wanted to get more information about the biological relevance of this effect. It is known that p53 -/- cells are able to arrest only temporary in G2 phase of the cell cycle after DNA damage, an effect also called checkpoint recovery or adaptation depending on the existence of remaining DNA damage (Bunz, Dutriaux et al. 1998; Bartek and Lukas 2007). I assumed that this is probably due to the increased G2/M gene expression (Fig. 3.11) resulting from an increased binding

of B-MYB to the promoters of these genes (Fig. 3.14, 3.15). To test this possibility, I first checked if p53 -/- cells compared to p53 +/+ cells exhibit a shortened G2 arrest when treated with doxorubicin (Fig. 3.20 A). Therefore, I stained the cells for phospho-histone H3 (PH3), a marker for early mitotic cells, and quantified the cell population using FACS analysis. As shown in Figure 3.20 A, p53 +/+ cells did not enter mitosis until 96 h after DNA damage induction. In contrast, a small fraction of p53 -/- cells were released into the cell cycle approximately 40 h after DNA damage induction. This indicates that the maintenance of the DNA damage-induced G2 block is disrupted in a small fraction of p53 -/- cells probably due to increased G2/M gene expression after DNA damage seen before (Fig. 3.11). Inhibition of LINC switch and the increased binding of B-MYB to LIN-9 in p53 -/- cells after DNA damage, effects also detectable on promoter level, probably causes this increased G2/M gene expression.

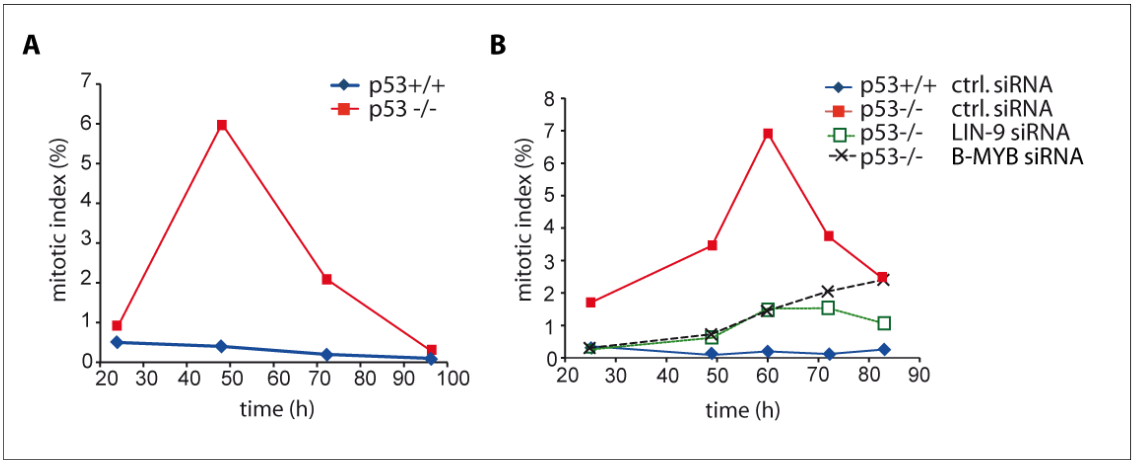

Figure 3.20: Mitotic index of HCT-116 cells after doxorubicin treatment

(A) HCT-116 p53 +/+ and p53 -/- cells were treated with 1 µM doxorubicin for 2 h, washed twice with 1 x PBS and left growing in normal medium fort he indicated times. Cells were stained with PI and an antibody directed against PH3 and measured using FACS analysis. Mitotic cells are displayed as mitotic index (amount of mitotic cells within the whole cell population in percent). (B) HCT-116 p53 -/- cells were treated with siRNAs either directed against a control gene (ctrl), LIN-9 (LIN-9) or B-MYB (B-MYB). After treatment with doxorubicin for 2 h, the cells were washed twice with 1 x PBS and left growing in normal medium for the indicated time. Staining and measurement was performed as illustrated in (A).

To address the question if LIN-9 and B-MYB are responsible for G2 checkpoint recovery in p53 -/- cells (Fig. 3.20 A), I depleted one of the two proteins using siRNA, treated the cells with doxorubicin and again quantified the amount of mitotic cells via FACS analysis. As shown in Figure 3.20 B, p53 +/+ cells

arrested in the G2 phase of the cell cycle until 82 h after DNA damage induction. In contrast, p53 -/- cells reentered the cell cycle about 50 h after treatment with doxorubicin. Even though the mitotic index was higher in LIN-9 and B-MYB depleted p53 -/- cells (1.5 %) compared with p53 +/+ cells (< 0.5 %), I could nevertheless reduce the amount of mitotic cells by B-MYB or LIN-9 depletion compared to p53 -/- cells treated with control siRNA (7 %). Strikingly, in p53 -/- cells depletion of either B-MYB or LIN-9 diminished mitotic entry after DNA damage induction suggesting that LINC together with B-MYB at least partially contributes to checkpoint recovery in p53 -/- cells.

3.5 B-MYB in primary breast tumors

As shown before, B-MYB is essential for p53 negative cells to escape G2/M arrest and enter mitosis. Additionally, from literature it is known that B-MYB expression levels are upregulated in breast cancer cells and can predict the probability of tumor reoccurrence (Bertucci, Houlgatte et al. 2000; Sorlie, Perou et al. 2001; Sotiriou, Neo et al. 2003; Amatschek, Koenig et al. 2004). To substantiate the relevance of these observations I re-evaluated microarray data sets from primary breast tumors (Fig. 3.21). I therefore examined three different breast cancer microarray data sets in which the p53 status and B-MYB levels were reported. First, I plotted B-MYB expression levels against p53 status and showed that B-MYB expression levels are consistently upregulated in p53 mutant tumors when compared to B-MYB gene expression levels in p53 wt tumors (Fig. 3.21 A). Secondly, high B-MYB expression levels not only correlated with the p53 status but also with the severity of the disease (Fig. 3.21 B). In p53 wildtype tumors in which B-MYB levels were mainly decreased compared to the average, the tumor was mostly characterized as not aggressive but as well-differentiated by classification according to elston grade. In contrast, high B-MYB levels in p53 mutated tumors had a dramatic effect on the histological grade. Nearly all of these tested tumors were characterized as aggressive and poorly differentiated resulting in a poor prognosis. Additionally, B-MYB expression levels also correlated with LINC target gene expression such as cyclin B1 and cdk1 (Fig. 3.21 C). Breast cancer tumors with high B-MYB levels also showed increased expression of LINC target genes such as cyclin

B1 and cdk1. In contrast, G1/S gene expression levels shown by the expression of dihydrofolate deductase (DHFR) were not altered in tumors with high B-MYB levels and did not correlate with the p53 status of breast cancer tumors. This examination showed how the severity of breast cancer tumors is determined by B-MYB and thereby LINC target gene expression levels, whereas both were increased in tumors carrying p53 mutations.

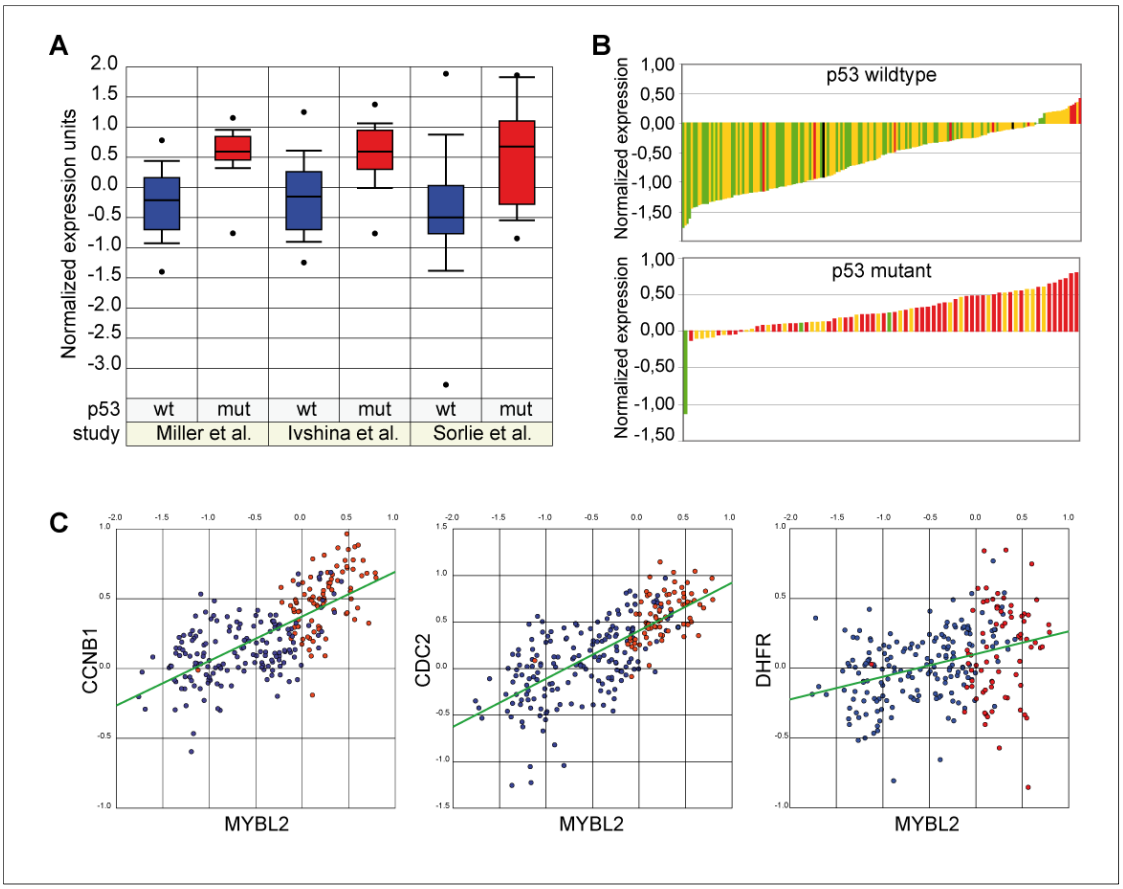

Figure 3.21: Expression levels of B-MYB and B-MYB target genes in p53 negative tumor samples

(A) B-MYB expression is dependent on the p53 status in primary human breast cancers. Three microarray data sets in which the p53 status were denoted were examined (Sorlie, Perou et al. 2001; Miller, Smeds et al. 2005; Ivshina, George et al. 2006). Relative B-MYB expression level was compared with the average as determined by the global mean method. (B) B-MYB expression levels were plotted against the p53 status and the histologic grade classified by elston grade (Miller, Smeds et al. 2005). Green, Elston grade 1; yellow, Elston grade 2; red, Elston grade 3. (C) Correlation between B-MYB expression, p53 status and LINC target gene (cyclin B1, cdk1) or G1/S gene (DHFR) expression in human breast cancer (Miller, Smeds et al. 2005).

4 Discussion

The mammalian LIN core complex is composed of 5 different proteins which can associate with B-MYB or E2F4 and p130 in a cell cycle dependent manner. During G0, LINC binds together with E2F4 and p130 to G2/M gene promoters at a time when their gene expression is repressed. In contrast, during S phase LINC/B-MYB binds at the G2/M promoters and contributes to the activation of G2/M gene expression (Schmit, Korenjak et al. 2007). After DNA damage, cells arrest within the cell cycle during G1 or G2 phase to enable DNA-repair or, if the damage cannot repaired, induction of apoptosis. Correct down regulation of G2/M gene expression after induction of DNA damage is needed for sustained G2 arrest and is known to be dependent on p130- and E2F4-binding to their promoters (Badie, Itzhaki et al. 2000; Lange-zu Dohna, Brandeis et al. 2000; Crosby, Jacobberger et al. 2007; Plesca, Crosby et al. 2007). Because E2F4 and p130 are known components of LINC during G0 and because LINC is known to regulate G2/M gene expression during cell cycle progression, this work addressed the question if LINC plays a role in the decrease of G2/M gene expression after induction of DNA damage.

Several lines of evidence suggest that LINC plays an important part in the DNA damage response. LINC changes its composition from a B-MYB containing complex in growing cells to a p130 containing complex in DNA damaged cells (Fig. 3.1 and 3.3). Secondly, this rearrangement is reflected on promoters of LINC target genes as demonstrated by ChIP (Fig. 3.13). Finally, LINC rearrangement correlates with reduced expression of target genes (Fig. 3.10) thereby probably contributing to a sustained G2 arrest.

Because LINC composition changed before major effects on cell cycle distribution were detectable, LINC rearrangement is unlikely an indirect effect triggered by cell cycle inhibition (Fig. 3.1). The hypothesis that LINC switch is induced independently of cell cycle inhibition is also supported by the observation that the LINC switch was not only detectable in cells mainly blocking in G1 phase of the cell cycle such as MCF-7 cells (Fig. 3.1 and 3.9) but also detectable in DNA damaged synchronized U2OS cells mainly blocking in

G2 (Fig. 3.5). Together, this indicates that the LINC rearrangement is not induced by a block in the G1 phase of the cell cycle. Additionally, LINC rearrangement is not induced indirectly by a cell cycle arrest in G2 since HCT-116 cells deficient in p21 -/- and p53 -/-, like wt cells block in G2 (Fig. 3.7, 3.8, 3.16) (Waldman, Kinzler et al. 1995; Bunz, Dutriaux et al. 1998) but only in wildtype cells a change in LINC composition after DNA damage was observed.

Interestingly, LINC rearrangement is not restricted to the G2/M checkpoint response but is also induced in cells mainly blocking in G1. This could possibly demonstrate a failsafe mechanism which is responsible to catch cells which escaped the G1 block thereby inhibiting entry into mitosis. This hypothesis is supported by the fact that LINC rearrangement contributes to the repression of G2/M genes in G1 arrested cells (Fig. 3.10).

4.1 How does the composition of LINC switch in response to DNA-damage?

Similar to the situation during cell cycle progression (Schmit, Korenjak et al. 2007), during the DNA damage-induced rearrangement, composition of the LIN core complex remained constant - independently of the associated protein (Fig. 3.2). By treatment with etoposide and cisplatin I could show that LINC rearrangement is not dependent on a specific agent but is rather a general phenomenon after DNA damage induction (Fig. 3.3).

The upstream pathway which mediates LINC rearrangement is dependent on the activation of p53 and p21, since HCT-116 cells deficient for p53 or p21 do not show a change in LINC composition after DNA damage induction. Additionally, this finding is supported by the fact that the repression of many G2/M genes following DNA damage is dependent on the function of p53 and p21 (Azzam, de Toledo et al. 1997; de Toledo, Azzam et al. 1998; Taylor, Schonthal et al. 2001). Since Nutlin-3 treatment, which activates p53 without inducing DNA damage, is sufficient to induce p130 binding to LIN-9, it is unlikely that other pathways are involved in passing the signal upstream of LINC.

Concerning the mechanism leading to LINC switch, it appears that dephosphorylation of p130 could play an important role in inducing LINC reorganization. This finding is supported by the fact that LIN-9 can only bind to the faster migrating hypophosphorylated form of p130 and not to the hyperphosphorylated form present in untreated cells (Fig. 3.1 A, 3.2 A, 3.3 A, 3.5 A and 3.6). Additionally, the fact that LINC rearrangement is dependent on p21 and moreover, that p21 activation can – by inhibition of cyclin-cdk complexes - lead to p130 dephosphorylation supports the idea that p130 dephosphorylation enables its binding LINC (Fig. 3.6). It is already known, that 9 out of 22 phosphorylation sites within the p130 protein have to be dephosphorylated to enable binding to E2F4 (Farkas, Hansen et al. 2002). Furthermore, genotoxic stress as well as oxidative stress are known trigger for p130 dephosphorylation and induction of E2F4 binding (Cicchillitti, Fasanaro et al. 2003; DuPree, Mazumder et al. 2004; Crosby, Jacobberger et al. 2007). The fact that binding of E2F4 to p130 is regulated by p130 phosphorylation and additionally, E2F4 and p130 both associate to LINC after DNA damage induction supports the idea that p130 binding to LIN-9 is also regulated by phosphorylation. So far it is not clear if p130 has to be completely dephosphorylated to bind to LIN-9. Based data obtained in U2OS cells, suggest that p130 has to be partially phosphorylated for binding to LIN9 because nocodazole treatment in U2OS cells seems to induce almost complete dephosphorylation of p130 compared to doxorubicin treated cells but did not induce p130 binding to LIN-9 (Fig. 3.5). Mechanistically, partially de-phosphorylated p130 could displace B-MYB from LINC after DNA damage induction. Consistent with this notion, B-MYB and p130 cannot be found in the same complex at any time point tested after DNA damage induction (Fig. 3.4).

4.2 LINC function in DNA damage response

Data in this thesis support the idea that changes in LINC composition play a role in the transcriptional repression of G2/M genes in response to DNA damage. This notion is supported by published studies showing that pocket proteins and E2F4 are involved in DNA damage response and DNA damage induced cell cycle arrest (Badie, Itzhaki et al. 2000; Lange-zu Dohna, Brandeis

et al. 2000; Taylor, Schonthal et al. 2001; Polager and Ginsberg 2003; Jackson, Agarwal et al. 2005). By repressing many G2/M genes, E2F4 and p130 contribute to the maintenance of the DNA damage induced G2 arrest (Taylor, Schonthal et al. 2001; Jackson, Agarwal et al. 2005). So far it is not clear, if the decreased binding of B-MYB or the stronger binding of p130 to LIN-9 or both effects together are crucial for LINC function in G2/M gene repression (Fig. 3.13). First, to test whether E2F4-p130/LINC directly contributes to G2/M gene repression, DNA damage has to be induced in LIN-9 depleted p53 +/+ cells and in parallel gene expression has to be analyzed.

Conceivable, E2F4 and p130 could, additionally to their function together with LINC, function in G2/M gene repression independently or together with other complexes than LINC. In different breast cancer cell lines as well as neuronal cell lines, complexes containing p130, E2F4, HDACs, SUV39 H1, p300 or DNMT1 were found, showing that p130 and E2F4 could repress G2/M gene expression by recruitment of chromatin modifying complexes/proteins (Macaluso, Cinti et al. 2003; Liu, Nath et al. 2005). Therefore, the additional question is, whether E2F4- and p130-function after DNA damage induction is restricted to their binding to LINC possibly together with some chromatin modifying proteins or whether E2F4 and p130 proteins can additionally be found in other complexes than LINC-containing ones. To address this question, p130 containing complexes have to be purified and the associated proteins identified.

Our results suggest that LINC is rather involved in maintaining the G2 arrest than in its induction. It is known, that the induction of a G2 arrest is not dependent on transcriptional regulation but triggered by phosphorylation events which lead to the inhibition of cyclin-cdk complexes thereby avoiding cdc25c activation (see Introduction). Moreover, E2F4- and p130-mediated repression of G2/M gene expression, is known to be absolute essential for maintaining an otherwise shortened G2 arrest (see Introduction). Although LINC switch is absent in HCT-116 p53 -/- and p21 -/- cells, the cells are still able to induce an arrest in G2 which supports the idea that LINC – by influencing G2/M gene expression – is a regulator of the G2 checkpoint maintenance rather than the checkpoint initiation. Since p53 -/- cells display an increased G2/M gene

expression after DNA damage induction (Fig. 3.11) and an enrichment of B-MYB at the G2/M gene promoters (Fig. 3.14, 3.15), I assume that the loss of a proper LINC switch directly prevents/impedes a proper G2/M gene repression. Importantly, by depletion of B-MYB and/or LIN-9 we found that the combined function of these proteins together contributes to the increased G2/M gene expression in p53 -/- cells after treatment with doxorubicin (Fig. 3.18, 3.19)(Bunz, Dutriaux et al. 1998; Taylor, Schonthal et al. 2001).

On the one hand, the impact of B-MYB and LINC on G2/M gene expression could be due to the increased B-MYB expression (Fig. 3.11) consequently leading to an increased binding of B-MYB to LIN-9 (Fig. 3.8) and enrichment of B-MYB at the G2/M gene promoters (Fig. 3.14, 3.15) thereby possibly directly activating target gene expression. On the other hand, increased G2/M gene expression in p53 -/- cells after DNA damage induction can be due to the decreased binding of E2F4-p130/LINC to target gene promoters (Fig. 3.14, 3.15). Even the fact that B-MYB depletion itself leads to a decrease in G2/M target gene expression does not exclude the possibility that B-MYB depletion could indirectly lead to an increased association of E2F4-p130/LINC to target gene promoters thereby enabling E2F4- and p130-dependent gene repression. To test this hypothesis, ChIP experiments using B-MYB depleted HCT-116 p53 -/- cells should be performed to see if B-MYB depletion leads to the increased enrichment of E2F4 and p130 to the target gene promoters.

I speculated that the B-MYB- and LINC-dependent increased G2/M gene expression in p53 -/- cells after DNA damage could be a trigger for the premature cell cycle re-entry seen in this cell line (Fig. 3.20). Indeed, by depletion of LIN-9 and B-MYB in p53 -/- cells I could show that LINC together with B-MYB contributes to the premature cell cycle re-entry of p53 -/- cells after DNA damage induction.

The function of B-MYB together with LINC in promoting premature cell cycle re-entry is probably directly linked to its ability to upregulate the transcription of mitotic genes and supported by the finding that B-MYB depletion partially inhibited G2/M gene activation in p53 -/- cells. High B-MYB levels lead to an

increased target gene expression which in turn could contribute to premature cell cycle re-entry. This hypothesis is supported by the finding that high levels of cyclin B1, a B-MYB/LINC target, are known to shorten the G2 checkpoint in HeLa cells (Ianzini and Mackey 1997; Kao, McKenna et al. 1997). But more important, our results suggest that LINC together with B-MYB activates Plk1 expression in p53 -/- cells after DNA damage thereby leading to a premature cell cycle re-entry. Plk1 is a key protein responsible for checkpoint recovery as well as checkpoint adaptation. As mentioned before, Plk1 is one of the genes whose expression is repressed by p53, p21, E2F4 and p130 after DNA damage thereby contributing to a sustained G2 arrest supporting the idea that Plk-1 could be the key protein responsible for premature cell cycle re-entry induced by B-MYB/LINC-dependent gene activation. So far, regulation of Plk1 itself during checkpoint recovery and checkpoint activation is not completely clear. Solely, Aurora A, another LINC target gene, is known to be involved in Plk-1 activation before checkpoint recovery occurs (Macurek, Lindqvist et al. 2008). Additionally, during normal cell cycle progression Aurora A and Bora cooperatively activate Plk1 by phosphorylation resulting in mitotic entry (Seki, Coppinger et al. 2008). With premature B-MYB/LINC activation, we provide a mechanism of how premature activation of Plk1 in p53 -/- cells after DNA damage could be induced.

Since a double knockdown of B-MYB and LIN-9 did not show additive effects in G2/M gene expression I assume that B-MYB and LIN-9 function in the same pathway, or rather, that the effect of B-MYB on G2/M gene expression is due to the function of the activating LIN complex. Additionally, depletion of either B-MYB or LIN-9, reduced cell cycle re-entry of p53 -/- cells after DNA damage, suggesting that premature cell cycle re-entry is no isolated function of B-MYB opposed to transcription-independent B-MYB function such as the recently reported function of the MYB-Clafi complex (Yamauchi, Ishidao et al. 2008). To confirm that activation of G2/M gene expression after DNA damage induction in p53 -/- cells and consequent premature cell cycle re-entry is due to LINC function, other LINC members such as LIN-54 and LIN-52 could be depleted and premature cell cycle re-entry analyzed by PH3 staining.

Furthermore, I assume that the premature cell cycle re-entry as a consequence of B-MYB and LINC function has to be termed as checkpoint adaptation since doxorubicin treatment of p53 +/+ and p53 -/- cells should lead to the same or at least comparable amount of DNA damage and additionally p53 +/+ cells did not enter mitosis prematurely after DNA damage within the tested period. To assure this hypothesis, γH2AX staining has to be performed in p53 -/- cells after entry into mitosis was initiated to see if p53 -/- cells re-enter cell cycle with (adaptation) or without (recovery) DNA damage.

Whether premature cell cycle re-entry after DNA damage induction seen in p53 -/- cells removes unfixable defective cells by “mitotic catastrophe” or “mitosis-linked cell death” is still questionable (Bartek and Lukas 2007). Especially when considering the resulting consequences whenever damaged cells survive this kind of cell death it rather seems that premature cell cycle re-entry is not a controlled cellular process but is mainly due to failures in checkpoint regulation such as premature activation of Plk1 e.g. due to prematurely arising activating LIN complex (see 4.3). Therefore, the next step is to unravel the effects of premature cell cycle re-entry on tumor cell survival and in the first step mainly address the question, if doxorubicin treated p53 -/- cells enter the G1 phase of the next cell cycle or die during mitosis due to mitotic catastrophe (Fig. 4.1).

In case those damaged cells are not eliminated by mitotic catastrophe the resulting consequences can be disastrous for intact cell survival. Thus, accelerated progression through the cell cycle before DNA damage repair is completed probably leads to the accumulation of errors and probably facilitates tumor development and progression without the possibility to eliminate the cells by apoptosis. In the end this would lead to impaired/worsened therapy/treatment options and hence to a bad prognosis and perhaps reoccurrence. Based on our findings, it seems possible that overexpression of B-MYB in p53 mutant tumors allows premature cell cycle restart and thus proliferation of cells with damaged DNA which could contribute to genomic instability and thereby lead to transformation events. So far, only a loss of B-MYB function was implicated with increased genomic instability due to its

function in G2/M gene expression and additionally, its function during mitosis at the mitotic spindle within the MYB-Clafi-complex.

Importantly, similar to reduced B-MYB activity, also high B-MYB expression levels, by inducing transcriptional activation of target genes, could lead to errors during mitosis. In turn, the resulting acceleration of cell cycle progression could contribute to genomic instability. E.g. for the E2F target gene Mad2 it is known that its exact regulation is absolutely essential for proper mitosis and therefore maintenance of genomic stability. Deregulation in either direction was shown to induce aneuploidy (Hernando, Nahle et al. 2004; Orr, Bousbaa et al. 2007; Sotillo, Hernando et al. 2007). The fact that defects in mitosis can lead to aneuploidy and additionally, that B-MYB regulates expression of genes important for proper mitosis supports the idea, that B-MYB deregulation in general can induce genomic instability probably by influencing target gene expression such as cyclin B, Plk1 and others. Importantly, it is known that overexpression of cyclin B, which is a B-MYB/LINC target gene, can lead to tetraploidy (Yin, Grove et al. 2001) and that Plk-1 is necessary for maintaining genomic stability during mitosis (Feng, Lin et al. 2009). Additionally, Plk1 overexpression in bladder cancer was associated with chromosomal instability and aneuploidy (Yamamoto, Matsuyama et al. 2006). Also Aurora A, another B-MYB/LINC target gene, was reported to induce chromosomal instability (Sen, Katayama et al. 2008).

4.3 LINC function in tumors

Since p53 -/- cells lack a proper G1 arrest, they are strongly dependent on a functional G2 checkpoint (Fig. 3.8 (Li, Nagasawa et al. 1995)). But p53 -/- cells show a weakened G2 checkpoint during which the DNA damage induced G2 arrest is disrupted in the end leading to a premature entry into mitosis due to B-MYB and LINC activity (Fig. 3.20). As mentioned in the previous section, checkpoint adaptation due to increased B-MYB expression in p53 -/- cells could negatively influence cancer therapy and thereby support reoccurrence through several mechanisms. Therefore, the next section discusses the clinical

relevance of increased B–MYB expression levels seen in p53 mutant tumors regarding the resulting consequences for prognosis.

By examination of microarray data sets (Fig. 3.21) I found that increased B-MYB expression levels are often found in breast cancer tumors deficient for p53 (Fig.3.21) and correlate with increased LINC target gene expression such as cyclin B1 and cdc2. In contrast, G1/S gene expression levels such as DHFR are independent of B-MYB expression levels (Fig. 3.21 C). Additionally, in Figure 3.11, I showed that not only G2/M gene expression but also B-MYB expression levels are increased after DNA damage induction in p53 -/- colon cancer cells. Supporting our hypothesis that B-MYB expression levels in cancer cells are often elevated due to the loss of p53-dependent repressive effects, also in bladder cancer high B-MYB expression levels were correlated with a p53 mutant status (Lindgren, Liedberg et al. 2006). Additionally, numerous hepatocellular carcinomas (HCC) display high levels of B-MYB expression. Importantly, these tumors frequently contain mutations within the p53 gene (He, Tang et al. 1996; Chen, Merchant et al. 2003).

Whether B-MYB levels are increased as a result of p53 deficiency and if so, how B-MYB levels are increased in p53 deficient cells is not clear so far. Since transcriptional activation of B-MYB is regulated by the family of E2F transcription factors, it seems possible, that – after DNA damage induction - loss of cdk inhibition due to p53 deficiency triggers phosphorylation of pocket proteins thereby allowing transcriptional activation of B-MYB by E2F1-3 (Takahashi, Rayman et al. 2000; Wells, Boyd et al. 2000). Simultaneously, loss of cdk inhibition leads to the disruption of E2F4-p130 complexes which in turn impedes target gene repression of genes such as B-MYB (Liu, Lucibello et al. 1996). Importantly, E2F1 depletion in hepatocellular carcinoma cell lines results in a significant decrease in B-MYB expression (Nakajima, Yasui et al. 2008). Additionally, deregulation of E2F1 is observed in many different cancers, including hepatocellular carcinoma (HCC), and directly correlates with high B-MYB expression levels (Nakajima, Yasui et al. 2008). A function of E2F1 together with the nuclear epidermal growth factor receptor (EGFR) in increasing B-MYB expression was postulated before (Hanada, Lo et al. 2006) supporting

the hypothesis that B-MYB expression is increased in p53 -/- or mutant cells after DNA damage induction due to E2F1 activity. The fact that expression of HPV-16 E7, a known pocket protein inhibitor, activates B-MYB transcription supports the hypothesis that missing pocket protein function due to cdk-dependent inhibition can lead to increased B-MYB expression (Lam, Morris et al. 1994; Lin, Fiscella et al. 1994). Additionally, overexpression of p53 correlates with decreased B-MYB expression levels during G1 arrest indicating that p53-dependent pathways indirectly contribute to B-MYB transcriptional regulation (Lin, Fiscella et al. 1994). But moreover, a pathway which is based on E2F1 activation due to cdk-mediated pocket protein inhibition would also affect transcriptional activation of other G1/S genes which are under the control of E2F transcription factors. Because neither the gene expression data (Fig. 3.11, 3.18, 3.19) nor the microarray data (Fig. 3.21) showed a obvious correlation between G1/S gene expression and the p53 status, it seems that increased B-MYB expression levels are at least partially due to different mechanisms. This hypothesis is supported by the recent finding that p53-dependent activation of microRNAs such as mir-34 play an important role in the DNA damage response by regulating transcription of genes relevant in tumor development in mammalian cells as well as *C. elegans* (Bommer, Gerin et al. 2007; Kato, Paranjape et al. 2009). After mir-34 activation a decreased phosphorylation of the retinoblastoma tumor suppressor (pRb) was reported. Importantly, MYB was shown to be repressed either directly due to mir-34b/c activation (Toyota, Suzuki et al. 2008) or by mir-34-dependent silencing of E2F3 expression (He, He et al. 2007). It would be interesting to analyze whether increased B-MYB expression levels seen in p53 -/- cells after DNA damage induction are – at least partially - dependent on the loss of mir-34 activation. Therefore, B-MYB expression in mir-34-inhibited p53 +/+ cells or additionally, since mir-34 activation is not dependent on p21 activation, B-MYB expression in HCT-116 p21 -/- cells has to be analyzed after DNA damage induction.

Conceivable, a copy-number gain of the B-MYB gene as seen in hepatocellular, breast, liver and ovarian carcinomas could also in other cancers contribute to increased B-MYB levels (Sala 2005). Additional to transcriptional regulation, B-

MYB levels also regulated on protein level. Because B-MYB mRNA is relatively stable, regulation on protein level is mainly mediated by regulating its degradation. It is known that degradation of B-MYB is increased by cyclin A dependent phosphorylation at its C terminus (Charrasse, Carena et al. 2000). Additionally, it was shown that hypophosphorylated B-MYB in neuroblastoma cells is resistant to degradation. Interestingly, cyclin D, by direct binding to B-MYB, on the one hand inhibits B-MYB activity by inhibiting its phosphorylation and on the other hand increases its stability (Schwab, Caccamo et al. 2007). Interestingly, alterations in the cyclin D1-pRb pathway are known to be hallmarks of human cancer (Nakajima, Yasui et al. 2008). Additionally, it was postulated before, that p53 is able to repress cyclin D1 transcription (Rocha, Martin et al. 2003). Therefore, in p53 mutant cells, cyclin D1 gene repression is lost, thereby contributing to an increased B-MYB stability. Nevertheless, it has to be analyzed whether B-MYB, when bound to cyclin D, is accessible for LINC and able to fulfill its function together with LINC after induction of the DNA damage response in p53 -/- cells. Additionally, the half-life of B-MYB should be compared between HCT-116 wt and p53 -/- cells after doxorubicin treatment to detect potential differences in the regulation of B-MYB degradation. Conceivable, cooperation of several pathways could lead to an increased B-MYB gene expression or activity - on the one hand by transcriptional activation and on the other hand by inhibiting B-MYB degradation.

Importantly, B-MYB levels do not only correlate with the p53 status of breast cancer tumors but additionally correlate with the severity of the disease. Several studies showed that B-MYB expression levels are upregulated in breast cancer cells and predict the probability of tumor reoccurrence (Bertucci, Houlgatte et al. 2000; Sorlie, Perou et al. 2001; Sotiriou, Neo et al. 2003; Amatschek, Koenig et al. 2004). Additionally, Ahlbory and colleagues could show that chicken DT40 cells lacking B-MYB are more sensitive to DNA damage-induced UV radiation and alkylation (Ahlbory, Appl et al. 2005). In the study of Thorner et al, high B-MYB expression levels were shown to decrease the probability of relapse-free and overall survival in breast cancer patients.

Additionally, overexpression of Plk-1, a B-MYB/LINC target gene, is reported for many cancers such as colorectal cancer, esophageal squamous cell carcinoma and non-small cell lung cancer and often correlates with poor prognosis (Wolf, Elez et al. 1997; Takahashi, Sano et al. 2003; Feng, Lin et al. 2009). Importantly, Kanaji and colleagues demonstrated that Plk1 expression was significantly associated with a poorer prognosis for gastric carcinoma (Kanaji, Saito et al. 2006). This supports our hypothesis that Plk1 could be the key target of B-MYB responsible for premature cell cycle re-entry and thereby leading to a poorer prognosis.

Even though no data regarding the correlation between prognosis, B-MYB expression levels and p53 status are available for colon tumors, our obtained data from HCT-116 cells and the postulated mechanism seem to be relevant for the therapy of tumors with high B-MYB expression levels in general. E.g. B-MYB expression is increased in metastatic vs. localized prostate tumors supporting the finding that B-MYB correlates with poor prognosis also in other cancer types than breast tumors (Sala 2005). In neuroblastoma, high B-MYB expression levels were associated with an increased risk of death (Raschella, Cesi et al. 1999). Additionally, numerous hepatocellular carcinomas (HCC) display high levels of B-MYB expression. Importantly, these tumors frequently contain mutations within the p53 gene which in turn correlates with a shortened interval between surgical resection and the appearance of recurrence (He, Tang et al. 1996; Chen, Merchant et al. 2003). The fact that expression of B-MYB as well as target genes such as Plk1 are deregulated in many tumors and often correlate with poor prognosis and additionally, that high B-MYB expression levels are also found in colon carcinomas (Ki, Jeung et al. 2007), supports the hypothesis that our obtained data are not only relevant in breast cancer tumors but more importantly, supports the idea that the presented mechanism can be applied to different types of cancer.

In the case of B-MYB being a predictor of reoccurrence and bad prognosis, inhibition of B-MYB function or B-MYB expression by therapeutic agents could be relevant in tumors with p53 mutant background by blocking re-entry into cell cycle leading to a more efficient G2 arrest after DNA damage induction. Using a

luciferase-based screen, agents that inhibit B-MYB expression could be identified and tested for their advantage in medical application. Additionally, since B-MYB activity is known to be regulated via its degradation (Charrasse, Carena et al. 2000), agents who target B-MYB stability could be new substances for advanced medical application. To test whether the additional application of B-MYB inhibitors in this context has positive effects on the therapeutic outcome, in vivo models should be used and e.g. nude mice assays performed. Therefore, p53 -/- cells, in which B-MYB and/or LIN-9 is depleted, would be injected into nude mice and the developing tumors treated with doxorubicin. Using this assay, B-MYB and LINC function during the DNA damage response in p53 -/- cells could be monitored - concerning not only treatment of an existing tumor but also tumor development. Thereby, contribution of B-MYB and LINC to tumor development and their impact on tumor therapy could be studied in p53 -/- cells (Fig. 4.1).

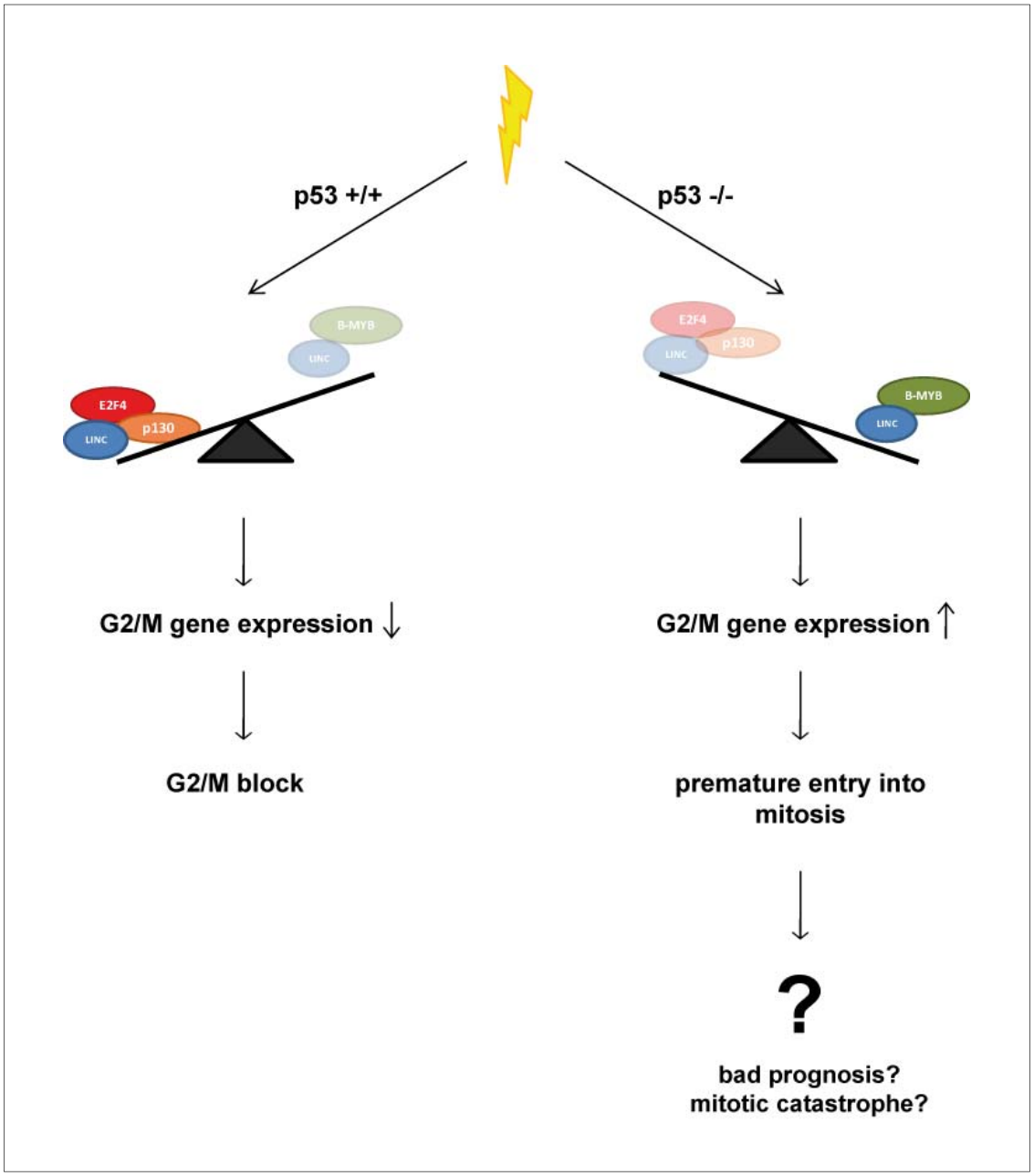

Figure 4.1: Simplified model of LINC function in DNA damage response

Dependent on the genetic background binding of p130 and E2F4 to LINC is induced after DNA damage induction. As a consequence, target gene expression is increased thereby leading to G2 block. In contrast, in p53 -/- where the LINC switch is absent, the balance between the activating and the repressing LIN complex is shifted towards the B-MYB binding LIN complex. Premature re-entry into mitosis is a direct consequence of the no longer decreased but instead even increased G2/M gene expression. Whether re-entry into cell cycle has positive or negative consequences for cell survival and/or prognosis is not known so far and has to be unraveled.

In Figure 4.1 the results of this work are summarized. In p53 +/+ cells a complex composed of LINC, p130 and E2F4 is build up after DNA damage induction. Thus, by direct binding of LINC to the promoters of target genes, G2/M gene expression is decreased leading to a sustained block in the G2

phase of the cell cycle. In contrast, in p53 -/- cells LINC switch is absent or rather not inducible and additionally B-MYB levels are increased by an unknown mechanism. Therefore, the balance between the repressing and the activating LIN complex is shifted towards B-MYB/LINC. As a consequence of this, G2/M gene expression is not decreased but even increased leading to premature entry into mitosis. Whether premature cell cycle re-entry leads to mitotic catastrophe and therefore cell death or further proliferation with the possibility of error accumulation has to be investigated in more detail. Up to date, the outcome for cell survival and therefore, the resulting implications for cancer treatment are controversial. Nevertheless, it seems that targeting B-MYB function by inhibition enables a more effective and adjuvant therapy especially in p53 mutant tumors.

5 Summary

Around 10.000 – 150.000 endogenous DNA damage-induced lesions occur in a human body per day and cell. Accumulation of unrepaired lesions can lead to aneuploidy and the loss of genomic integrity which in turn contributes to tumor formation. Therefore, an efficient DNA damage response has to be initiated, in the end leading to cell cycle inhibition and induction of repair.

Since it is known that a recently characterized human multiprotein complex named LINC (or human dREAM) together with B-MYB is involved in the regulation of G2/M gene expression (Plk1, cyclin B1, cdc2 etc.), its function in the DNA damage response was analyzed in this study. In growing cells B-MYB is associated to the LIN core complex which consists of 5 different proteins named LIN-9, LIN-54, LIN-52, LIN-37 and RbAp48. After induction of DNA damage B-MYB leaves the complex and binding of E2F4 and p130 to LINC is induced. Importantly, the upstream pathway leading to LINC rearrangement is dependent on the activation of p53 and p21.

Interestingly, p53 -/- cells solely have the potential to block in the G2 phase of the cell cycle, thereby making them vulnerable for errors during G2 arrest induction or maintenance. Here I demonstrate that LINC rearrangement is absent in p53 -/- cells and that B-MYB/LINC binding to target gene promoters is increased. This in turn leads to an increased G2/M gene expression after DNA damage induction and triggers premature cell cycle re-entry (checkpoint adaptation). Significantly, B-MYB expression is increased in p53 mutated primary breast cancer tumors and correlates with poor prognosis and reoccurrence probably due to its function in checkpoint adaptation. This study gives evidence that inhibition of B-MYB gene expression or B-MYB function in p53 mutant tumors could be a good choice for adjuvant therapy.

6 Zusammenfassung

In jeder menschlichen Zelle entstehen täglich ca. 10.000 – 150.000 endogene DNA Schäden. Eine Anhäufung dieser Läsionen kann zu genetischer Instabilität führen und dadurch zur Krebsentwicklung beitragen. Daher ist eine schnelle DNA Schadensantwort nötig, um schwerwiegende Folgen für die Zelle zu vermeiden.

Da bekannt ist, dass der Multiproteinkomplex LINC (auch humaner dREAM-Komplex genannt) an der transkriptionellen Regulation mitotischer und G2-spezifischer Gene beteiligt ist, sollte in dieser Arbeit seine Beteiligung an der DNA Schadensantwort genauer untersucht werden. In der vorliegenden Arbeit wird gezeigt, dass in normal wachsenden Zellen B-MYB an den LINC-Kernkomplex bindet, welcher sich aus 5 Proteinen zusammensetzt: LIN-9, LIN-54, LIN-52, LIN-37 und RbAp48. Treten DNA Schäden auf, dissoziiert B-MYB vom LINC Kernkomplex wobei gleichzeitig die Bindung von p130 und E2F4 an LINC induziert wird. Zusätzlich konnte gezeigt werden, dass der Signalweg, der die LINC Umlagerung vermittelt, sowohl p53- als auch p21-abhängig ist.

p53 negative Zellen können nach Schädigung der DNA weder einen G1 Block induzieren noch einen G2 Block langfristig aufrechterhalten. Eine Erklärung für diese Schwächung des G2 Arrests liefern Daten dieser Arbeit: Da in DNA geschädigten p53 -/- Zellen keine LINC Umlagerung beobachtet werden kann und zusätzlich B-MYB verstärkt an LINC und die Zielpromotoren bindet, kommt es zu einer erhöhten G2/M Genexpression. Dies resultiert häufig in einem verfrühten Wiedereintritt in den Zellzyklus („checkpoint adaptation“). Eine Daten-Analyse primärer Brustkrebstumore zeigte außerdem, dass erhöhte B-MYB Genexpressionslevel mit einer erhöhte Rückfallgefahr und einer schlechten Prognose korrelieren, was möglicherweise auf die Funktion von B-MYB während der „checkpoint adaptation“ zurückzuführen ist. Schlussendlich lassen die Ergebnisse dieser Arbeit vermuten, dass die Hemmung der B-MYB Funktion in solchen Tumoren, die p53 Mutationen tragen, die Wahrscheinlichkeit eines Behandlungserfolges vergrößern und die Wahrscheinlichkeit eines Rückfalls senken könnte.

7 Appendix

7.1 Table of figures

7.2 Abbreviations

APS	Ammonium persulfate
BSA	Bovine serum albumine
DTT	Dithiothreitol
CDE	Cell cycle-dependent element
Cdk	Cyclin-dependent kinase
ChIP	Chromatin immunoprecipitation
CHR	Cell cycle genes homology region
DMSO	Dimethylsulfoxyde
DNA	Deoxyribonucleic acid
dNTP	deoxyribonucleotide triphosphate
DSB	double strand break
dREAM	Drosophila RBF E2F and Myb complex
DREAM	DP, RB-like, E2F and MuvB complex
DRM	DP, RB and MuvB complex
ECL	Enhanced chemiluminescence
EDTA	ethylenediaminetetraacetic acid
ESB	Electrophoresis sample buffer
FACS	Fluorescence-associated cell sorting
FCS	Fetal calf serum
Fig.	Figure
G0, G1, G2	Gap phases
GAPDH	glyceraldehyde-3-phosphate dehydrogenase
GST	Glutathione S-transferase
HDAC	Histone deacetylase
HRP	Horseradish peroxydase
IP	Immunoprecipitation
kDa	kiloDalton
LB	Luria Bertani
LINC	LIN complex
mip	Myb-interacting protein
M	Mitosis
PBS	Phosphate buffered saline

PCNA	Proliferating Cell Nuclear Antigen
PH3	Phospho-histone H3 (Ser10)
PI	Protease Inhibitor
PMSF	Phenylmethylsulphonyl fluoride
pRB	Retinoblastoma protein
qPCR	Quantitative polymerase chain reaction
RNA	Ribonucleic acid
RNAi	RNA interference
siRNA	small interfering RNA
rpm	Revolutions per minute
RT	Reverse transcriptase
	Room temperature
SDS	Sodium dodecyl sulfate
shRNA	Short hairpin RNA
S	Synthesis phase
synMuv	Synthetic multivulva
TAE	Tris-acetate-EDTA
TBS	Tris-buffered saline
WB	Western blot

7.3 References

Ahlbory, D., H. Appl, et al. (2005). "Disruption of B-myb in DT40 cells reveals novel function for B-Myb in the response to DNA-damage." Oncogene **24**(48): 7127-34.

Amatschek, S., U. Koenig, et al. (2004). "Tissue-wide expression profiling using cDNA subtraction and microarrays to identify tumor-specific genes." Cancer Res **64**(3): 844-56.

Azzam, E. I., S. M. de Toledo, et al. (1997). "CDC2 is down-regulated by ionizing radiation in a p53-dependent manner." Cell Growth Differ **8**(11): 1161-9.

Badie, C., J. E. Itzhaki, et al. (2000). "Repression of CDK1 and other genes with CDE and CHR promoter elements during DNA damage-induced G(2)/M arrest in human cells." Mol Cell Biol **20**(7): 2358-66.

Barabas, K., R. Milner, et al. (2008). "Cisplatin: a review of toxicities and therapeutic applications." Vet Comp Oncol **6**(1): 1-18.

Bartek, J. and J. Lukas (2001). "Mammalian G1- and S-phase checkpoints in response to DNA damage." Curr Opin Cell Biol **13**(6): 738-47.

Bartek, J. and J. Lukas (2007). "DNA damage checkpoints: from initiation to recovery or adaptation." Curr Opin Cell Biol **19**(2): 238-45.

Beall, E. L., P. W. Lewis, et al. (2007). "Discovery of tMAC: a Drosophila testis-specific meiotic arrest complex paralogous to Myb-Muv B." Genes Dev **21**(8): 904-19.

Bertucci, F., R. Houlgatte, et al. (2000). "Gene expression profiling of primary breast carcinomas using arrays of candidate genes." Hum Mol Genet **9**(20): 2981-91.

Bommer, G. T., I. Gerin, et al. (2007). "p53-mediated activation of miRNA34 candidate tumor-suppressor genes." Curr Biol **17**(15): 1298-307.

Bradford, M. M. (1976). "A rapid and sensitive method for the quantitation of microgram quantities of protein utilizing the principle of protein-dye binding." Anal Biochem **72**: 248-54.

Bunz, F., A. Dutriaux, et al. (1998). "Requirement for p53 and p21 to sustain G2 arrest after DNA damage." Science **282**(5393): 1497-501.

Chan, T. A., H. Hermeking, et al. (1999). "14-3-3Sigma is required to prevent mitotic catastrophe after DNA damage." Nature **401**(6753): 616-20.

Charrasse, S., I. Carena, et al. (2000). "Degradation of B-Myb by ubiquitin-mediated proteolysis: involvement of the Cdc34-SCF(p45Skp2) pathway." Oncogene **19**(26): 2986-95.

Chen, G. G., J. L. Merchant, et al. (2003). "Mutation of p53 in recurrent hepatocellular carcinoma and its association with the expression of ZBP-89." Am J Pathol **162**(6): 1823-9.

Cicchillitti, L., P. Fasanaro, et al. (2003). "Oxidative stress induces protein phosphatase 2A-dependent dephosphorylation of the pocket proteins pRb, p107, and p130." J Biol Chem **278**(21): 19509-17.

Cobrinik, D. (2005). "Pocket proteins and cell cycle control." Oncogene **24**(17): 2796-809.

Crosby, M. E., J. Jacobberger, et al. (2007). "E2F4 regulates a stable G2 arrest response to genotoxic stress in prostate carcinoma." Oncogene **26**(13): 1897-909.

Cummings, J. and J. F. Smyth (1993). "DNA topoisomerase I and II as targets for rational design of new anticancer drugs." Ann Oncol **4**(7): 533-43.

de Toledo, S. M., E. I. Azzam, et al. (1998). "Regulation by ionizing radiation of CDC2, cyclin A, cyclin B, thymidine kinase, topoisomerase IIalpha, and RAD51 expression in normal human diploid fibroblasts is dependent on p53/p21Waf1." Cell Growth Differ **9**(11): 887-96.

Dimova, D. K. and N. J. Dyson (2005). "The E2F transcriptional network: old acquaintances with new faces." Oncogene **24**(17): 2810-26.

DuPree, E. L., S. Mazumder, et al. (2004). "Genotoxic stress induces expression of E2F4, leading to its association with p130 in prostate carcinoma cells." Cancer Res **64**(13): 4390-3.

Dyson, N. (1998). "The regulation of E2F by pRB-family proteins." Genes Dev **12**(15): 2245-62.

Farkas, T., K. Hansen, et al. (2002). "Distinct phosphorylation events regulate p130- and p107-mediated repression of E2F-4." J Biol Chem **277**(30): 26741-52.

Feng, Y. B., D. C. Lin, et al. (2009). "Overexpression of PLK1 is associated with poor survival by inhibiting apoptosis via enhancement of survivin level in esophageal squamous cell carcinoma." Int J Cancer **124**(3): 578-88.

Fornari, F. A., J. K. Randolph, et al. (1994). "Interference by doxorubicin with DNA unwinding in MCF-7 breast tumor cells." Mol Pharmacol **45**(4): 649-56.

Gagrica, S., S. Hauser, et al. (2004). "Inhibition of oncogenic transformation by mammalian Lin-9, a pRB-associated protein." EMBO J **23**(23): 4627-38.

Gaubatz, S., G. J. Lindeman, et al. (2000). "E2F4 and E2F5 play an essential role in pocket protein-mediated G1 control." Mol Cell **6**(3): 729-35.

Giacinti, C. and A. Giordano (2006). "RB and cell cycle progression." Oncogene **25**(38): 5220-7.

Graves, P. R., C. M. Lovly, et al. (2001). "Localization of human Cdc25C is regulated both by nuclear export and 14-3-3 protein binding." Oncogene **20**(15): 1839-51.

Hanada, N., H. W. Lo, et al. (2006). "Co-regulation of B-Myb expression by E2F1 and EGF receptor." Mol Carcinog **45**(1): 10-7.

Hande, K. R. (1998). "Etoposide: four decades of development of a topoisomerase II inhibitor." Eur J Cancer **34**(10): 1514-21.

Harrison, M. M., C. J. Ceol, et al. (2006). "Some C. elegans class B synthetic multivulva proteins encode a conserved LIN-35 Rb-containing complex distinct from a NuRD-like complex." Proc Natl Acad Sci U S A **103**(45): 16782-7.

He, B., Z. Y. Tang, et al. (1996). "Analysis of the cellular origin of hepatocellular carcinoma by p53 genotype." J Cancer Res Clin Oncol **122**(12): 763-6.

He, L., X. He, et al. (2007). "A microRNA component of the p53 tumour suppressor network." Nature **447**(7148): 1130-4.

Hernando, E., Z. Nahle, et al. (2004). "Rb inactivation promotes genomic instability by uncoupling cell cycle progression from mitotic control." Nature **430**(7001): 797-802.

Horstmann, S., S. Ferrari, et al. (2000). "Regulation of B-Myb activity by cyclin D1." Oncogene **19**(2): 298-306.

Ianzini, F. and M. A. Mackey (1997). "Spontaneous premature chromosome condensation and mitotic catastrophe following irradiation of HeLa S3 cells." Int J Radiat Biol **72**(4): 409-21.

Ivshina, A. V., J. George, et al. (2006). "Genetic reclassification of histologic grade delineates new clinical subtypes of breast cancer." Cancer Res **66**(21): 10292-301.

Jackson, M. W., M. K. Agarwal, et al. (2005). "p130/p107/p105Rb-dependent transcriptional repression during DNA-damage-induced cell-cycle exit at G2." J Cell Sci **118**(Pt 9): 1821-32.

Jin, P., S. Hardy, et al. (1998). "Nuclear localization of cyclin B1 controls mitotic entry after DNA damage." J Cell Biol **141**(4): 875-85.

Johnson, T. K., R. E. Schweppe, et al. (1999). "Phosphorylation of B-Myb regulates its transactivation potential and DNA binding." J Biol Chem **274**(51): 36741-9.

Jordan, M. A., D. Thrower, et al. (1992). "Effects of vinblastine, podophyllotoxin and nocodazole on mitotic spindles. Implications for the role of microtubule dynamics in mitosis." J Cell Sci **102 (Pt 3)**: 401-16.

Kanaji, S., H. Saito, et al. (2006). "Expression of polo-like kinase 1 (PLK1) protein predicts the survival of patients with gastric carcinoma." Oncology **70**(2): 126-33.

Kao, G. D., W. G. McKenna, et al. (1997). "Cyclin B1 availability is a rate-limiting component of the radiation-induced G2 delay in HeLa cells." Cancer Res **57**(4): 753-8.

Kato, M., T. Paranjape, et al. (2009). "The mir-34 microRNA is required for the DNA damage response in vivo in C. elegans and in vitro in human breast cancer cells." Oncogene **28**(25): 2419-24.

Ki, D. H., H. C. Jeung, et al. (2007). "Whole genome analysis for liver metastasis gene signatures in colorectal cancer." Int J Cancer **121**(9): 2005-12.

Kleinschmidt, M. A., T. U. Wagner, et al. (2009). "lin9 Is Required for Mitosis and Cell Survival during Early Zebrafish Development." J Biol Chem **284**(19): 13119-27.

Korenjak, M. and A. Brehm (2005). "E2F-Rb complexes regulating transcription of genes important for differentiation and development." Curr Opin Genet Dev **15**(5): 520-7.

Korenjak, M., B. Taylor-Harding, et al. (2004). "Native E2F/RBF complexes contain Myb-interacting proteins and repress transcription of developmentally controlled E2F target genes." Cell **119**(2): 181-93.

Lam, E. W., J. D. Morris, et al. (1994). "HPV16 E7 oncoprotein deregulates B-myb expression: correlation with targeting of p107/E2F complexes." EMBO J **13**(4): 871-8.

Lange-zu Dohna, C., M. Brandeis, et al. (2000). "A CDE/CHR tandem element regulates cell cycle-dependent repression of cyclin B2 transcription." FEBS Lett **484**(2): 77-81.

Leng, M. and V. Brabec (1994). "DNA adducts of cisplatin, transplatin and platinum-intercalating drugs." IARC Sci Publ(125): 339-48.

Lewis, P. W., E. L. Beall, et al. (2004). "Identification of a Drosophila Myb-E2F2/RBF transcriptional repressor complex." Genes Dev **18**(23): 2929-40.

Li, X. and D. P. McDonnell (2002). "The transcription factor B-Myb is maintained in an inhibited state in target cells through its interaction with the nuclear corepressors N-CoR and SMRT." Mol Cell Biol **22**(11): 3663-73.

Lin, D., M. Fiscella, et al. (1994). "Constitutive expression of B-myb can bypass p53-induced Waf1/Cip1-mediated G1 arrest." Proc Natl Acad Sci U S A **91**(21): 10079-83.

Lindgren, D., F. Liedberg, et al. (2006). "Molecular characterization of early-stage bladder carcinomas by expression profiles, FGFR3 mutation status, and loss of 9q." Oncogene **25**(18): 2685-96.

Lipinski, M. M. and T. Jacks (1999). "The retinoblastoma gene family in differentiation and development." Oncogene **18**(55): 7873-82.

Lipsick, J. S. (2004). "synMuv verite--Myb comes into focus." Genes Dev **18**(23): 2837-44.

Litovchick, L., S. Sadasivam, et al. (2007). "Evolutionarily conserved multisubunit RBL2/p130 and E2F4 protein complex represses human cell cycle-dependent genes in quiescence." Mol Cell **26**(4): 539-51.

Liu, D. X., N. Nath, et al. (2005). "Regulation of neuron survival and death by p130 and associated chromatin modifiers." Genes Dev **19**(6): 719-32.

Liu, N., F. C. Lucibello, et al. (1998). "A new model of cell cycle-regulated transcription: repression of the cyclin A promoter by CDF-1 and anti-repression by E2F." Oncogene **16**(23): 2957-63.

Liu, N., F. C. Lucibello, et al. (1996). "Cell cycle-regulated repression of B-myb transcription: cooperation of an E2F site with a contiguous corepressor element." Nucleic Acids Res **24**(15): 2905-10.

Macaluso, M., C. Cinti, et al. (2003). "pRb2/p130-E2F4/5-HDAC1-SUV39H1-p300 and pRb2/p130-E2F4/5-HDAC1-SUV39H1-DNMT1 multimolecular complexes mediate the transcription of estrogen receptor-alpha in breast cancer." Oncogene **22**(23): 3511-7.

Macurek, L., A. Lindqvist, et al. (2008). "Polo-like kinase-1 is activated by aurora A to promote checkpoint recovery." Nature **455**(7209): 119-23.

Mailand, N., S. Bekker-Jensen, et al. (2006). "Destruction of Claspin by SCFbetaTrCP restrains Chk1 activation and facilitates recovery from genotoxic stress." Mol Cell **23**(3): 307-18.

Malumbres, M. and M. Barbacid (2001). "To cycle or not to cycle: a critical decision in cancer." Nat Rev Cancer **1**(3): 222-31.

Mamely, I., M. A. van Vugt, et al. (2006). "Polo-like kinase-1 controls proteasome-dependent degradation of Claspin during checkpoint recovery." Curr Biol **16**(19): 1950-5.

Maya, R., M. Balass, et al. (2001). "ATM-dependent phosphorylation of Mdm2 on serine 395: role in p53 activation by DNA damage." Genes Dev **15**(9): 1067-77.

Miller, L. D., J. Smeds, et al. (2005). "An expression signature for p53 status in human breast cancer predicts mutation status, transcriptional effects, and patient survival." Proc Natl Acad Sci U S A **102**(38): 13550-5.

Molinari, M. (2000). "Cell cycle checkpoints and their inactivation in human cancer." Cell Prolif **33**(5): 261-74.

Nakajima, T., K. Yasui, et al. (2008). "Activation of B-Myb by E2F1 in hepatocellular carcinoma." Hepatol Res **38**(9): 886-95.

Niida, H. and M. Nakanishi (2006). "DNA damage checkpoints in mammals." Mutagenesis **21**(1): 3-9.

Nitiss, J. L. (2002). "DNA topoisomerases in cancer chemotherapy: using enzymes to generate selective DNA damage." Curr Opin Investig Drugs **3**(10): 1512-6.

Nurse, P. (1997). "Checkpoint pathways come of age." Cell **91**(7): 865-7.

Orr, B., H. Bousbaa, et al. (2007). "Mad2-independent spindle assembly checkpoint activation and controlled metaphase-anaphase transition in Drosophila S2 cells." Mol Biol Cell **18**(3): 850-63.

Osterloh, L., B. von Eyss, et al. (2007). "The human synMuv-like protein LIN-9 is required for transcription of G2/M genes and for entry into mitosis." EMBO J **26**(1): 144-57.

Peschiaroli, A., N. V. Dorrello, et al. (2006). "SCFbetaTrCP-mediated degradation of Claspin regulates recovery from the DNA replication checkpoint response." Mol Cell **23**(3): 319-29.

Pilkinton, M., R. Sandoval, et al. (2007). "Mammalian Mip/LIN-9 interacts with either the p107, p130/E2F4 repressor complex or B-Myb in a cell cycle-phase-dependent context distinct from the Drosophila dREAM complex." Oncogene **26**(54): 7535-43.

Plesca, D., M. E. Crosby, et al. (2007). "E2F4 function in G2: maintaining G2-arrest to prevent mitotic entry with damaged DNA." Cell Cycle **6**(10): 1147-52.

Polager, S. and D. Ginsberg (2003). "E2F mediates sustained G2 arrest and down-regulation of Stathmin and AIM-1 expression in response to genotoxic stress." J Biol Chem **278**(3): 1443-9.

Raschella, G., V. Cesi, et al. (1999). "Expression of B-myb in neuroblastoma tumors is a poor prognostic factor independent from MYCN amplification." Cancer Res **59**(14): 3365-8.

Rocha, S., A. M. Martin, et al. (2003). "p53 represses cyclin D1 transcription through down regulation of Bcl-3 and inducing increased association of

the p52 NF-kappaB subunit with histone deacetylase 1." Mol Cell Biol **23**(13): 4713-27.

Sala, A. (2005). "B-MYB, a transcription factor implicated in regulating cell cycle, apoptosis and cancer." Eur J Cancer **41**(16): 2479-84.

Santilli, G., M. N. Cervellera, et al. (2001). "PARP co-activates B-MYB through enhanced phosphorylation at cyclin/cdk2 sites." Oncogene **20**(57): 8167-74.

Schmit, F., M. Korenjak, et al. (2007). "LINC, a human complex that is related to pRB-containing complexes in invertebrates regulates the expression of G2/M genes." Cell Cycle **6**(15): 1903-13.

Schwab, R., A. Caccamo, et al. (2007). "B-MYB is hypophosphorylated and resistant to degradation in neuroblastoma: implications for cell survival." Blood Cells Mol Dis **39**(3): 263-71.

Seki, A., J. A. Coppinger, et al. (2008). "Bora and the kinase Aurora a cooperatively activate the kinase Plk1 and control mitotic entry." Science **320**(5883): 1655-8.

Sen, S., H. Katayama, et al. (2008). "Functional significance of Aurora kinase A in centrosome amplification and genomic instability." Adv Exp Med Biol **617**: 99-108.

Shangary, S. and S. Wang (2009). "Small-molecule inhibitors of the MDM2-p53 protein-protein interaction to reactivate p53 function: a novel approach for cancer therapy." Annu Rev Pharmacol Toxicol **49**: 223-41.

Shimada, M. and M. Nakanishi (2006). "DNA damage checkpoints and cancer." J Mol Histol **37**(5-7): 253-60.

Sorlie, T., C. M. Perou, et al. (2001). "Gene expression patterns of breast carcinomas distinguish tumor subclasses with clinical implications." Proc Natl Acad Sci U S A **98**(19): 10869-74.

Sotillo, R., E. Hernando, et al. (2007). "Mad2 overexpression promotes aneuploidy and tumorigenesis in mice." Cancer Cell **11**(1): 9-23.

Sotiriou, C., S. Y. Neo, et al. (2003). "Breast cancer classification and prognosis based on gene expression profiles from a population-based study." Proc Natl Acad Sci U S A **100**(18): 10393-8.

Syljuasen, R. G., S. Jensen, et al. (2006). "Adaptation to the ionizing radiation-induced G2 checkpoint occurs in human cells and depends on checkpoint kinase 1 and Polo-like kinase 1 kinases." Cancer Res **66**(21): 10253-7.

Takahashi, T., B. Sano, et al. (2003). "Polo-like kinase 1 (PLK1) is overexpressed in primary colorectal cancers." Cancer Sci **94**(2): 148-52.

Takahashi, Y., J. B. Rayman, et al. (2000). "Analysis of promoter binding by the E2F and pRB families in vivo: distinct E2F proteins mediate activation and repression." Genes Dev **14**(7): 804-16.

Taylor, W. R., A. H. Schonthal, et al. (2001). "p130/E2F4 binds to and represses the cdc2 promoter in response to p53." J Biol Chem **276**(3): 1998-2006.

Tessema, M., U. Lehmann, et al. (2004). "Cell cycle and no end." Virchows Arch **444**(4): 313-23.

Toczyski, D. P., D. J. Galgoczy, et al. (1997). "CDC5 and CKII control adaptation to the yeast DNA damage checkpoint." Cell **90**(6): 1097-106.

Tommasi, S. and G. P. Pfeifer (1995). "In vivo structure of the human cdc2 promoter: release of a p130-E2F-4 complex from sequences immediately upstream of the transcription initiation site coincides with induction of cdc2 expression." Mol Cell Biol **15**(12): 6901-13.

Toyota, M., H. Suzuki, et al. (2008). "Epigenetic silencing of microRNA-34b/c and B-cell translocation gene 4 is associated with CpG island methylation in colorectal cancer." Cancer Res **68**(11): 4123-32.

van Vugt, M. A., A. Bras, et al. (2004). "Polo-like kinase-1 controls recovery from a G2 DNA damage-induced arrest in mammalian cells." Mol Cell **15**(5): 799-811.

Vassilev, L. T. (2005). "p53 Activation by small molecules: application in oncology." J Med Chem **48**(14): 4491-9.

Waldman, T., K. W. Kinzler, et al. (1995). "p21 is necessary for the p53-mediated G1 arrest in human cancer cells." Cancer Res **55**(22): 5187-90.

Wang, Y., C. Jacobs, et al. (2000). "Binding of 14-3-3beta to the carboxyl terminus of Wee1 increases Wee1 stability, kinase activity, and G2-M cell population." Cell Growth Differ **11**(4): 211-9.

Wang, Z., M. Jonca, et al. (2007). "Exploration of liquid and supercritical fluid chromatographic chiral separation and purification of Nutlin-3--a small molecule antagonist of MDM2." J Pharm Biomed Anal **45**(5): 720-9.

Wells, J., K. E. Boyd, et al. (2000). "Target gene specificity of E2F and pocket protein family members in living cells." Mol Cell Biol **20**(16): 5797-807.

Wolf, G., R. Elez, et al. (1997). "Prognostic significance of polo-like kinase (PLK) expression in non-small cell lung cancer." Oncogene **14**(5): 543-9.

Yamamoto, Y., H. Matsuyama, et al. (2006). "Overexpression of polo-like kinase 1 (PLK1) and chromosomal instability in bladder cancer." Oncology **70**(3): 231-7.

Yamauchi, T., T. Ishidao, et al. (2008). "A B-Myb complex containing clathrin and filamin is required for mitotic spindle function." EMBO J **27**(13): 1852-62.

Yang, J., K. Song, et al. (2008). "Rb/E2F4 and Smad2/3 link survivin to TGF-beta-induced apoptosis and tumor progression." Oncogene **27**(40): 5326-38.

Yin, X. Y., L. Grove, et al. (2001). "Inverse regulation of cyclin B1 by c-Myc and p53 and induction of tetraploidy by cyclin B1 overexpression." Cancer Res **61**(17): 6487-93.

Yoo, H. Y., A. Kumagai, et al. (2004). "Adaptation of a DNA replication checkpoint response depends upon inactivation of Claspin by the Polo-like kinase." Cell **117**(5): 575-88.

Zhang, J., S. Wang, et al. (2007). "Nitric oxide down-regulates polo-like kinase 1 through a proximal promoter cell cycle gene homology region." J Biol Chem **282**(2): 1003-9.

Zhu, W., P. H. Giangrande, et al. (2004). "E2Fs link the control of G1/S and G2/M transcription." EMBO J **23**(23): 4615-26.

Ziebold, U., O. Bartsch, et al. (1997). "Phosphorylation and activation of B-Myb by cyclin A-Cdk2." Curr Biol **7**(4): 253-60.

7.4 Danksagung

An erster Stelle möchte ich mich herzlich bei Herrn Prof. Dr. Stefan Gaubatz für die Möglichkeit bedanken, meine Doktorarbeit mit seiner Unterstützung und Betreuung anzufertigen. Viele seiner wertvollen Tipps und die von ihm eingebrachte Erfahrung haben sehr zum Erfolg meiner Doktorarbeit beigetragen.

Ich danke Herrn Dr. Alsheimer vielmals für die unkomplizierte und kurzfristige Zusage, meine Dissertation als Zweitkorrektor zu begutachten.

Vor allem „meiner“ Arbeitsgruppe bin ich zu großem Dank verpflichtet. In diesen 3 Jahren haben wir allen „Ups“ und „Downs“ zum Trotz in vielen „Stunden der Weisheit“ gemeinsam gelacht, geweint, vor Lachen geweint, gelästert, „Kaffeepausen“ gemacht, Feierabendbierchen (und –weinchen) getrunken, gelitten, Launen ertragen, aufgemuntert, gestützt, gefeiert, Sachen geschmissen, nicht zuletzt natürlich gearbeitet und vor allem am Ende doch überlebt. Dafür und für die vielen kleinen anderen Dinge, die diese Zeit so unvergesslich machen, möchte ich Euch von ganzem Herzen danken: Fabienne Schmit, Nina Reichert, Lisa Osterloh, Kathrin Schmitt, Susi Spahr, Jasmina Esterlechner, Tanja Ulrich, Piero Ocone, Adelgunde Wolpert, Markus Kleinschmidt, Leona Probst (beste Bachelorette), Katharina Brauburger (beste Diplomandin), Steffi Hauser und Sarah Cremer.

Der größte Dank gebührt meiner Familie und meinem Freund Steffen, die mich in jeder Lebenssituation unterstützt und es mir damit ermöglicht haben, das Beste aus mir herauszuholen, positiv zu denken und damit auch schwierige Situationen durchzustehen. Ihr habt mir nicht nur beruflich sondern auch privat in guten und schlechten Zeiten beigestanden und mir mit eurer Unterstützung, Fröhlichkeit und Liebe geholfen mich wieder aufzurappeln, nach vorne zu schauen und den Mut nicht zu verlieren, wenn etwas nicht so lief wie geplant und erhofft.

Nicht zuletzt möchte ich meinen Freunden danken, die mir seit 1999 eine unvergesslich tolle Zeit in Würzburg beschert haben. Von Labby bis Impro, von Genie bis Wahnsinn. Mit Eurer Freude und Eurem Ideenreichtum, Eurem schier

unerträglich-lustigen Witz und Charme und natürlich Eurer Verrücktheit und Lebensfreude habt Ihr mich immer wieder aufgemuntert und motiviert. Ganz besonders zu erwähnen ist natürlich die beste Michaela der Welt (ohne Gruppenzugehörigkeit, dafür aus Barcelona), die Labby-Fraktion, die KOMA-Truppe und die Füchslein-Dabljutschi.

„Wo die Praxis des Lebens fehlt, ist das Studium immer nur eine halbtätige Arbeit.“ August Graf von Platen Hallermund (Hallermünde), (1796 - 1835), deutscher Dramatiker, Theaterschriftsteller und Lyriker

7.5 Own publications

Mannefeld M, Klassen E, Gaubatz S
B-MYB is required for recovery from the DNA damage-induced G2 checkpoint in p53 mutant cells
Cancer Research, 2009, 69 (9), 4073-4080

Schmit F, Korenjak M, Mannefeld M, Schmitt K, Franke C, von Eyss B, Gagrica S, Hänel F, Brehm A and Gaubatz S.
LINC, a human complex that is related to pRb-containing complexes in invertebrates regulates the expression of G2/M genes.
Cell Cycle. 2007, 6: 1903-13

Conference contributions:
Mannefeld M, Schmitt K, Gaubatz S.
Regulation of G2/M gene expression by the human DREAM/ LIN complex in response to DNA damage. Poster. Cancer and the cell cycle
August 21 – August 23, 2008, Lausanne.

7.7 Eidesstattliche Erklärung

Hiermit erkläre ich an Eides statt, dass ich die vorliegende Dissertation selbständig verfasst habe und dabei keine anderen, als die von mir angegebenen Hilfsmittel und Quellen benutzt habe. Zitate sind als solche gekennzeichnet.

Ich erkläre außerdem, dass die vorliegende Dissertation weder in gleicher noch in ähnlicher Form bereits in einem anderen Prüfungsverfahren vorgelegen hat.

Ich habe früher, außer den mit dem Zulassungsantrag urkundlich vorgelegten Graden, keine weiteren akademischen Grade erworben oder zu erwerben versucht.

Würzburg, den 24. Juli 2009

_____

Mirijam Mannefeld